CO_2 transport: Data and models – a review

Svend Tollak Munkejord*, Morten Hammer, Sigurd W. Løvseth

SINTEF Energy Research, P.O. Box 4761 Sluppen, NO-7465 Trondheim, Norway

Abstract

This review considers data and models for CO_2 transport. The thermophysical properties of CO_2 and CO_2-rich mixtures are needed as a basis for various models within CO_2 capture and storage (CCS). In particular, this is true for transient models of pipes and vessels. Here, the data situation for phase equilibria, density, speed of sound, viscosity and thermal conductivity is reviewed, and property models are considered. Further, transient flow data and models for pipes are reviewed, including considerations regarding running-ductile fractures, which are essential to understand for safety. A depressurization case study based on recently published expansion-tube data is included as well. Non-equilibrium modelling of flow and phase equilibria are reviewed. Further, aspects related to the transport of CO_2 by ship are considered. Many things are known about CO_2 transport, e.g., that it is feasible and safe. However, if full-scale CCS were to be deployed today, conservative design and operational decisions would have to be made due to the lack of quantitative validated models.

Keywords: CO_2 transport, fluid dynamics, thermodynamics, thermophysical properties, depressurization, decompression,

1. Introduction

In the two-degree scenario (2DS) of the International Energy Agency [1], which is one possible way of reaching the two-degree goal, CO_2 capture and storage (CCS) contributes to reducing the global CO_2 emissions by about six billion tonnes per year in 2050. To achieve this scenario, CO_2 must be transported from the points of capture to the storage sites. A large fraction of the captured CO_2 is likely to be transported in pipeline networks. Pipeline transport of CO_2 is different from that of natural gas in a number of ways. First, the CO_2 will normally be in a liquid or dense liquid state [2, 3], whereas the natural gas most often is in a dense gaseous state, see e.g. Aursand *et al.* [4]. Second, depending on the capture technology, the CO_2 will contain various impurities [5–7], which may, even in small quantities, significantly affect the thermophysical properties [8, 9]. The thermophysical properties, in their turn, influence the depressurization and flow behaviour [10]. Transport of CO_2 by pipeline is in operation for the purpose of enhanced oil recovery (EOR), mainly in the USA [11, 12]. The CCS case is likely to be different, due to different impurities, and the proximity to densely populated areas. Thus, there is a need to develop modelling tools which can aid in the safe and economical design and operation of CO_2-transport pipelines.

Flow models for CO_2 transport should be able to take a number of phenomena into account. As already alluded to, multiple chemical components need to be catered for. Already in a single-phase case, CO_2 mixtures from different capture technologies will give different dynamic behaviour in pipeline transport [13]. Depending on the conditions, hydrates [14], or other solids, may form. Two-phase liquid-vapour flow may also occur, even if the pipeline is designed to be operated in the single-phase region. This may be due to varying CO_2 supply [15], or during transient events, such as start-up, shut-in or depressurization [16–18]. During these events, among other things, it is important to be able to estimate the temperatures, since the construction materials may have a minimum temperature below which they begin to lose their toughness, e.g. the ductile-brittle transition temperature of steel. Furthermore, it is of great importance to be able to calculate the single-phase and two-phase (mixture) speed of sound. This is because a given pipeline filled with CO_2 is more susceptible to running-ductile fracture than if filled with natural gas [2, 19, 20], and the running fracture is governed by a 'race' between the fracture velocity and the speed of sound.

The dispersion of CO_2 resulting from a leakage [21–24] is an input to risk assessments. To obtain realistic input boundary conditions to dispersion models, it is necessary to have good depressurization models for pipes and vessels.

Koornneef *et al.* [25] pointed out various knowledge gaps which affect the uncertainties of quantitative risk assessments for CO_2 pipelines. However, the fact that CO_2 pipelines have different challenges when compared to natural gas pipelines does not mean that CO_2-pipeline networks will be associated with high risks. The study by Duncan and Wang [26] suggested a very small likelihood of having potentially lethal releases for CO_2 from pipelines, assuming, among other things, that fracture propensity can be successfully mitigated.

Due to the large investments associated with offshore pipelines,

*Corresponding author.
Email address: svend.t.munkejord [a] sintef.no (Svend Tollak Munkejord)

transportation by ship may be a viable alternative due to its flexibility, especially in a start-up phase with relatively low CO_2 volumes. Among the issues needing further attention, is the design of the offloading system, which also has to be compatible with the restrictions imposed by the storage site. Such considerations require modelling tools accurately representing the thermophysical properties of CO_2 and CO_2-rich mixtures, including the vapour-liquid phase boundary and the precipitation of solids. Further, the emptying or depressurization of vessels have similarities with the depressurization of pipelines.

Regarding the content of other substances ('impurities') in the CO_2 to be transported, there appears to be at least two views. The first is that one should arrive at a 'transport specification' listing the maximum allowable content of impurities. The second is to perform knowledge-based optimization for each case. We believe that the latter approach may lead to a more efficient CCS system, preventing e.g. the oversizing of capture and conditioning plants. In the case of ship transport in particular, the liquefaction process should be optimized together with the capture process.

In view of the above, we want to review the state of the art with respect to data and models for transient two- and multiphase flow of CO_2 and CO_2-rich mixtures in CO_2-transport systems. Emphasis is put on developments having taken place after the reviews by Aursand *et al.* [4], Li *et al.* [8, 9], Gernert and Span [27], or on relevant subjects not covered therein. We put our boundary conditions around the transport system itself, focusing on thermo- and fluid dynamics in, and out of, pipes and vessels.

Although it would lead too far to enter into details in this paper, it should not be forgotten that the accuracy of a simulation not only depends on the accuracy of the physical model, but also on the employed numerical method. Numerical methods for multiphase flow models is a subject where there are still challenges with respect to robustness, accuracy and efficiency. For instance, numerical diffusion can smear out the resolution of a depressurization wave in a pipeline [28, 29]. The numerical methods employed to solve for the thermophysical properties also need to be highly consistent, robust and efficient. This is particularly true in conjunction with CFD methods, where the thermophysical properties are needed in each computational cell at each time step.

The remainder of this article is organized as follows. In Section 2 we review the data situation for phase equilibria, density, speed of sound, viscosity and thermal conductivity of CCS-relevant CO_2-rich mixtures. Section 3 deals with property models and briefly discusses implementation in fluid-dynamic models and flow through restrictions, which is relevant for decompression calculations. In Section 4, we review published data and models for transient multiphase flow of CO_2-rich mixtures in pipes. In particular, we include pipe-depressurization case study. Section 5 considers ship transport of CO_2. The study is concluded in Section 6.

2. Thermophysical property data

Knowledge of the relevant thermophysical properties of the relevant fluids is needed to optimize CO_2 transport with respect to economy, operability and safety. A few examples will be provided in the following. We will then review the situation regarding thermophysical property data for CO_2-rich CCS-relevant mixtures.

In pipeline transport it is usually desirable to have the fluids in dense phase, and hence knowledge of the vapour-liquid *phase behaviour* is essential [30, 31]. Accurate knowledge of vapour-liquid phase behaviour is particularly important when water is present in the CO_2-rich fluid to be transported, since even small amounts of water may lead to accelerated corrosion, in particular when in combination with other impurities [32–36]. At even lower water concentrations, CO_2 may form hydrates [37], in particular in combination with methane [38]. Phase behaviour will also be an important factor to determine the temperature and pressure characteristics of the CO_2-rich liquid in ship transport, and is particularly important in the design of the liquefaction process, for instance in order to avoid solid-state formation. Finally, phase behaviour models are very important to predict transient phenomena such as sudden (de-)pressurization of pipelines [39] and liquid loading and unloading of vessels.

For dimensioning of both pipelines and vessel size in ship transport, knowledge of the *density* as a function of pressure, temperature and composition is required. Density is also important for the design of important processing equipment such as compressors and pumps. In future large-scale CCS, accurate flow metering will be needed, both for government control and to facilitate a working CCS market and in order to optimize the processes involved. Many of the most relevant methods used today for fiscal natural gas metering are volumetric and hence need accurate density information for the transported mixtures.

Speed of sound has readily apparent importance in determining the flow rate in choked flow or in order to model any transient phenomena involving pressure waves. However, in addition, speed of sound often has an important role in the development and verification of equations of state (EOSs). The thermodynamic speed of sound is defined from the isentropic pressure variation with density, and for single-phase flow it is a purely thermodynamic function. In multiphase flow this is complicated by the interaction of the phases.

Among transport properties, *viscosity* is needed to estimate the pressure drop in pipes, reservoir modelling, as well as for the design of processing equipment. *Thermal conductivity* and *heat capacity* are needed for heat-transfer calculations, heat-exchanger design and a range of transient phenomena. Likewise, *diffusion coefficients* are needed to properly model e.g. reservoir behaviour and tank unloading.

Although the focus of this work is on CO_2 transport, thermophysical properties are also of high relevance in other sections of the CCS chain, both during capture, processing, injection and storage.

2.1. CCS capture product and transport fluid specifications

In real-life applications, the CO_2 to be transported will not be pure, but will be mixed with a certain amount of different impurities. As indicated in Table 1, the concentration range of different impurities in the CO_2 product from CCS capture processes can be quite large, depending on the capture technology and e.g. the purity of the fuel. It should be clear that the high level of impurities from some of the capture processes will lead to thermophysical properties that are drastically different from that of pure CO_2. For instance, the presence of only small amounts of dry air gases will increase the power consumption of transport chains [40], high levels of oxygen may be undesirable for instance in EOR and storage in depleted oil reservoirs, and toxic components may be unacceptable from regulator's point of view. The effects of water have already been discussed above. Hence, conditioning of the captured CO_2 product may be needed in many cases to enable efficient transport and storage. However, conditioning comes at a cost depending on the specified purity level, and hence, the levels of impurities allowed should be determined based on accurate models for the behaviour of the CO_2-rich mixtures.

For the different CO_2 pipelines in operation today, there is no consensus with regard to the specifications of CO_2 product composition and operational pressure. For instance, the maximum water content specifications vary between 50 ppm and 630 ppm [41]. In the Sleipner project, Hansen *et al.* [42] even indicate that the water content is more than 1000 ppm, which could lead to hydrate formation or even water-rich liquid phase at prolonged shut-ins. From a corrosion perspective, this example has less general relevance due to the use of stainless steel, which will be too expensive in projects of larger scale. It should be noted that most of the US EOR pipelines are transporting gas from geological CO_2 sources, which, depending on the capture and conditioning process, have different compositions than what is expected in CCS systems. During the last decade, various CO_2 quality recommendations for CCS pipeline transport have been proposed [2, 5, 43–46]. They vary a lot, for instance when it comes to water content (50 to 500 ppm), other impurities and overall CO_2 purity (95 to 99.5 %).

2.2. Data situation for equilibrium properties

Relatively recently, a review by Gernert and Span [27] has mapped the availability of experimental data on various thermodynamic properties of mixtures containing CO_2, H_2O, N_2, O_2, Ar, and CO. The last experimental data points considered were from 2012. Li *et al.* [8] published a review on density and phase equilibria data on CO_2-rich mixtures, with the last data considered being from 2002. Further, Li *et al.* [9] published a review on the data situation with regard to viscosity, thermal conductivity and diffusivity, with the last data points considered being from 2004. For fluid-phase equilibria, there is a series of articles covering high-pressure vapour-liquid equilibrium (VLE) measurements of many systems [47–53]. In order to get an up-to-date overview of data availability, free databases such as NIST's ThermoLit [54, 55] could be a useful source.

In the current work, a rather up-to-date overview of the data situation for phase behaviour, density, speed of sound, viscosity and thermal conductivity relevant for CCS will be provided. A warning is however warranted: Often data reviews are given in terms of parameters such as number of data points, pressure, temperature, and composition range. This information can in some cases be quite misleading. Firstly, there will often be large regions without data between the bounds of the pressure, temperature and composition range. Secondly, the usefulness of the data will depend on their real accuracy. In practice, accuracy is often not indicated in the data source. If it is indicated, there could be large discrepancies between what is claimed and the reality. Hence, for modelling purposes, careful study and consistency checks of the actual data should be performed, where the data often are categorized as either primary data used for modelling or secondary data. In EOS-CG [27], the new mixing rules were based only on 14 % of the data points available for the respective binary systems. It is beyond the scope of this work to perform such a critical review, and hence even for the systems and properties with the most measurements, a satisfactory data situation cannot be claimed. However, the overview provided indicates the strong need for more measurement data for certain properties, conditions, and mixtures, and should provide a useful starting point for further data mining and analysis.

The results of the data survey are shown in Tables 2–8. The information provided for the systems covered includes the number of sources, the number of sources during the last 40 years, the location of references, the number of data points, and ranges in temperature, pressure, and composition. New data do not at all have to be better than historic data, but generally, both the measurement techniques and physical understanding of the different measurement principles have improved during the last decades. Secondary referencing using some existing reviews [8, 9, 27, 56–63] are used for some of the sources, both because some of these references go deeper into the data, and to limit the number of references in the current work somewhat. In the tables, the number of references provided by each secondary source is given in an exclusive manner, such that primary sources are only counted once.

For all properties, data have been surveyed for binary mixtures between CO_2 and the other components listed in Table 1, which we will call primary mixtures in the following. If no data are found for such a binary system for a given property, no entry is provided in the relevant table. For phase equilibrium, also data from binary mixtures with water as well as ternary mixtures are provided. The reason is that even a small presence of a second phase in CCS transport could have a large impact. For some of the properties, also pure CO_2 is considered because of the rather small number of experimental papers found.

2.2.1. Vapour-liquid-liquid equilibrium (VLE)

An overview of VLE data relevant for CCS is provided in Table 2. Regarding some important binary systems for CCS, like CO_2-N_2, CO_2-CH_4, and CO_2-H_2O, the reports of a number of recent experimental studies seem to indicate a satisfactory data situation. Nevertheless, gaps and inconsistencies have recently been pointed out. For instance, with regard to CO_2-N_2, it was argued in [65] that prior to recent measurements [65, 79], the data situation was not very satisfactory at high temperatures and around the critical pressure. This is illustrated around 298.15 K in Figure 1, where the presence of data is not equivalent to a satisfactory data situation. Recently, the data situation for CO_2-O_2 has drastically been improved [82], and also the data situation for CO_2-H_2 is now better than it used to be thanks to

Table 1: Lower ($x_{i,\mathrm{min}}$) and upper ($x_{i,\mathrm{max}}$) range of typical impurity mole fractions from different capture processes. From [9] based on data from [2].

	CO_2	N_2	O_2	Ar	SO_2	H_2S/ COS	NO_x	CO	H_2	CH_4	H_2O	Amines	NH_3
$x_{i,\mathrm{min}}$ (%)	75	0.02	0.04	0.005	$<10^{-3}$	0.01	<0.002	$<10^{-3}$	0.06	0.7	0.005	$<10^{-3}$	$<10^{-3}$
$x_{i,\mathrm{max}}$ (%)	99	10	5	3.5	1.5	1.5	0.3	0.2	4	4	6.5	0.01	3

Table 2: VLE data for CCS-relevant systems.

System	# Sources		Location of References	# Points	Data ranges		
(1)-(2)-(3)-(4)	Total	1975→			T (K)	p (MPa)	x_{CO_2}
CO_2-N_2	34	26	12 in [8] + 12 in [27] +[65, 72–80]	> 700	208–303	0.6–21.4	0.15–0.999
CO_2-O_2	8	2	5 in [8] + 1 in [27] + [81, 82]	> 292	218–298	0.9–14.7	0.15–0.99
CO_2-Ar	4	2	2 in [8] + 1 in [27] +[83]	~ 200	233–299	1.5–14.0	0.25–0.99
CO_2-SO_2	3	0	1 in [8]+[84, 85]	~ 425	293–418	2.1–9.5	0.09–0.93
CO_2-H_2S	8	3	2 in [8] + [86–91]	> 270	248–365	1.0–8.9	0.01–0.97
CO_2-N_2O	1	0	1 in [8]	> 100	293–307	5.3–7.2	0.26–0.88
CO_2-NO_2/ CO_2-N_2O_4	2	1	1 in [8] + [92]	26	262–328	0.17–9.0	0.005–0.88
CO_2-CO	3	1	1 in [8] + 1 in [27] + [93]	106	223–293	0.8–14.2	0.20–0.996
CO_2-H_2	8	4	2 in [8] + [64, 71, 79, 80, 94, 95]	> 400	218–303	0.9–172	0.07–0.999
CO_2-CH_4	19	15	9 in [8]+ [74, 75, 96–103]	>180	153–320	0.68–48	0.026–0.99
CO_2-H_2O	>50		Eg. 41 refs. in [27]	>1500	251–623	0.1–350	0.08–1.00
CO_2-NH_3	2	0	2 in [8]	62	413–531	4.3–81.7	0.023–0.33
H_2O-N_2	29	15	26 in [27] + [104–106]	> 876	233–657	0.045–270	0.01–1.00
H_2O-O_2	9	5	5 in [27] + [107–110]	246	273–711	0.1–280	0.00–0.99
H_2O-Ar	12	10	9 in [27] + [111–113]	> 460	258–663	0.1–340	0.00–0.95
H_2O-SO_2	30	8	23 in [56] + [114–120]	> 756	273–423	$2\cdot10^{-4}$–345	0.86–0.999
H_2O-H_2S	17	6	13 in [58] + [121–124]	> 700	273–589	0.01–20.7	$5\cdot10^{-4}$–0.9997
H_2O-N_2O	3	2	[125–127]	> 52	286–303	0.1–7.3	0.95–0.9996
H_2O-CO	2	2	[122, 128]	41	304–589	1.1–13.8	0.001–0.99995
H_2O-H_2	6	5	[122, 129–133]	> 25	310–713	0.34–250	$6\cdot10^{-4}$–0.99996
H_2O-CH_4	This system is nominally well covered, for instance with more than 30 sources found in [54]						
H_2O-MEA H_2O-DEA H_2O-MDEA H_2O-NH_3	These systems are nominally relatively well covered, see [54, 134]						
CO_2-N_2-O_2	3	0	2 in [8] + 1 in [27]	80	218–273	5.1–13	–0.925
CO_2-N_2-H_2	1	1	[80]	36	253–302	2.1–8.7	0.95–0.93
CO_2-CO-H_2	1	1	1 in [8]	36	233–283	2–20	0.17–0.98
CO_2-CH_4-N_2	2	2	2 in [8]	> 100	220–293	6–10	0.27–0.99
CO_2-CH_4-H_2S	1	0	1 in [8]	16	222–239	2.1–4.8	0.024–0.78
CO_2-H_2O-CH_4	5	5	[38, 135–138]	> 132	243–423	0.1–100	0.001–0.83
CO_2-H_2O-NaCl CO_2-brines	16	15	10 in [62]+[62, 139–143]	> 1150	278–673	0.0–40	10^{-4}–0.998
CO_2-O_2-Ar-N_2	1	1	[144]	5	252–293	7.1–9.0	0.892

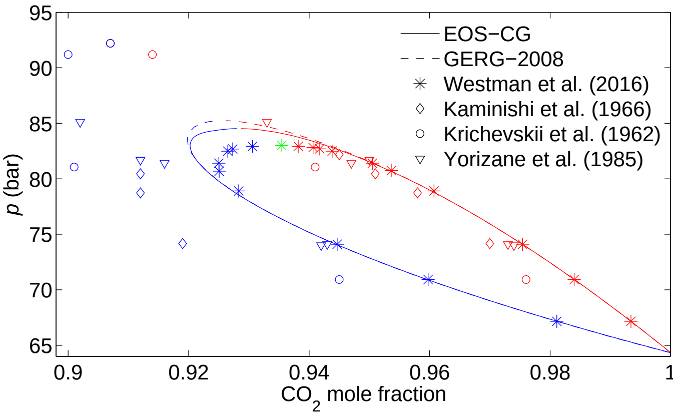

Figure 1: Data situation for CO_2-N_2 VLE around 298.15 K. Experimental data from [64–67] are plotted with the GERG-2008 [68] and EOS-CG [27] models. Bubble points are shown in red, dew points in blue, and a supercritical measurement from the measurement campaign reported in [65] is shown in green.

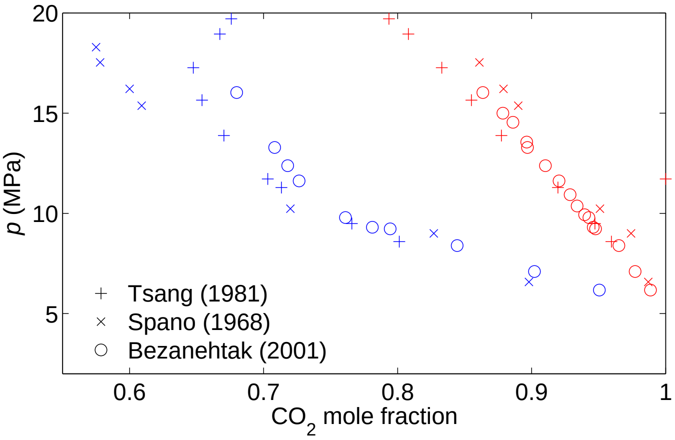

Figure 2: Available data for CO_2-H_2 VLE. All data at (290.00 ± 0.15) K. Data from [69–71]. Bubble points are shown in red and dew points in blue.

recent measurements [79, 80]. That an improvement was much needed despite the presence of literature data is illustrated in Figure 2. For CO_2-Ar there is one recent data set which seems to be of high quality [145], but the region around the critical locus is not well covered. For the other primary mixtures listed, the data situation is generally poor. For CO_2-SO_2 for instance, there are many data points, but most of the data are from a single author around the year 1902, and the latest data are from 1931. For CO_2-NO_x and CO_2-CO there are big gaps in the data. No VLE data have been found for the binary systems CO_2-COS, CO_2-NO, or CO_2-amines / CO_2-NH_3.

In order to avoid corrosion, it is of high importance to accurately determine the threshold for the formation of a water-rich liquid phase, and hence also VLE measurements on binary mixtures between water and the other impurities have been included in Table 2. Also here the amount of data varies significantly. It should be noted that a large part of the data are on gas solubility in water. For H_2O-SO_2 and H_2O-H_2S, a large fraction of the data is very old, in the case of H_2O-SO_2, 16 of the sources were published before 1940, the first one in 1855. Again the coverage of e.g. CO and NO_x seems poor, and no data have been found for binary mixtures between H_2O and COS, NO and NO_2/N_2O_4.

For completeness, also multicomponent CO_2 mixtures have been included in Table 2. Perhaps the most interesting systems here are CO_2-H_2O-NaCl and CO_2-brines, for which there are some data to be studied, and which are relevant for injection and storage. Ternary mixtures between CO_2, H_2O, and amines or NH_3, which are seen as more important for some capture processes than for transport and injection, have not been included in Table 2, but some data have been identified.

2.2.2. *Vapour-liquid-liquid equilibrium (VLLE)*

Some of the primary mixtures, like methane and CO_2 and water and CO_2, are known to form immiscible liquids at certain conditions, i.e., vapour-liquid-liquid equilibrium (VLLE). Again, it is of considerable practical interest to accurately characterize when a water-rich liquid phase forms. As seen in Table 3, the experimental data found for this kind of systems are scarce.

2.2.3. *Equilibria involving solids and hydrates*

In Table 4, the relevant phase equilibrium measurements found for systems involving solids are listed. During depressurization, the temperature of dry CO_2 mixtures could drop significantly, facilitating the formation of solid CO_2 (dry ice). New equilibria models for pure CO_2 with solids have recently been developed [169, 170], although, as stated in [170], the amount of thermodynamic data on solid CO_2 is very limited. For CCS, it is of interest to quantify also the change in freezing point due to impurities. For most impurity components, we would expect a freezing point depression. As seen in Table 4, very few measurements have been performed with such systems, except for CO_2 mixed with CH_4 or N_2. For these mixtures, the main focus has, however, been on low temperatures and hence relatively low CO_2 concentrations in the fluid phase(s), and the measurements on CO_2-N_2 are mostly quite old and incomplete.

With water involved, solid or hydrate phases can be introduced at much higher temperatures. Quite a bit of data have been found for the binary CO_2-H_2O system. With additional components present, far less data are available, and for the systems that are covered, a significant part of the data comes from a single source [63].

2.2.4. *Density and related properties*

Available data found for density and the related properties virial coefficients and compressibility are shown in Table 5. At first glance, density seems to be relatively well covered for a number of the primary binary mixtures, such as CO_2-N_2, CO_2-Ar, CO_2-CH_4, and CO_2-H_2O, but approximately 99 % of the data points for CO_2-CO and 80 % of the data points on CO_2-CH_4 come from the same experimental setup, all with a mole fraction of 0.97 CO_2 or more [93, 189]. It should also be noted that density measurements have an added degree of freedom as the composition of the fluids can be varied, in contrast to phase equilibria measurements of binary mixtures where the composition of each phase at a given temperature and pressure is fixed. Furthermore, it should be noted that for CO_2-H_2O, most data are for low CO_2 content, and no data have been found below

Table 3: VLLE equilibrium data for CCS-relevant systems.

System	# Sources		Location of References	# Points	Data ranges		
(1)-(2)	Total	1975→			T (K)	p (MPa)	x_{CO_2}
CO_2-H_2O	3	3	2 in [27] + [146]		278–313	6.4–29.5	
H_2O-H_2S	2	1	[121, 124]	> 15	311–373	4–20.7	0.018–0.95
H_2O-N_2O	2	1	[121, 146]				
CO_2-H_2O-CH_4	1	1	[138]	37	293–301	6.5–7.7	$4{\cdot}10^{-5}$–0.22

Table 4: Phase equilibrium data involving solids and hydrates for CCS-relevant systems.

System	# Sources		Location of References	# Points	Data ranges		
	Total	1975→			T (K)	p (MPa)	x_{CO_2}
CO_2-N_2	6	2	[79, 94, 147–150]	> 16	140–190	4.8–200	
CO_2-O_2	1	1	[151]	12	91–119	0.4–0.4	$4{\cdot}10^{-6}$–10^{-5}
CO_2-SO_2	1	0	[152]			0.1	
CO_2-H_2S	1	0	[152]			0.1	
CO_2-H_2	1	1	[79]	3	217–218	4.3–13.7	
CO_2-CH_4	7	2	[153–159]		98–217	0.1–10	0.01–0.58
CO_2-H_2O	>50		E.g. 44 in [160]+3 in [63]+[63, 161, 162]				
CO_2-H_2O-N_2	4	4	3 in [63]+[63]		273–289	2.1–55.1	0–1
CO_2-H_2O-CO	2	2	1 in [63]+[63]		273–286	1.4–21.3	0.1–0.97
CO_2-H_2O-H_2	4	3	3 in [63]+[63]		274–287	1.6–16.5	0.19–0.97
CO_2-H_2O-CH_4	2	10	9 in [63]+[63]		264–288	1.8–20.0	0–1
CO_2-brines	4	4	[163–166]	199	259–281	0.9–28	
CO_2-H_2O-SO_2	1	1	[167]	3	277–280	1.8–2.7	
CO_2-H_2O-N_2-SO_2	1	1	[168]	3	273–276	7.2–8.7	
CO_2-H_2O-NO_2-O_2	1	1	[167]	3	277	1.9	

Table 5: Data for density, virial coefficients and compressibility for CCS-relevant systems.

System	# Sources		Location of References	# Points	Data ranges		
	Total	1975→			T (K)	p (MPa)	x_{CO_2}
CO_2-N_2	37	25	6 in [8] + 24 in [27] + [63, 171–176]	>5210	208–673	–273	0.01–0.98
CO_2-O_2	7	2	5 in [27] + [63, 171]	377	268–423	–47.8	0.49–0.95
CO_2-Ar	19	11	3 in [8] + 8 in [27] + [63, 174, 176–181]	>1480	213–573	0.1–101	0.01–0.96
CO_2-SO_2	3	2	1 in [8] + [84, 181]	168	287–347	0.1–20	0.13–0-97
CO_2-H_2S	6	4	1 in [8] + [182–186]	>900	220–501	0.1–60.5	0.5–0.94
CO_2-N_2O	1	1	[187]	42	238–358	1–5.9	0.09–0.91
CO_2-CO	9	7	1 in [8] + 3 in [27] + [63, 93, 174, 188, 189]	> 50000	223–423	0.1–48.6	0.29–0.996
CO_2-H_2	11	7	[63, 71, 171, 174, 190–196]	>632	223–473	0.05–50.7	0.22–0.98
CO_2-CH_4	22	19	5 in [8]+[63, 75, 100, 174, 189, 191, 194, 197–206]	>6250	206–573	0.08–100	0.01–0.996
CO_2-H_2O	35	29	21 in [27] + 10 in [61] + [207–210]	>3619	273–1023	–600	0.001–0.997

273.25 K, although data for low H_2O concentrations and below 273.25 K would be highly relevant for CCS. Most of the data for CO_2-O_2 are old, and have a limited concentration range. For CO_2-SO_2 most of the data are from 1901 [84], and about 94 % of the data points for CO_2-H_2S are from a single source [186]. No data have been found for CO_2-COS, CO_2-NO, CO_2-NO_2 or CO_2- N_2O_4, or CO_2-amines or CO_2-NH_3 for these important properties.

2.2.5. *Speed of sound*

Perhaps due to the high attenuation of acoustic waves in CO_2, there is not a lot of speed-of-sound data available. Hence also pure CO_2 is included in the speed-of-sound data overview of Table 6. For mixtures, there is only limited-range data available for CO_2-N_2, CO_2-Ar, and CO_2-H_2O. Except for CO_2-N_2 and CO_2-H_2O, all the liquid mixture speed-of-sound data come from a single source [63]. The claimed uncertainty of Al-Siyabi [63] is $1\ m\,s^{-1}$, but no uncertainty analysis is provided, and data is only provided for a single composition per binary system. For a number of the primary mixtures, no liquid and / or vapour speed-of-sound measurements have been found. The few measurements found for CO_2-H_2O are not in a relevant range for CO_2 transport and storage.

2.2.6. *Viscosity*

The identified viscosity data for pure CO_2 and primary binary mixtures relevant for CCS are summarized in Table 7. The available data in the 80s and 90s for pure CO_2 were reviewed in [57, 59, 60]. In the modelling work of Vesovic *et al.* [59], the liquid data had all to be abandoned because of their inconsistencies, and a data-based reference model for the liquid phase could only be made once new measurements were available eight years later [60]. Works prior to 1957 were discarded due to inaccurate working equations. It should be noted that since the work of Fenghour and Wakeman [60], Vogel reportedly [230, 235] has reevaluated measurements from the 80s and 90s [236, 237] using accurate ab-initio correlations for helium. The data situation for viscosity is relatively thin for pure CO_2 but much worse for mixtures. For five binary systems, CO_2-O_2, CO_2-Ar, CO_2-CO, CO_2-H_2, and CO_2-CH_4, all liquid data are again provided by Al-Siyabi [63] for a single composition per system, using a single capillary viscometer. The uncertainty is claimed to be 1 %, with only uncertainty contributions from pressure measurements considered. No liquid viscosity data have been found for an important binary system such as CO_2-N_2. For CO_2-H_2O, only liquid-phase measurements on water-rich mixtures are available. For gas phase, there are a few more sources, but many of the measurements are quite old. No data have been found for either liquid or vapour/supercritical phase for CO_2-H_2S, CO_2-COS, CO_2-NO, CO_2-NO_2, CO_2-N_2O_4, CO_2-amines, or CO_2-NH_3.

2.2.7. *Thermal conductivity*

Like for viscosity, the data situation for thermal conductivity for CCS mixtures is highly unsatisfactory. The data available for pure CO_2 and binary mixtures between CO_2 and impurities of CCS are shown in Table 8. A relatively high number of sources are found for pure CO_2. However, when analysing the data in order to set up a model for thermal conductivity of pure CO_2, Vesovic *et al.* [59] discarded most of the data sources and had to use theoretical predictions in the liquid-phase and high temperature zero-density regions. Only a limited number of data sets have been published since, but a new set of measurements from [235] appears to be fairly complete. Except for CO_2-H_2O, no liquid-phase mixture data have been found, and only a handful of modern measurements for the vapour or supercritical phase are available for mixtures.

3. Thermophysical property models

In this section, we briefly review models and methods for calculating the thermophysical properties of CO_2 and CO_2-rich mixtures. Highly relevant topics, such as implementation in fluid-dynamic models, and methods for calculating flow through restrictions, are also covered.

3.1. *Property models for pure CO_2 and CO_2-rich mixtures*

During transport by pipeline or ship, the CO_2-rich fluid is normally in equilibrium. However, equilibrium properties are also needed as a useful starting point for non-equilibrium models. The thermodynamic properties of pure CO_2 are well described by the Span-Wagner EOS [243]. The Span-Wagner EOS is very accurate when it comes to prediction of density and saturation line. The estimated uncertainty for density predictions in the pressure and temperature domain relevant for transport of CO_2 is 0.05 %. The uncertainty in vapour pressure predictions is 0.006 %. Speed of sound and isobaric heat capacity are reported to be within 1.0 % and 1.5 %, respectively. In order to describe dry-ice in equilibrium with liquid and vapour, an auxiliary model is required. Trusler [169] developed a Helmholtz free energy model, and Jäger and Span [170] developed a Gibbs free energy model, that can be used to describe solid-liquid-vapour equilibrium for pure CO_2 and mixtures containing CO_2 in combination with a model for the fluid CO_2. Considering only pure CO_2, the auxiliary equations for the sublimation line published by Span and Wagner [243], have been used together with the Clausius-Clapeyron equation to describe vapour-solid equilibrium [244]. This approach is, however, not as easily extendable to CO_2-rich mixtures.

The Span-Wagner formulation is CPU demanding to solve compared to simpler models, like the commonly used Peng-Robinson (PR) EOS [245]. To address this, a new EOS for pure CO_2 has been developed by Demetriades *et al.* [246]. The EOS is designed for accuracy between 0 °C and the critical temperature of CO_2. The pressure of interest is set to be below 150 bar. This pressure-explicit EOS is relatively fast to evaluate, and it gives significant predictive improvements over Peng-Robinson, and contains much fever parameters than the Span-Wagner EOS. How the Demetriades *et al.* [246] EOS performs compared to other alternatives, e.g. the modified Benedict-Webb-Rubin (MBWR) EOS [247], is unknown. The accurate technical equations of state for CO_2 used in GERG-2004 [248], also represent a less CPU-demanding alternative to the Span-Wagner reference EOS. Demetriades and Graham [249] extended the pure-fluid

Table 6: Speed-of-sound data for CCS-relevant systems.

System	Vap/ Liq	# Sources Total	# Sources 1975→	Location of References	# Points	Data ranges T (K)	Data ranges p (MPa)	Data ranges x_{CO_2}
CO_2	V	6	4	[202, 211–215]	> 445	220–450	0.22–14.2	1
	L	5	2	[63, 216–219]	> 484	248–473	3.6–450	1
CO_2-N_2	V	1	1	1 in [27]	65	250–350	0.5–10.3	0.5
	L	2	2	[63, 220]	79	268–423	9.5–400	0.40–0.96
CO_2-O_2	L	1	1	[63]	62	268–301	8.9–41	0.94
CO_2-Ar	V	1	1	[221]	30	275–500	< 8	0.50–0.75
	L	1	1	[63]	62	268–301	8.93–41	0.93
CO_2-CO	L	1	1	[63]	61	268–301	9.71–41.1	0.96
CO_2-H_2	L	1	1	[63]	57	268–301	9.71–40.8	0.95
CO_2-CH_4	L	1	1	[63]	61	268–301	8.87–38.2	0.95
CO_2-H_2O	V	1	1	[222]		281–297	0.1	
	L	1	1	[223]	27	293–575	570–6000	0.05
CO_2-Ar-CO	L	1	1	[63]	58	268–301	10.3–41.2	0.97
CO_2-Ar-CO	L	1	1	[63]	58	268–301	10.3–41.2	0.97
CO_2-CH_4-H_2-N_2	L	1	1	[63]	60	268–301	7.6–40.6	0.95

Table 7: Viscosity data for CCS-relevant systems.

System	Vap/ Liq	# Sources Total	# Sources 1975→	Location of References	# Points	Data ranges T (K)	Data ranges p (MPa)	Data ranges x_{CO_2}
CO_2	V	39	18	26 in [57, 59, 60] + [215, 224–230]	> 1150	202–1871	0.02–8000	1
	L	34		28 in [59] + 7 in [60]		220–543	0.6–350	1
CO_2-N_2	V	5	0	5 in [9]	150	289–873	0.1–120	0–1
CO_2-O_2	V	2	1	2 in [9]	24	297–673	0.1	0–1
	L	1	1	[63]	60	280–343	9.1–47.3	0.95
CO_2-Ar	V	4	2	3 in [9] + [231]	198	213–673	0.02–2.5	0–0.92
	L	1	1	[63]	48	280–343	7.8–50.4	0.95
CO_2-SO_2	V	3	0	3 in [9]	69	238–353	0.1	0–1
CO_2-N_2O	V	3	1	2 in [9]+[232]	> 34	298–550	0.1	0–1
CO_2-CO	V	1	1	1 in [9]	10	298–473	0.1	0.31&0.77
	L	1	1	[63]	56	280–343	8.9–49.4	0.95
CO_2-H_2	V	6	2	6 in [9]	65	291–1100	0.1–0.3	0–1
	L	1	1	[63]	51	280–343	8.7–45.4	0.95
CO_2-CH_4	V	5	1	4 in [9] + [233]	406	293–673	0.1–172	0–1
	L	1	1	[63]	52	280–343	6.5–50.1	0.95
CO_2-H_2O	V	1	0	1 in [9]	8	303	0.1	0.96–0.99
	L	8	5	5 in [9] + [210, 234]	175	273–449	0.1–100	0.003–0.030
CO_2-H_2O-NaCl	L	2	2	2 in [9]	90	273–278	0.1–30	0–0.016

Table 8: Thermal conductivity data for CCS-relevant systems.

System	Vap/ Liq	# Sources Total	# Sources 1975→	Location of References	# Points	Data ranges T (K)	Data ranges p (MPa)	Data ranges x_{CO_2}
CO_2	V/L	65	12	60 in [59] + [235, 238–242]		186–2000	–2000	1
CO_2-N_2	V	10	1	10 in [9]	257	273–1033	0.1–300	0–1
CO_2-O_2	V	1	0	1 in [9]	4	369 & 370		0.22–0.73
CO_2-Ar	V	3	2	3 in [9]	270	273–473	0.1–11.3	0–1
CO_2-SO_2	V	1	0	1 in [9]	9	323 & 373		0.1–0.90
CO_2-N_2O	V	2	1	2 in [9]	90	300.65–723	0.1–4.25	0–1
CO_2-H_2	V	7	1	7 in [9]	120	258–893	0.1–7.5	0–1
CO_2-CH_4	V	4	3	3 in [9] + [240]	390	228–433	0.1–17.7	0.075–0.88
CO_2-H_2O	V/L	4	0	3 in [9]	41	298–603	0.1	0–1

EOS [246] with mixture rules to describe the binaries CO_2-H_2, CO_2-O_2 and CO_2-N_2 with good agreement with experimental data.

Analogous to the GERG equations for description of natural gas with impurities, EOSs are being developed for combustion gases (CG), where CO_2 is the main component. EOS-CG [27, 250, 251] is based on a single-component reference equation for Helmholtz free energy in the natural variables temperature and density/volume. In contrast to GERG-2004/2008, the single-component reference EOS is used, and not a simplification. I.e. for pure CO_2, EOS-CG becomes the Span-Wagner EOS. If the binary interaction parameters are correlated to accurate measurements, especially in the critical region, the use of accurate pure-fluid EOSs will give an improvement over GERG. In order to describe mixtures, Helmholtz free energy mixing rules are used [252–255]. Improved binary mixture models and parameters have been developed so far for the exhaust-gas components CO_2, H_2O, N_2, O_2, Ar and CO. One challenge with mixtures is the extrapolation of the pure-fluid reference equations. A species may exist in a mixture phase where the pure fluid is unstable, and therefore not tuned to experimental data. Despite some difficulties, good results have been published, and significant improvement over GERG-2008 is seen for mixtures containing CO_2 and H_2O [27].

Wilhelmsen *et al.* [256] compared density predictions for pure CO_2 and CO_2 mixtures, using five EOSs. Soave-Redlich-Kwong (SRK) [257] (with and without Péneloux shift [258]), Lee-Kesler [259], Peng-Robinson [245], GERG-2004, and SPUNG [260] were evaluated against the Span-Wagner EOS and experimental data. Wilhelmsen *et al.* focused on an extended corresponding state approach, termed SPUNG. SPUNG uses SRK and classical van der Waals mixing rules to scale a reference EOS. Here the MBWR equation [261] for propane was used. The extended corresponding state approach was found to be an excellent compromise between computational speed and accuracy.

Statistical Associating Fluid Theory (SAFT) [262, 263] models are popular for many application, and are also of interest for CCS fluid mixtures. Diamantonis *et al.* [264] compared SAFT and Perturbed-Chain SAFT (PC-SAFT) [265] with cubic EOSs, Redlich-Kwong (RK) [266], SRK and PR, and assessed the vapour-liquid equilibrium modelling capabilities for CO_2 binary and ternary mixtures. For the impurities CH_4, N_2, O_2, SO_2, Ar and H_2S, it was concluded that the SAFT, PC-SAFT, RK, SRK and PR are of comparable accuracy when binary interaction parameters are fitted to experimental data. In this case, there is little benefit of using the more complex and more CPU demanding SAFT and PC-SAFT models over cubic EOSs. In Diamantonis *et al.* [264], H_2S was the only component considered as associating when using SAFT, but no components were treated as associating with PC-SAFT, as this gave the best fit to experimental data. SAFT and PC-SAFT are expected to perform better than cubic EOSs in systems with components which are more strongly associating than H_2S, such as H_2O.

There has also been an effort to combine SAFT-based EOSs with molecular-dynamics simulations [267]. By tuning pure-fluid saturation data to SAFT-γ, force field parameters can be established [268]. These parameters are used in coarse-grained molecular dynamics simulations, allowing for predictions of other properties, like interfacial tension. The model was extended to binary and ternary mixtures by Lobanova *et al.* [269], and good agreement with experimental data was observed for low-pressure data. As for many of the SAFT-based models, the pure-fluid critical points were overestimated, something which also leads to poor correlation in the critical region for mixtures. For CO_2, the critical point is close to the operational area for pipeline transport, making good predictions in this region important. The critical point must therefore be accounted for when tuning parameters used for pure-fluid description with SAFT. Herdes *et al.* [270] have developed a new parameter set for the SAFT-γ model, for CO_2 and other components, using the pure-fluid critical point explicitly. These parameters potentially improve the prediction of CO_2 and CO_2-rich mixtures in the critical region.

Cubic EOSs can predict VLE quite well, but are known for poor density predictions in the liquid phase and in the critical region. Li and Yan [271] also found SRK to predict VLE properties in CO_2 mixtures satisfactorily. In process modelling, the poor density predictions can to some extent be overcome using density corrections. Using a three-parameter EOS might also give improved density predictions [272]. For fast transients in pipelines, where also the speed of sound comes into play, a density correction is not sufficient. In this case, the more detailed modelling approach of EOS-CG/GERG is far superior [39], as these systems have been tuned to both density and speed-of-sound experimental data.

For EOS-CG, the CO_2 and H_2O system has been extended to include hydrate formation [160]. Early work was performed by Chapoy *et al.* [273] measuring and modelling hydrate temperatures in CO_2 and CO_2-rich mixtures. Later, Chapoy *et al.* [274] used the Cubic-Plus-Association [275] method to describe the fluid chemical potentials and the solid solution theory of van der Waals and Platteeuw [276] to describe the hydrate phase appearance in CO_2-rich mixtures. Very few data sets are identified for CO_2-hydrate formation under saturated conditions. Chapoy *et al.* therefore saw a need for more experiments in order to improve the thermodynamic modelling of CO_2-hydrate systems. Duan and Sun [277] modified a van der Waals and Platteeuw model for CO_2-hydrate prediction, and obtained good agreement with experimental data. To describe the fluid phases, an ab initio quantum chemical method was used. The water activity was corrected using the Pitzer model to account for the presence of electrolytes.

Viscosity of pure CO_2 for conditions relevant for transport and capture is described using the correlation of Fenghour and Wakeman [60] to an accuracy below 2 %. In the low-pressure area, the viscosity predictions are much better. This is also confirmed by recent experiments, but Schäfer *et al.* [230] saw room for improvements in the models. Thermal conductivity of pure CO_2 is correlated to a similar degree of accuracy by Vesovic *et al.* [59]. New models which are claimed to better predict e.g. the critical enhancement, i.e. behaviour around the critical point, have been announced for both viscosity and thermal conductivity [235].

Viscosity of mixtures can be described by the extended corresponding-principle-state approach. One such model is TRAPP [278]. TRAPP is also used for thermal conductivity modelling of mixtures [279]. Friction theory is another interesting approach [280] for viscosity predictions. Those models will be able to describe the properties of CO_2-rich mixtures, but this is not documented in the public literature.

3.2. Implementation in fluid-dynamic models

In compressible two-phase flow models, integrated using finite volume methods, the iso-choric-iso-energetic phase-equilibrium problem must be solved, unless modelling simplifications are made. Giljarhus *et al.* [281] described a framework for solving the iso-choric-iso-energetic phase-equilibrium problem using the Span-Wagner [243] EOS. Later, Hammer *et al.* [244] extended the framework by including dry-ice at the sublimation line, using the Gibbs-Duhem equation together with an auxiliary model for the the sublimation line. Solving the EOS directly for single-component CO_2 depressurization has been performed by several authors [20, 244, 281–284].

For multi-component systems, the iso-choric-iso-energetic phase-equilibrium problem becomes more difficult, and an approach like the one presented by Michelsen [285] must be taken. For CO_2 systems, this method has successfully been used for depressurization simulations by Munkejord and Hammer [39]. Due to the time consumption solving the EOS directly during CFD simulations, the use of pre-calculated interpolation tables may be preferable. Elshahomi *et al.* [286] performed simulations of pipeline depressurizations in 2D with Fluent® using thermodynamic look-up tables.

3.3. Flow through restrictions

Simulation models for depressurization of pipes or valves normally require the flow through valves or restrictions to be implemented as a boundary condition. The first stages of the depressurization often involve choked flow, in which the flow velocity is restricted by the effective two-phase speed of sound. The most common way of modelling choked flow is by using a homogeneous equilibrium model (HEM), and assuming steady-state flow, thus obtaining a general Bernoulli formulation, i.e., energy and mass conservation for an isentropically expanding flow. The choking condition is found by equating the velocity of the expanding fluid with the speed of sound. A major problem of this formulation is the singularity of the triple point. The speed of sound becomes zero, as the density can change isentropically without a change in pressure [287, Sec. 2.8.1]. This is illustrated in Figure 3. Figure 3a shows an isentropic depressurization path plotted in density-entropy space. The isentrope starts from a dense liquid state, continues through the liquid-vapour two-phase area before passing through the triple point, ending at atmospheric pressure in the two-phase solid-vapour region. In Figure 3b, the homogeneous mixture speed of sound is plotted against density for the same isentropic path. It is seen that the speed of sound is discontinuous at all phase boundaries.

Martynov *et al.* [288] described a choke model following the HEM principle, handling the triple point by maximizing mass flux as a function of dry-ice mass fraction (x_s) in the triple point. This is equivalent to using the mass flux found at the triple point entry from the liquid-vapour region, ($x_s = 0$). The model was subsequently applied for simulating experiments of CO_2 release from a pipeline [289].

Martynov *et al.* [290] modelled the dry ice in equilibrium with pure CO_2 with an extended Peng-Robinson approach. Three different parameter sets for the cubic EOS were used; one for liquid and vapour, one for the melting line and the properties of dry ice in equilibrium with liquid, and one for the sublimation line and the properties of dry ice in equilibrium with vapour. It is unclear whether this gave consistent properties of dry ice in the triple point. Given the development of a Gibbs free energy function [170], and a Helmholtz free energy function for dry ice [169, 291], cubic equations of state can be coupled directly with the dry-ice models. This has found an application in the modelling of supersonic separation of CO_2 from an exhaust gas [292].

4. Pipeline transport of CO_2

Some challenges related to CO_2 transport in pipes, such as enlarged two-phase region, free water, etc., increase with an increasing amount of impurities in the CO_2. On the other hand, the removal of impurities at the capture plant entails increased investment and operational costs. This constitutes a techno-economic optimization problem which has to be considered for each specific project. Some of the data and models needed to perform detailed studies are yet lacking.

For CO_2-transport pipelines operating in a single-phase state, several quantities, such as pressure drop and pump or compressor work, can be estimated if sufficiently accurate thermodynamic and transport property models are available. It should be noted that CO_2 mixtures from different capture technologies will have different dynamic behaviour in pipelines [13]. An important issue is also the effect of impurities on corrosion [293].

Here we will concentrate on transient two-phase flow effects, which need to be accounted for during design and operation of CO_2-transport pipeline networks.

4.1. Pipe depressurization

The depressurization of a pipe filled with CO_2 constitutes a relatively well defined case, and it is suitable for model validation for several reasons. First, the pressure-wave propagation during depressurization needs to be understood due to its application to fracture-propagation control. Second, transient flow-model formulations have inherent wave-propagation velocities, which ought to agree with the experimental observations, something which is particularly challenging in the two-phase region. Third, models predicting CO_2 dispersing in the atmosphere due to a leak, are dependent on a realistic specification of the outflow state of the pipe.

The thermo- and fluid dynamics of pipe depressurizations are tightly intertwined. As an example, both CO_2-mixture composition and phase slip influence the pressure-propagation velocity [10]. Based on a homogeneous equilibrium pipeline decompression model, Brown *et al.* [294] performed a global sensitivity

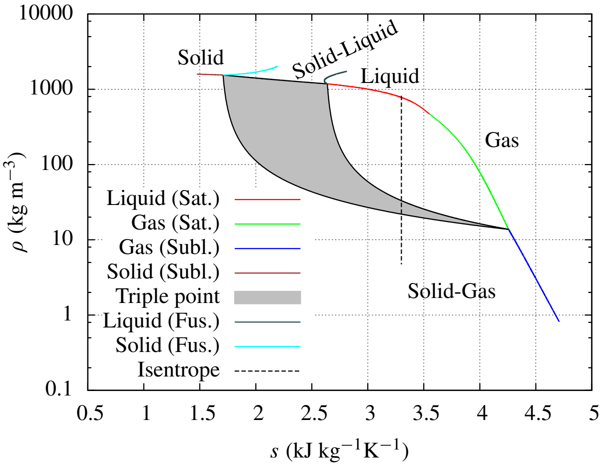

(a) Density-entropy phase map for CO_2.

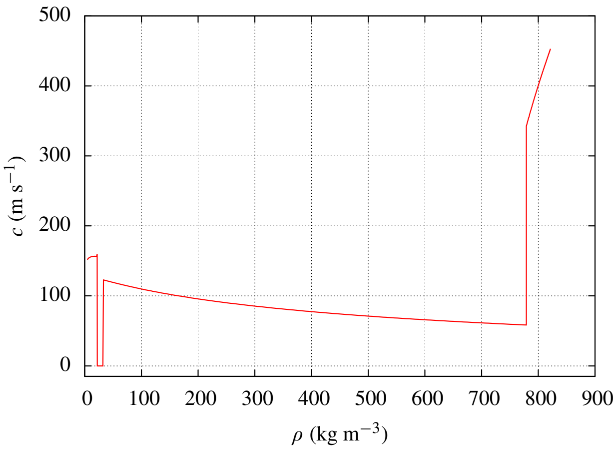

(b) CO_2 equilibrium speed of sound for the isentrope drawn in Figure 3a.

Figure 3: Illustration of the speed of sound along an isentrope (3.3 kJ kg^{-1} K^{-1}) starting in a dense liquid state at 12.5 MPa, 29 °C and passing the triple point. The plots are made using the Span and Wagner [243] EOS together with the dry-ice model of Jäger and Span [170].

analysis of the impact of impurities on CO_2 pipeline failure, and found that the outflow rate is highly sensitive to the composition during the early stages of depressurization, where the effect of the impurities on phase equilibrium has a significant impact on the outflow.

Experimental facilities where pressure and temperature are dynamically recorded along a tube or pipe after one end of the tube is opened to the atmosphere, are commonly referred to as ‘shock tubes’ or ‘expansion tubes’. We prefer the latter designation, since, for such an experimental set-up, the shock will appear outside the tube.

As shown in Table 9, pipe-depressurization data for CO_2 and CO_2-rich mixtures are relatively scarce in the literature. Here we have included studies at least giving pressure as a function of time. In the table, l and d denote tube length and inner diameter, respectively.

de Koeijer *et al.* [37] compared pressure-temperature plots of measured data of a tube depressurization and model predictions using OLGA® [302, 303] employing the Span and Wagner [243] EOS. It was noted that there is room for model improvement.

Clausen *et al.* [298] measured pressure and temperature at the outlets during the depressurization of a 50 km long 24” buried onshore pipeline filled with almost-pure CO_2. The case was also simulated using OLGA®, again employing the Span and Wagner [243] EOS. Good agreement was obtained for the pressure, while some discrepancies were observed for the temperature. Since the pipeline was only instrumented at the outlets, and because of some uncertainty regarding the initial conditions, clear conclusions regarding the reason for the disagreement could not be reached. Clausen *et al.* mentioned several possible reasons: The effect of impurities not being accounted for, incorrectly estimated mass-transfer rate during phase transition, incorrect flow-regime prediction, and uncertainties in the modelling of heat transfer to the surroundings.

Huh *et al.* [304] considered a tube of length 51.96 m and inner diameter 3.86 mm. See also Cho *et al.* [305]. Pressure and temperature were measured during depressurization of pure CO_2 and CO_2-N_2 mixtures with up to 8 % N_2. The experimental data were compared to simulations performed using OLGA®. Rather larger discrepancies were seen than what was observed by Clausen *et al.* [298]. The experiments of Huh *et al.*, were, however, carried out in a much smaller tube and lasting 40 s instead of 10 h.

Tu *et al.* [306] conducted a somewhat different study, in which a 23 m long tube loop with an inner diameter of 3 cm filled with CO_2 was depressurized through nozzles of diameter 1 mm to 5 mm. The main focus was the temperature development in the leakage jet as a function of initial pressure and nozzle size.

Botros *et al.* [296] discussed an experiment designed to measure and study the decompression wave speed, which is the velocity of the rarefaction wave propagating into a pipeline, after the bursting of a disc. A specialized expansion tube with a smooth inner surface was employed, to be more representative for larger industrial pipes. Further details of the experimental facility are given in Botros [307]. The CO_2-CH_4 mixture studied was chosen to be relevant for EOR. The single-phase speed of sound predicted by the GERG-2008 EOS was found to agree very well with the experiment, although the measured plateau pressure was found to be slightly higher than predicted using GERG-2008. This is an important aspect when it comes to designing pipelines to arrest ductile fracture. Based on the present state of knowledge of pipeline ductile fracture of CO_2 mixtures with impurities, Botros *et al.* recommended at least one or two full-scale burst tests for each design case.

Mahgerefteh *et al.* [308] studied measured and predicted decompression-wave speed for CO_2 and CO_2 mixtures where the initial state was gaseous. For the cases tested, it was observed that impurities in the CO_2 stream lowered the phase-transition pressure plateaux. This is the reverse of what is observed for depressurizations from a dense phase, see below.

Cosham *et al.* [299] studied the decompression behaviour of CO_2 and CO_2-rich mixtures in the dense phase. An expansion tube of length 144 m and inner diameter 146 mm was employed. Decompression curves were shown for several experiments, but

Table 9: Experimental data of CO_2-pipe depressurization.

Author	Mixture (mol %)	p (bar)	T (°C)	l (m)	d (mm)	Emphasis
Armstrong and Allason [295]	CO_2	98.4–105.0	6.0–13.7	200	50	p & T, release rate, dispersion
Botros *et al.* [296]	72.6 % CO_2, 27.4 % CH_4	285.7	40.5	42	38.1	Wave prop.
Brown *et al.* [297]	CO_2	153.4	5.2	144	150	p only
Brown *et al.* [297]	CO_2	70	25.2	37	40	p only
Brown *et al.* [283]	CO_2 (99.8 %)	36	1	256	233	p & T
Clausen *et al.* [298]	CO_2 (99.14 %)	81	31	50×10^3	587	p & T, full scale
Cosham *et al.* [299]	CO_2	153.4	5.0	144	146	Wave prop.
Cosham *et al.* [299]	91.03 % CO_2, 1.15 % H_2, 4.00 % N_2, 1.87 % O_2, 1.95 % CH_4	150.5	10.0	144	146	Wave prop.
Drescher *et al.* [300]	89.8 % CO_2, 10.1 % N_2	119.9	19.5	141.9	10	p & T
Drescher *et al.* [300]	80.0 % CO_2, 20.0 % N_2	120.8	19.7	141.9	10	p & T
Drescher *et al.* [300]	70.0 % CO_2, 30.0 % N_2	120.0	17.3	141.9	10	p & T
Jie *et al.* [301]	CO_2	39.1	5.0	144	146	Wave prop., gas

two of them, one with pure CO_2 and one with a multicomponent mixture, were discussed in some more detail, including pressure-time traces. The study was motivated by the fact that an understanding of the decompression behaviour is required in order to predict the steel toughness required to arrest a running-ductile fracture. The authors concluded that dense-phase CO_2 has three opposite trends with respect to gas-phase CO_2: Increasing the initial temperature will increase the required arrest toughness (although this is not always the case for CO_2 mixtures, as discussed by Elshahomi *et al.* [286]); Decreasing the initial pressure will increase the required arrest toughness; The addition of components such as hydrogen, oxygen, nitrogen or methane will increase the required arrest toughness. In the decompression experiments, the measured pressure plateaux were consistently lower than predicted using the GERG-2008 EOS. Further, the measured pressure plateaux increased along the pipe. Cosham *et al.* hypothesized that this may be due to 'delayed nucleation', i.e., thermodynamic non-equilibrium, and suggested that the subject requires further investigation in order to understand it in more detail. The effect of impurities (here N_2) on the saturation pressure, and hence the required arrest toughness, is illustrated in Figure 4a, whereas the influence of initial temperature is illustrated in Figure 4b.

Data from Cosham *et al.* [299] were considered by Jie *et al.* [301], who employed a semi-implicit numerical method to solve the HEM (see Xu *et al.* [309] for more details) with the Peng–Robinson–Stryjek–Vera EOS [310]. It was found that the plateau pressures were overpredicted, particularly for depressurizations starting in the gaseous region. Jie *et al.* [301] hypothesized that this may be due to non-equilibrium effects not being captured by the HEM.

As part of their validation of a homogeneous relaxation model (HRM), Brown *et al.* [297] presented pressure-time traces from two depressurization experiments for pure CO_2. In the HRM, the phase transition is not instantaneous, as in the HEM. Instead, it is modelled using a 'relaxation time'. This gave a slightly lower predicted pressure. The presented pressure plots indicated, in our interpretation, that the relaxation versus full-equilibrium modelling was not the main cause of uncertainty with respect to the experimental data. Since the pressure data were presented on a longer time scale than what is needed to capture pressure waves (10 s), effects of friction and heat transfer to the surroundings could also be relevant.

Brown *et al.* [283] presented pressure and temperature measured at different locations during the first part of the depressurization of a 233 mm inner-diameter pipe. Calculations were performed with a HEM and a two-fluid model (TFM) where the mass-transfer between the phases was modelled based on relaxation of enthalpy. Overall, the TFM gave slightly better results than the HEM, but with an increased advantage for the TFM further away from the outlet. The authors found that during the first 1 s of the depressurization, a relatively short relaxation time of 5×10^{-6} s produced good agreement between computation and experiment. After that, however, a longer relaxation time of 5×10^{-4} s gave better agreement. The physical reason why the flow would need shorter time to reach equilibrium during the first part of the depressurization, seems, however, to remain elusive. Both studies [283, 297] employed the Peng-Robinson EOS.

Drescher *et al.* [300] performed depressurization experiments with three binary CO_2-N_2 mixtures in a tube of length 141.9 m and diameter 10 mm. Pressure and temperature traces were plotted at four different positions, at a time scale including the dry-out point. The cases were modelled using a HEM employing the Friedel [311] friction correlation and a radial heat-transfer model accounting for the heat capacity of the tube. The predicted pressures matched the measured values well, although with a tendency to underprediction. The temperatures were underpredicted to a larger degree. Nevertheless, the calculated dry-out times agreed well with the experiments. In general, computations and experiments matched best near the middle of the tube. The calculated single-phase pressure-propagation velocity was overpredicted when compared to the experiments. This was mainly attributed to the use of the EOS of Peng and Robinson [245].

Munkejord and Hammer [39] expanded the modelling work of Drescher *et al.* [300], adding a two-fluid model (TFM) in which the friction was calculated using the model of Spedding and Hand [312]. Data from Botros *et al.* [296] and Cosham *et al.* [299] were also included in the study. Despite its increased

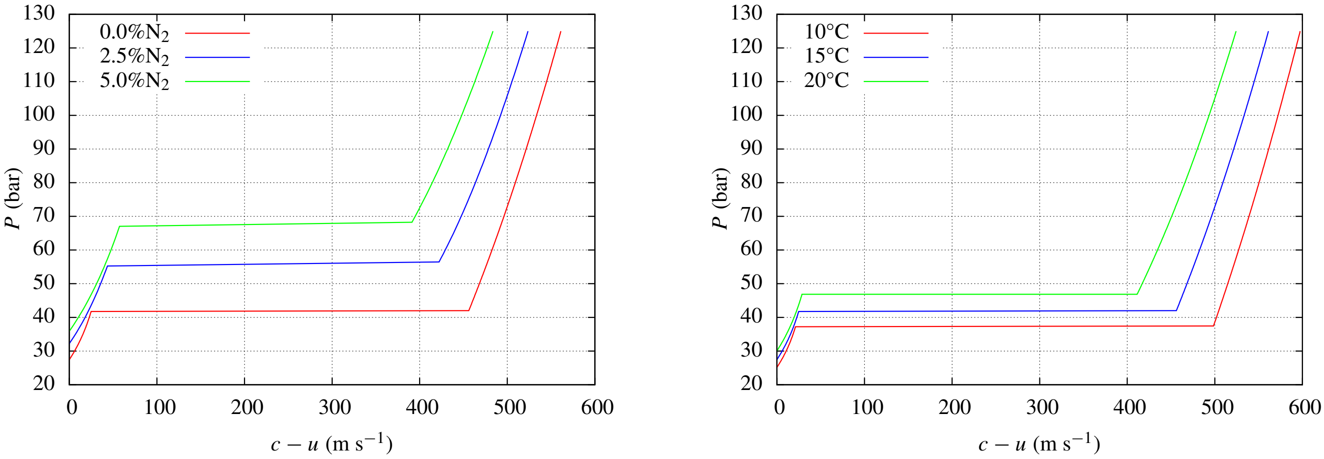

(a) Decompression speed for pure CO_2 and two CO_2-N_2 mixtures. Initial pressure 12.5 MPa and initial temperature 15 °C.

(b) Decompression speed for pure CO_2, at an initial pressure of 12.5 MPa and at three different initial temperatures.

Figure 4: CO_2 decompression-speed dependency of N_2 impurity and initial temperature. The EOS-CG [250, 251] reference EOS is used.

complexity, the TFM could not be said to yield better results than the HEM in general. The authors hypothesized that TFM predictions may be improved with more detailed modelling and experimental studies. The effect of heat-transfer modelling was also studied. For the experiments of Drescher *et al.* [300], the effect of the tube heat capacity was shown to be very large. Not including it yielded far too low temperatures and pressures. Further, for the cases studied, the in-tube heat-transfer correlation of Gungor and Winterton [313] yielded somewhat better results than that of Colburn (see e.g. Bejan [314, Chap. 6]).

The data of Botros *et al.* [296] and Cosham *et al.* [299] were also studied by Elshahomi *et al.* [286], who implemented a 2D HEM employing the GERG-2008 EOS [68]. It seems that for these cases, the main cause of differences between the model of Elshahomi *et al.* [286] and that of Munkejord and Hammer [39], is the different EOS, not the effect of 1D versus 2D.

A technical report by Armstrong and Allason [295], and accompanying documents and data files, have recently been made publicly available. A series of pipe-depressurization experiments with pure CO_2 have been conducted, with full-bore opening and varying restrictions at the outlet. Data were recorded both inside and outside the pipe. We have made an initial study of one of the reported cases, see Section 4.2.

4.2. Depressurization case

To illustrate the modelling of CO_2-pipeline depressurization, we consider experimental data of Test 4 recently published in a technical report by Armstrong and Allason [295] with accompanying data files. See also Table 9. A pipe of length 200 m, inner diameter 51.92 mm and thickness 4.23 mm is filled with pure CO_2 at a pressure of 101.51 bar and a temperature of 4.9 °C. At time $t = 0$ s, a rupture disc is cut by an explosive, and the pipe is opened to the atmosphere, such that a decompression wave travels into the pipe.

To calculate the radial heat transfer, we assume that the pipe is made of stainless steel with a density of 8000 kg m^{-3}, a specific heat capacity of 485 J kg^{-1} K^{-1} and a thermal conductivity of 14 W m^{-1} K^{-1}. We also assume that the surrounding air temperature is equal to the initial temperature.

The case has been calculated using the homogeneous equilibrium model (HEM) described by Munkejord and Hammer [39] employing the Span-Wagner EOS solved by the method of Hammer *et al.* [244]. For the wall-friction, the correlation of Friedel [311] was employed. A spatial grid of 1200 cells and a CFL number of 0.85 were used. Temperature and pressure are plotted as a function of time at position 5 m (close to the outlet) in Figure 5 and at position 195 m (near the closed end) in Figure 6. The sensitivity to the choice of model for the in-tube heat-transfer coefficient is indicated. The legend ‘C’ denotes the simple correlation of Colburn (see e.g. Bejan [314, Chap. 6]), while ‘GW’ denotes the correlation of Gungor and Winterton [313] accounting for saturated flow boiling.

In Figures 5b and 6b, it can be observed that there is good agreement for the pressure, although with a tendency towards underprediction, particularly near the outlet in the first part of the depressurization (Fig. 5b). This is consistent with the results reported by Munkejord and Hammer [39], but in contrast to those of Brown *et al.* [283], where their HEM overpredicted the measured pressure.

For the temperature near the outlet, plotted in Figure 5a, there is also good agreement between computation and experiment. The HEM, both when the Colburn and when the Gungor–Winterton heat-transfer correlation is used, predicts the appearance of solid CO_2 at about 28 s. When all the solid is sublimated, the temperature starts rising. With Gungor–Winterton, this point is predicted at 29 s, which appears to be in very good agreement with the experiment. With Colburn, on the other hand, the predicted minimum temperature appears nearly 3 s late.

The temperature near the closed end of the pipe is plotted in Figure 6a. In the first part of the depressurization, there is good agreement between computation and experiment. After about 30 s, however, the use of the Gungor–Winterton correlation first leads to an underpredicted temperature, and then to a significant

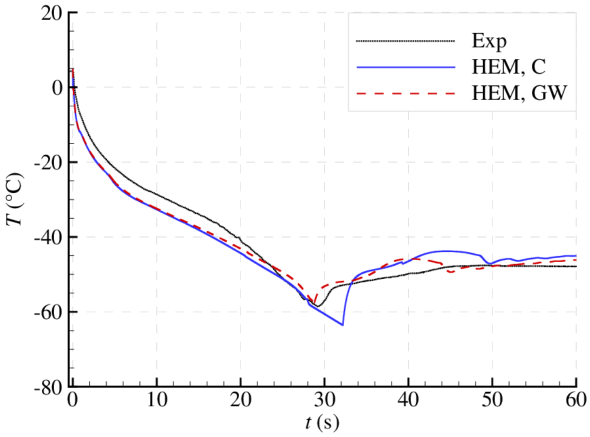

(a) Temperature.

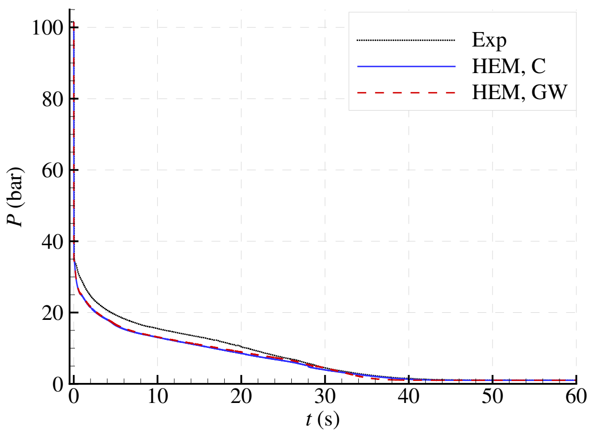

(b) Pressure.

Figure 5: Depressurization case: Comparison of data from experiments (Exp) and homogeneous equilibrium model (HEM) at position 5 m (from the outlet) using Colburn (C) and Gungor–Winterton (GW) heat-transfer coefficient.

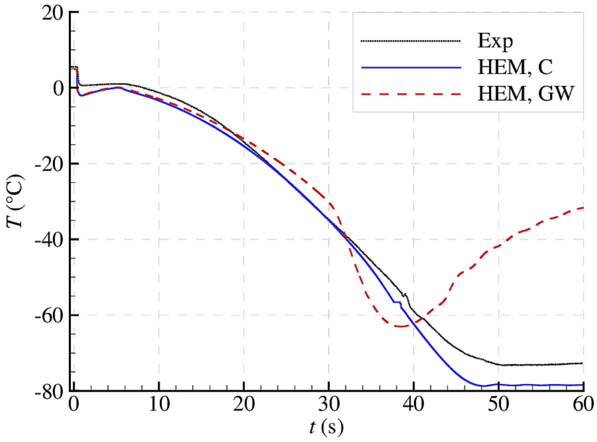

(a) Temperature.

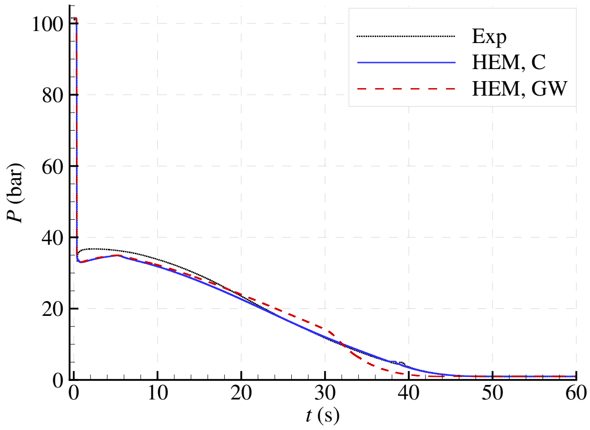

(b) Pressure.

Figure 6: Depressurization case: Comparison of data from experiments (Exp) and homogeneous equilibrium model (HEM) at position 195 m (from the outlet, i.e., near the closed end) close using Colburn (C) and Gungor–Winterton (GW) heat-transfer coefficient.

overprediction. The Colburn correlation gives far better results here: At about 38 s, there is a kink in the calculated temperature due to the triple point. It is interesting to note that there is a corresponding feature in the measured temperature at about the same time. After this, both the calculated and measured temperature flatten out, but the calculated temperature is about 5 K lower than measured. The main reason for the difference between the temperature calculated with Gungor–Winterton and with Colburn, is that with the former, the heat transfer is higher, such that the triple point is avoided and no solid is formed. The measured temperature, on the other hand, gives a clear indication that there is solid CO_2 present in the experiment, since the presence of solid CO_2 keeps the temperature down. Flow models should, therefore, be able to take solid CO_2 into account.

Although there are no flow-regime observations for this case, our interpretation of these results is that close to the outlet, there is a strongly dispersed flow regime, where the no-slip assumption in the HEM is not too far off. Near the closed end of the pipe, however, we expect the flow to have a tendency to stratification, for which the HEM cannot account. In view of this, the results presented in Figure 6 for the Colburn correlation are rather better than what we had expected.

Armstrong and Allason [295] presented more data than what we have analysed here, e.g., depressurizations with orifices and pressure and temperature data taken at different positions. A modelling study considering more of the data set would constitute an interesting continuation of this work.

It should also be mentioned that we have accounted for the heat capacity of the pipe, as described by Munkejord and Hammer [39]. The assumption of adiabatic flow would lead to a significant underprediction of temperatures and pressures, although not as dramatic as for the 10 mm tube considered in Case 3 of Munkejord and Hammer [39]. This illustrates the different challenges in pipe-depressurization modelling: The prediction of quantities both near the outlet and near the closed end, as well as capturing both the initial waves, and the slower phenomena involving heat and mass transport.

As alluded to by e.g. Cosham *et al.* [299], detailed experimental observations of the first instants of pipe depressurizations often seem not to be compatible with an assumption of full thermodynamic equilibrium, with measured pressure plateaux lower than predicted. It appears that flow models accounting for 'delayed nucleation' may be needed to describe this behaviour. This is of importance e.g. for the modelling of running-ductile fracture in CO_2 pipelines, and it constitutes an interesting avenue for further research.

4.3. Running-ductile fracture in CO_2 pipes

For pipelines transporting pressurized fluids, including CO_2, it is important to ensure that a leak do not form a running ductile fracture, and that any running fracture be quickly arrested [315]. For CO_2 pipelines, ensuring running-ductile fracture arrest will often be a restrictive design criterion. It has been found that a pipeline carrying CO_2 in a dense phase will have higher propensity to running-ductile fracture than a pipeline transporting e.g. natural gas [19, 20, 316]. In simple terms, this is due to the high saturation pressure reached from a 'typical' dense-phase state, as well as the very large difference between the single-phase and two-phase decompression speed illustrated in Figure 4. The fracture propagation is governed by a 'race' between the decompression speed in the fluid and the fracture velocity in the steel. If the fracture velocity is faster, the pressure at the crack tip will remain high, and the fracture will propagate. On the other hand, if the decompression speed is faster, then the pressure at the crack tip will fall, and the crack will arrest.

The most common engineering design method against running-ductile fracture, the semi-empirical Battelle two-curve method [317], cannot be directly applied to dense-phase CO_2 pipelines [318]. CO_2 pipelines are commonly equipped with fracture arresters at regular intervals [2, Sec. 4.2.3]. Botros *et al.* [296] recommended at least one to two full-scale burst tests for each design case. Whence there is a need better to understand running-ductile fracture, which is a coupled fluid-structure problem [319].

One hypothesis is that additional insight may be gained by building models representing more of the fluid and structure physics, see Aursand *et al.* [4], Nordhagen *et al.* [320] and the references therein.

Some work has been undertaken in the development of fluid-structure interaction models, in which both the fluid and the steel structure are simulated to predict running-ductile fracture [321–324]. However, there is a need to develop models accounting for the behaviour of CO_2. Aihara and Misawa [316] presented a model in which the pipe radial displacement was determined by a single parameter, and they showed that a fracture in a pipeline with CO_2 and small amounts of impurities will tend to propagate longer than in natural-gas pipelines. Mahgerefteh *et al.* [19] coupled a homogeneous equilibrium model with the fracture-propagation model of Makino *et al.* [325]. Validation cases were presented for natural gas. For a case with CO_2, they found that the fracture-propagating distance increases for increasing pipeline temperature. Further, they found that larger amounts of impurities in the CO_2 increase the fracture-propagation distance.

A coupled fluid-structure methodology to predict fracture arrest for natural gas and hydrogen was discussed by Nordhagen *et al.* [320], Berstad *et al.* [326]. The pipe was modelled in a finite-element framework using shell elements while the fluid was modelled using a one-dimensional finite-volume method. Good agreement with the burst tests of Aihara *et al.* [327] was obtained. In Aursand *et al.* [20], the model was extended to account for CO_2 properties, using a homogeneous equilibrium model. Coupled-model predictions were compared to uncoupled two-curve models by Aursand *et al.* [284]. The coupled fluid-structure model predicted significantly thicker pipe walls to be necessary for fracture arrest than the uncoupled two-curve models, indicating that the latter may not be conservative for CO_2. Experimental validation against medium-scale crack-arrest experiments for CO_2 was performed by Aursand *et al.* [328]. The coupled-model calculations showed that the pressure load on a bursting pipeline filled with CO_2 is significantly more severe than in the case of natural gas. This may be one reason why two-curve methods have been found to fail for CO_2.

For coupled fluid-structure models, the leakage rate will affect the pressure distribution and hence the forces on the pipe walls. As noted by Aursand *et al.* [4], different flow-modelling assumptions will, in turn, affect the leakage rate. The homogeneous-equilibrium assumption will typically yield the lowest leakage rate, and will therefore be conservative in this context. Expressions to be applied at the outflow boundary for a HEM are given e.g. by Munkejord and Hammer [39], Hammer *et al.* [244]. It is foreseeable that similar expressions may be difficult to derive for more complex flow models. It may then instead be worthwhile to apply the same CFD method as the one employed inside the pipe [329].

More work is needed to validate the above-mentioned coupled models against experiments conducted with CO_2. As far as we know, the only published results from full-scale pipeline burst tests with CO_2-rich mixtures are those of Jones *et al.* [318], Cosham *et al.* [330]. In addition, some medium-scale ('West Jefferson') tests have been performed [318, 331]. The scale here relates to the pipeline length; over 100 m for full scale, and around 10 m for medium scale.

Many CO_2-storage sites are expected to be located offshore. It is therefore relevant to consider the integrity of offshore pipelines. Long running fractures may be a smaller challenge offshore, due to the high surrounding pressure. However, should a pipe rupture occur, it is of interest to estimate the leakage rate and the extent of the plume. Herein, it may be necessary to consider the relatively complex phase behaviour of CO_2-water mixtures [160]. Some modelling considerations for subsea pipelines were made by Meleddu *et al.* [332]. The leakage of air through a fracture in a pipeline submerged in shallow water was calculated using a 3D CFD model. Herein, the pipe cross-section was approximated to be of a square shape, and the fracture development was prescribed. The modelling results could be compared to available experimental data, and good agreement was obtained for the pressure development. Further, the model was employed to simulate the full-bore rupture of a deep-water CO_2-transport pipeline, assuming CO_2 and water to be immiscible. An experimental validation of these results would be interesting, but challenging.

4.4. *Wave-propagation, equilibrium and flow modelling*

Pressure-wave propagation is a determining factor in several phenomena of practical interest. During a pipeline depressurization, the flow will often be choked at the outlet, which means that the local flow velocity is equal to the local pressure-propagation velocity (speed of sound). For typical conditions for CO_2 pipelines, the choking will occur for a two-phase state. As is well known, the single-phase speed of sound is a thermodynamic quantity. For a two-phase state, the case is more complicated, since the observable pressure-propagation speed is a function of the flow topology. The simplest model example is the HEM, where the pressure-propagation speed (or mixture speed of sound) is a function of the gas volume fraction. The two-phase mixture speed of sound is typically lower than both the gas and the liquid speed of sound. The difference between the single-phase and the two-phase speed of sound is one of the factors affecting the propagation of running-ductile fracture in pipelines, see the previous section.

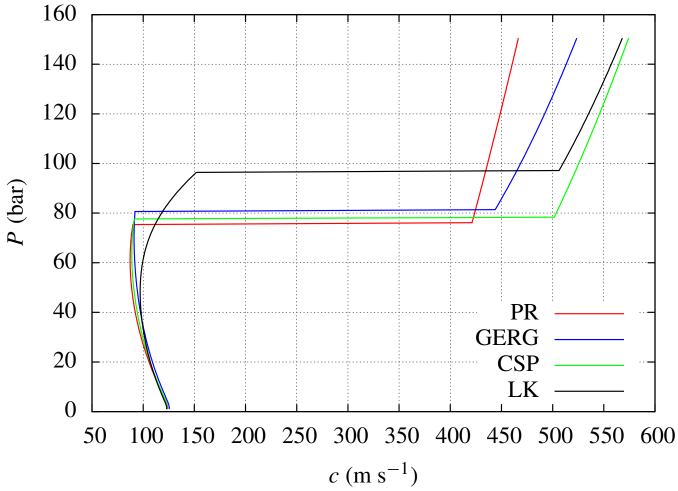

Figure 7: Speed of sound predicted using the Peng-Robinson (PR), GERG-2008 (GERG), a corresponding state approach [260] (CSP) and the Lee-Kesler [259] (LK) equations of state. The CSP method uses Peng-Robinson with van der Waals mixing rules to scale the propane properties calculated using the MBWR32 [247, 261] equation. The CO_2-H_2-N_2-O_2-CH_4 mixture and initial conditions of Cosham *et al.* [299] are employed, see Table 9.

Judging from the pipe-depressurization data presented by Cosham *et al.* [299], it appears that the flow may be in non-equilibrium, and more so during the first instants of the depressurization and close to the outlet. To our knowledge, it remains to develop and validate flow models properly accounting for this effect. This implies that flow models should not only allow slip between the phases, but that they should also accommodate non-equilibrium in one or more of the quantities temperature, chemical potential and pressure. Therefore, despite the good results in many cases (see Section 4.2), the HEM is not expected to be the ideal pipe-depressurization flow model. This is linked to the fact illustrated in Figure 3b, namely, that in the HEM, the speed of sound is discontinuous at the phase boundary, and moreover, it is zero at the triple point [287, Sec. 2.8.1]. This property is not believed to be physical, and it causes difficulties when developing numerical methods and performing simulations.

To illustrate that different models give very different speed-of-sound predictions, particularly above the saturation pressure, four common EOSs have been used to plot the equilibrium speed of sound for the Cosham *et al.* [299] mixture in Figure 7. Only the GERG-2008 model has been tuned to experimental speed-of-sound data, while the other EOSs mostly have been tuned to equilibrium data.

From a modelling viewpoint, a set of physical assumptions leads to a mathematical flow-model formulation. This formulation has inherent wave-propagation velocities. These velocities may be compared to experimental observations and this may serve as validation tests to be performed for the flow model.

Flow models allowing some degree of non-equilibrium are often formulated as *relaxation models*, see Aursand *et al.* [4]. Munkejord [333, 334] studied pressure relaxation in a two-fluid model. With instantaneous relaxation, the relaxation model approached the single-pressure model, but the numerical relaxation procedure introduced considerable numerical smearing.

Flåtten *et al.* [335] derived expressions for the wave velocities a multicomponent flow model with thermal relaxation. Martínez Ferrer *et al.* [336] studied temperature and velocity relaxation for the two-phase case. Flåtten and Lund [337], Lund [338] developed a relaxation-model hierarchy for no-slip two-phase flow models. It was shown that that the relaxed model always has a lower speed of sound than the relaxation model. In other words, the lowest two-phase mixture speed of sound is inherent in the HEM. The relaxation-model hierarchy was expanded by Linga [339], allowing slip between the phases.

Saurel *et al.* [340] considered a no-slip two-phase flow model with temperature and chemical-potential relaxation, albeit infinitely fast, near the gas-liquid interface. Zein *et al.* [341] studied a similar model, but with balance equations for the individual phasic velocities. A validation test was performed against data from a dodecane liquid-vapour shock tube. Rodio and Abgrall [342] presented an approach based on the discrete-equations method aimed at modelling flexibility and computational efficiency. So far, these models [340–342] employed the stiffened-gas EOS [343, 344]. We are not aware that these models have been validated for CO_2. A HEM using the stiffened-gas EOS for each phase was explored by Lund *et al.* [345], but lacked experimental data to compare with.

Most relaxation models so far have assumed the phase transfer either to be 'fast', or to be governed by a prescribed relaxation time. Future models should incorporate physical modelling of the phase transfer accounting for the relevant kinetics. As shown in the initial study by Lund and Aursand [346], statistical rate theory may provide a framework to do so.

Benintendi [347] discussed the effect of non-equilibrium phase transitions for expansions of liquid and supercritical CO_2, focusing on jet-flow characteristics after the stagnation point. Deficiencies of the HEM were described, and the author hypothesized that using a relaxation model (HRM) may improve the prediction of observed CO_2 expansion properties. One simplified steady-state numerical calculation was made along an expansion path, but the model is not directly applicable for handling non-equilibrium phase transitions in a CFD code.

Accounting for delayed homogeneous nucleation appears to be necessary to obtain a correct prediction of pressure and temperature for fast depressurizations. Further, the triple-point singularity resulting from the full equilibrium assumption must be overcome using non-equilibrium thermodynamics.

Tian *et al.* [348] performed a theoretical analysis of the liquid-to-vapour expansion mechanism in CO_2. They considered the critical energy barrier of a bubble nucleus as a function of saturation temperature. Using non-equilibrium thermodynamics, they calculated the entropy production during CO_2 expansion. Zero energy penalty was found at the critical point where the phases are identical. For lower pressures, further down the saturation line, the energy penalty (entropy production) increases.

Heermann *et al.* [349] performed molecular-dynamics simulations to determine the spinodal for pure CO_2. Fast temperature quenching and droplet nucleation relevant for polymer foams produced with a CO_2 blowing agent were of interest. Therefore, only the gas spinodal was studied. The same atomistic approach was used to calculate the saturation properties of CO_2. The results were in qualitatively good agreement with the predictions of the Span-Wagner EOS. However, the liquid density predicted by the molecular-dynamics simulations became too low for increasing temperature. The meta-stable region mapped from the molecular simulation was much smaller than the meta-stable region predicted from the van der Waals EOS and a virial expansion EOS.

4.5. Closure relations for CO_2

Existing flow maps and correlations for oil, natural gas and water in transport pipelines cannot necessarily be expected to be accurate for CO_2-rich mixtures, due to the significantly different thermodynamic and transport properties. Most of the flow maps and pressure-drop measurements and correlations for CO_2 are taken for tubes and channels in the millimetre range, often with heat-exchanger applications in mind, see e.g. [350–353].

Aakenes *et al.* [354] considered experimental data for frictional pressure drop in a 10 mm inner-diameter tube. See also de Koeijer *et al.* [37]. The data were compared to the model of Friedel [311] and that of Cheng *et al.* [353]. Although the latter was developed specifically for CO_2, the former fitted the data better, with a standard deviation of 9.7 %. This is perhaps because of its larger experimental database.

Cho *et al.* [305] performed an experimental study of the two-phase pressure drop for the flow of a CO_2-N_2 mixture in a tube of inner diameter 3.86 mm, using the same facility as in the study of Huh *et al.* [304]. The results were compared to different pressure-drop correlations, and rather large mean absolute errors in excess of 300 % were observed. It remains to provide an explanation for the deviations.

5. Ship transport of CO_2

CO_2 transport with ship is interesting in scenarios involving CO_2 sources close to the coast and offshore storage. Since ships are more flexible than pipelines, ship transport may be preferable for early CCS deployment, where the CO_2 quantities are small.

5.1. Techno-economic considerations

Publicly available work on ship transport of liquid CO_2 started appearing the early 2000s with several patents of Mitsubishi Heavy Industries [355]. Kaarstad and Hustad [356] conducted an overall assessment of ship and pipeline transportation of CO_2 to an oil field in the North Sea. The first detailed technical and economic study on CO_2 ship transport, by Aspelund *et al.* [357], recognized the potential role for shipping in developing the use of CO_2 for EOR, identifying the financial incentive of EOR, giving a value to CO_2. Further benefits of ship transport pointed out by this study were the flexible collection of CO_2 from several low-costs sources, flexibility for delivery to different locations and the relatively low capital expenditure for ship-based transport compared to pipeline transport.

When comparing ship transport to pipeline transport it is intuitive that transport distance is a key parameter. Economic studies show that long transport distance favours ship transport of CO_2 over pipe transport [358]. Technical-economic studies on ship transport of CO_2 were performed by Roussanaly *et al.* [359] who compared costs for CO_2 transport by ship or by onshore pipeline between Le Havre and a hub at Rotterdam, with the concept of onward transport for storage or EOR from there. In this specific case it was concluded that shipping cost around 10 % more. Skagestad *et al.* [360] pointed out that the liquefaction and operational costs are the main cost drivers for the ship, and capital investment cost is the main driver for pipeline transport.

Aspelund *et al.* [357] assumed pure CO_2 transported in a state close to the triple point, e.g. 6.5 bar and the corresponding saturation temperature, approximately −52 °C. These conditions are used in most later studies on CO_2 ship transport. However, a study by Nam *et al.* [361] optimized conditions over an entire transport chain, including pipeline sections and intermediate storage, and concluded on global optimum conditions of 10 bar and −39 °C.

Vermeulen [358] published a knowledge-sharing report considering the entire chain of liquid CO_2 transport by ship. Several types of infrastructure for offshore offloading system were considered, and well simulations were preformed to characterize the temperature dynamics stemming from the batchwise injection of CO_2. The hydrate temperature in the reservoir was identified as a defining criterion for the injection, requiring heat exchangers for conditioning at the injection site. The shipping solution considered was a modified liquefied petroleum gas (LPG) carrier with a cargo capacity of 30 000 m^3. The report encompassed most aspects of CO_2 transport by ship, but did not address impurities of CO_2, determined by the specification of the captured CO_2 and the liquefaction process.

Omata [362] considered LPG carriers and transport of saturated liquid at −10 °C (2.65 MPa to 2.8 MPa). The report covers the technical and economic feasibility of a concept for CO_2 transport using a carrier ship with injection equipment on board, to deliver directly to a subsea injection wellhead. It argues that in regions, such as Eastern Asia, where bulk resources are frequently traded long distances internationally by sea, it makes sense to consider the same for CO_2 transport.

Brownsort [363] summarized literature regarding CO_2 ship transport with the main purpose of EOR. It was pointed out that many publications do not debate liquefaction process options, focusing instead on a single process, which may be selected from corporate experience, but without clear justification.

The general conclusion from the CO_2 ship-transport studies are that this is technically feasible, albeit at a generally higher unit price than transport by pipeline. As mentioned earlier, this depends on the transport distance. Longer transport distance favours ship transport. However, there are still open technical questions, e.g., regarding the liquefaction process, the injection system and the well integrity as well as unloading time.

5.2. Vessel depressurization

The study of vessel depressurizations appears to be relevant for ship-transport of CO_2 and to other parts of the CO_2 chain where vessels are employed. Even though during normal unloading, the pressure in the storage vessels will be maintained by gas injection, accidental and uncontrolled depressurization might happen. Experimental data from vessel depressurizations could also be useful for model verification. This subject has received limited attention so far.

The blowdown of CO_2 from initially supercritical conditions was studied by Eggers and Green [364], Gebbeken and Eggers [365], motivated by the use of CO_2 in food-processing technology. The data may serve as validation cases for models involving CO_2 with phase transition induced by depressurization and heat transfer. Fredenhagen and Eggers [366] extended the study to CO_2-N_2 mixtures and presented a model based on local thermodynamic equilibrium and a drift-flux phase slip. The data of Gebbeken and Eggers [365] were considered in the modelling study of Zhang *et al.* [367] aimed at the safety analysis of supercritical water-cooled nuclear reactors.

Han *et al.* [368] studied the temperature and pressure development in 4.75 mm tubes used for the controlled depressurization of a CO_2 vessel.

Vree *et al.* [369] studied the depressurization of pure CO_2 in a tube of inner diameter 50 mm and length 30 m wound up in a coil of diameter 1.94 m and height 1.25 m. We expect the results to lie somewhere between those of vessels and straight tubes. The effect of nozzle sizes between 3 mm to 12 mm was investigated, as was the effect of depressurizing from the lower or upper end of the coil. The coldest temperature was observed for depressurization from the upper end of the coil.

5.3. Boiling liquid expanding vapour explosion

Boiling liquid expanding vapour explosion (BLEVE) may occur in storage and transportation of high-pressure liquefied CO_2. If the containing pipe or vessel ruptures, violent boiling of superheated CO_2 might cause a destructive shock wave. In Worms, Germany, a catastrophic failure of a liquid CO_2 storage vessel resulted in three fatalities, additionally eight people injured and significant material damage to a production facility [370]. A comprehensive review of the BLEVE phenomenon was presented by Abbasi and Abbasi [371].

Bjerketvedt *et al.* [372] conducted small-scale experiments with CO_2 BLEVE. By placing dry ice in a plastic container and applying heat, a phase change and pressure increase was induced. The pressure was increased until the tube ruptured, and pressure waves were measured at different distances from the container. A need to understand the boiling mechanisms of metastable CO_2 was identified. Bjerketvedt *et al.* concluded that there is a need for EOS validation and large-scale experiments to develop and validate CFD codes to perform risk analysis. Later, the same group performed rapid depressurization experiments of liquid CO_2 in a vertical shock tube [373]. With the aid of a high-speed camera, the evaporation wave propagating into the liquid was studied. A near-constant velocity of $20\,\mathrm{m\,s^{-1}}$ to $30\,\mathrm{m\,s^{-1}}$ of the liquid-vapour front was reported. The initial pressures were 3.5 and 5.5 MPa. Due to missing temperature and pressure measurements, the authors could not conclude regarding the thermodynamic path of the fluid.

van der Voort *et al.* [374] measured blast waves after fracturing 40 l liquid CO_2 bottles. Two cutting charges installed on opposite sides of the bottles were used in order to induce a fast and complete rupture of the CO_2 bottle. Simulations employing the Euler equations in 1D and 2D using simplified thermodynamics were compared with the measured blast wave, to give a qualitative fit. In order to give more realistic predictions of the BLEVE blast wave, explicit modelling of phase transition and proper fluid property models are required. The measured blast wave was disturbed by the initial detonation of the cutting charges and reflection from the walls of the test bunker.

Building on these experiments, van der Voort *et al.* [375] conducted 12 experiments using 40 l liquid CO_2 bottles to test the temperature dependence of the BLEVE problem. The temperature range was from −25.4 °C to 21.3 °C. The motivation was to evaluate the risk of BLEVE occurring below what the authors referred to as the homogeneous nucleation temperature. With data from a reference experiment with an empty bottle, some of the measurement disturbance from the initial detonation of the cutting charges could be removed. The conclusion regarding the homogeneous nucleation temperature remains, however, unclear.

5.4. Flow in wells

Whether the CO_2 has been transported by pipeline, ship, or other means, it will have to be injected into a reservoir through a well. Numerical models to perform calculations of transient scenarios in wells will have many similarities with those for pipelines.

For CO_2 injection into depleted gas reservoirs, or into relatively shallow reservoirs, pressures will be relatively low, such that CO_2 phase change will be more likely than what it usually is for EOR [376].

Many of the existing well-flow models for CO_2 are aimed at capturing essentially steady-state solutions, e.g. [377, 378], or slow transients. Cronshaw and Bolling [379] developed a finite-difference model for the flow of single- or two-phase CO_2 in wellbores, accounting for conduction to the surroundings. A semi-implicit integration procedure was employed. The thermophysical properties were taken from look-up tables. The solubility of water in liquid CO_2 and that of CO_2 in liquid water were neglected. The flow transients were assumed to be sufficiently slow, so that kinetic-energy changes across control volumes could also be neglected.

Pan *et al.* [380] developed a transient drift-flux model (DFM) for two-phase CO_2-brine mixtures to calculate leakages through the wellbore. A DFM was also studied by Lu and Connell [381, 382]. The Peng and Robinson [245] EOS was employed, with the assumption of full thermodynamic equilibrium. The computations included the effect of transient boundary conditions at the well inlet.

Ruan *et al.* [383] employed Fluent® to study the effect of water convection in the annulus surrounding the well assuming 2D axisymmetry. Musivand Arzanfudi and Al-Khoury [384] considered the leakage of CO_2 through an air-filled abandoned wellbore using a mixed finite-element discretization scheme. A main aim was to achieve a high numerical efficiency.

de Koeijer *et al.* [385] identified a need for experiments on shut-ins and depressurization in CO_2 injection wells. In order to characterize the reservoir, shut-in and depressurization operations are performed on the well. Especially the interaction between CO_2 and brine in the reservoir is of interest. A new infrastructure, drilling a 200 m to 250 m deep well, was suggested.

For safety, and to maintain the purpose of CCS, it is essential to ensure the integrity of CO_2 wells. Thermal cycling is one factor which can lead to debonding at the casing-cement or cement-rock interface. CO_2 injection may impose lower temperatures and stronger temperature variations on wells than what is done for oil and gas production. Therefore, it is of great interest to develop modelling tools which can assess various designs and operational procedures. Lund *et al.* [386] developed a radial heat-transfer model designed to account for the discontinuous thermal properties at the casing-cement and cement-rock interface. Good agreement with laboratory experiments was obtained. Future work should include the assessment of radial asymmetry, and the coupling to well-flow and reservoir models.

6. Conclusions

Although CO_2 is transported in various ways today, the amount required for full-scale CCS implementation motivates the search for solutions being as safe and reliable as required and as efficient as possible. To do this, simulation tools handling the transient flow of single- and multiphase CO_2 and CO_2-rich mixtures inside, and out of, pipes and vessels are needed to perform calculations relevant for design, operation and safety. Today's models are in need of improvement with respect to both fluid flow and thermophysical properties.

The risk associated with CO_2 pipelines has been evaluated to be very low, but the fracture propensity must be successfully mitigated. Today's semi-empirical fracture-propagation models cannot be applied to dense-phase CO_2 pipelines, and it has been recommended to perform at least two full-scale burst tests for each design case. The development of coupled fluid-structure fracture-propagation control models may lead to a better predictive capability.

Two-phase flow conditions can be expected to occur during various transient events even for systems designed to operate in the single-phase state. Such events can be varying CO_2 supply, start-up, shut-in or depressurization. Therefore, there is a need to develop validated simulation tools able to accurately predict these situations. Existing two-phase flow modelling tools can be expected to have moderate accuracy due to the limited data for CO_2 flow.

Depressurization experiments of pipes and tubes constitute one type of input needed for the development of fracture-propagation models, and two-phase flow models in general. It appears that two-phase flow models aiming to accurately describe rapid depressurizations need to take non-equilibrium effects into account. Among the different two-phase flow model formulations available today, there is not a 'generally preferred' one. Nevertheless, the relatively simple homogeneous equilibrium model has yielded good results in several cases. For depressurizations down to atmospheric conditions, models will, in many cases, need to take the formation of dry ice into account.

This was shown in our case study considering expansion-tube experimental data.

Regarding depressurizations of tubes, the shorter the time scale, the better the description provided by pure depressurization fluid dynamics and thermodynamics. For longer times, effects from friction, flow topology and heat transfer enter into play, rendering the interpretation of both experimental and modelling results complex.

The depressurization of vessels have, in many respects, a simpler flow configuration than the depressurization of pipes. Therefore, such data should be useful for validation of thermophysical and heat-transfer models relevant for CO_2 transport.

Regarding ship-transport of CO_2, one of the main challenges appears to be the optimal chain design. It has to include the liquefaction, conditioning and possible processing at the injection site. Issues like well integrity and the response of the CO_2 reservoir should also be considered. This will require good knowledge of the relevant CO_2-rich fluid properties, as well as flow in the well, the interaction of brine and CO_2, etc. There also seems to be a need for a better understanding of the safety aspects of transporting CO_2 in large vessels, such as the possible occurrence of boiling liquid expanding vapour explosion (BLEVE).

Removing a large portion of impurities produced by CO_2 capture processes could have a high cost. Hence the effect of impurities in CO_2-rich mixtures, which could be different in CCS than in the current US CO_2-transportation pipeline systems, must be known for cost and energy optimization. Even if strict purification standards are enforced, the impact of impurities will still have to be predicted in order to design efficient conditioning processes or to understand CO_2 injection processes or EOR or storage reservoir behaviour. For some properties, relatively accurate equilibrium models exist for pure CO_2. There are also thermodynamic models addressing the impact of impurities, but mixture models for transport properties are less developed.

Fiscal metering will be needed in order to facilitate government control and transactions in a future CCS market and the lack of accurate property models could have large cost impacts.

Currently, the best property models are empirical in nature, and hence cannot be more accurate than the experimental data to which they are fitted. In order to model mixtures, complete binary mixture data sets are desired, with ranges in temperature, pressure, and composition beyond what are expected for the given application. In the current work, the data situation of some important fluid equilibrium properties for CO_2-rich mixtures has been surveyed, combining and extending a number of more specialized reviews in the literature. Data for phase behaviour, density, speed of sound, viscosity, and thermal conductivity have been investigated, primarily for binary mixtures between CO_2 and 17 other components. With regard to density and vapour-liquid equilibria (VLE), the data situation for binary mixtures between CO_2 and water and the most common components in natural gas, like methane and nitrogen, appears to be satisfactory. For other relevant impurities, like for instance O_2, there are large holes in the data sets for density and VLE. For other binary systems, like for instance CO_2-COS and CO_2-NO, neither VLE nor density data have been found.

In addition to VLE, phase equilibria involving more than one liquid phase (VLLE) and equilibria involving solids / hydrates have been investigated. In general, there are very little experimental data for such phase equilibria, as well as for speed of sound, viscosity, and thermal conductivity. In many cases, there is either no data or only a single data set available per binary mixture system and phase even for the most common impurities, covering at best only a small part of the region of interest in terms of temperature, pressure, or composition. With regard to thermal conductivity, even the most reputable current model for pure CO_2 is still not based on data in the high-temperature zero density region or the important liquid phase.

Acknowledgements

This publication has been produced with support from the BIGCCS Centre, performed under the Norwegian research programme Centres for Environment-friendly Energy Research (FME), and from the CO_2Mix project in the CLIMIT research programme. The authors acknowledge the following partners for their contributions: Engie, Gassco, Shell, Statoil, TOTAL, and the Research Council of Norway (193816 and 200005).

The authors would like to thank Dr. Johannes Gernert and Professor Roland Span for sharing the literature database on which EOS-CG is based [27].

References

[1] IEA. *Energy Technology Perspectives*. 2015. ISBN 978-92-64-23342-3. doi:10.1787/energy_tech-2015-en.

[2] Metz B, Davidson O, de Coninck H, Loos M, Meyer L, editors. *Intergovernmental Panel on Climate Change (IPCC) Special Report on Carbon Dioxide Capture and Storage*. Cambridge University Press, 2005. ISBN 978-0-521-68551-1.

[3] Zhang ZX, Wang GX, Massarotto P, Rudolph V. Optimization of pipeline transport for CO_2 sequestration. *Energy Convers Manage* 2006; 47(6):702–715. doi:10.1016/j.enconman.2005.06.001.

[4] Aursand P, Hammer M, Munkejord ST, Wilhelmsen Ø. Pipeline transport of CO_2 mixtures: Models for transient simulation. *Int J Greenh Gas Con* 2013; 15:174–185. doi:10.1016/j.ijggc.2013.02.012.

[5] de Visser E, Hendriks C, Barrio M, Mølnvik MJ, de Koeijer G, Liljemark S, Le Gallo Y. Dynamis CO_2 quality recommendations. *Int J Greenh Gas Con* 2008; 2(4):478–484. doi:10.1016/j.ijggc.2008.04.006.

[6] NETL. CO_2 impurity design parameters. Tech. Rep. DOE/NETL-341-011212, National Energy Technology Laboratory, USA, 2013.

[7] Wetenhall B, Aghajani H, Chalmers H, Benson SD, Ferrari MC, Li J, Race JM, Singh P, Davison J. Impact of CO_2 impurity on CO_2 compression, liquefaction and transportation. In: Dixon T, Herzog H, Twinning S, editors, *GHGT-12 – 12th International Conference on Greenhouse Gas Control Technologies*. University of Texas at Austin / IEAGHGT, Austin, Texas, USA: Energy Procedia, vol. 63, 2014; pp. 2764–2778. doi:10.1016/j.egypro.2014.11.299.

[8] Li H, Jakobsen JP, Wilhelmsen Ø, Yan J. PVTxy properties of CO_2 mixtures relevant for CO_2 capture, transport and storage: Review of available experimental data and theoretical models. *Appl Energ* 2011; 88(11):3567–3579. doi:10.1016/j.apenergy.2011.03.052.

[9] Li H, Wilhelmsen Ø, Lv Y, Wang W, Yan J. Viscosity, thermal conductivity and diffusion coefficients of CO_2 mixtures: Review of experimental data and theoretical models. *Int J Greenh Gas Con* 2011; 5(5):1119–1139. doi:10.1016/j.ijggc.2011.07.009.

[10] Munkejord ST, Jakobsen JP, Austegard A, Mølnvik MJ. Thermo- and fluid-dynamical modelling of two-phase multi-component carbon dioxide mixtures. *Int J Greenh Gas Con* 2010; 4(4):589–596. doi:10.1016/j.ijggc.2010.02.003.

[11] US DOE. *Interagency Task Force on Carbon Capture and Storage*. Washington, DC, USA, 2010.

[12] Verma MK. Fundamentals of carbon dioxide-enhanced oil recovery (CO_2-EOR)—a supporting document of the assessment methodology for hydrocarbon recovery using CO_2-EOR associated with carbon sequestration. Open-File Report 2015-1071, U.S. Geological Survey, Reston, Virginia, USA, 2015. doi:10.3133/ofr20151071.

[13] Chaczykowski M, Osiadacz AJ. Dynamic simulation of pipelines containing dense phase/supercritical CO_2-rich mixtures for carbon capture and storage. *Int J Greenh Gas Con* 2012; 9:446–456. doi:10.1016/j.ijggc.2012.05.007.

[14] Uilhoorn FE. Evaluating the risk of hydrate formation in CO_2 pipelines under transient operation. *Int J Greenh Gas Con* 2013; 14:177–182. doi:10.1016/j.ijggc.2013.01.021.

[15] Klinkby L, Nielsen CM, Krogh E, Smith IE, Palm B, Bernstone C. Simulating rapidly fluctuating CO_2 flow into the Vedsted CO_2 pipeline, injection well and reservoir. In: Gale J, Hendriks C, Turkenberg W, editors, *GHGT-10 – 10th International Conference on Greenhouse Gas Control Technologies*. IEAGHGT, Amsterdam, The Netherlands: Energy Procedia vol. 4, 2011; pp. 4291–4298. doi:10.1016/j.egypro.2011.02.379.

[16] Liljemark S, Arvidsson K, McCann MTP, Tummescheit H, Velut S. Dynamic simulation of a carbon dioxide transfer pipeline for analysis of normal operation and failure modes. In: Gale J, Hendriks C, Turkenberg W, editors, *GHGT-10 – 10th International Conference on Greenhouse Gas Control Technologies*. IEAGHGT, Amsterdam, The Netherlands: Energy Procedia vol. 4, 2011; pp. 3040–3047. doi:10.1016/j.egypro.2011.02.215.

[17] Munkejord ST, Bernstone C, Clausen S, de Koeijer G, Mølnvik MJ. Combining thermodynamic and fluid flow modelling for CO_2 flow assurance. In: Dixon T, Yamaji K, editors, *GHGT-11 – 11th International Conference on Greenhouse Gas Control Technologies*. RITE / IEAGHGT, Kyoto, Japan: Energy Procedia, vol. 37, 2013; pp. 2904–2913. doi:10.1016/j.egypro.2013.06.176.

[18] Hetland J, Barnett J, Read A, Zapatero J, Veltin J. CO_2 transport systems development: Status of three large European CCS demonstration projects with EEPR funding. In: Dixon T, Herzog H, Twinning S, editors, *GHGT-12 – 12th International Conference on Greenhouse Gas Control Technologies*. University of Texas at Austin / IEAGHGT, Austin, Texas, USA: Energy Procedia, vol. 63, 2014; pp. 2458–2466. doi:10.1016/j.egypro.2014.11.268.

[19] Mahgerefteh H, Brown S, Denton G. Modelling the impact of stream impurities on ductile fractures in CO_2 pipelines. *Chem Eng Sci* 2012; 74:200–210. doi:10.1016/j.ces.2012.02.037.

[20] Aursand E, Aursand P, Berstad T, Dørum C, Hammer M, Munkejord ST, Nordhagen HO. CO_2 pipeline integrity: A coupled fluid-structure model using a reference equation of state for CO_2. In: Dixon T, Yamaji K, editors, *GHGT-11 – 11th International Conference on Greenhouse Gas Control Technologies*. RITE / IEAGHGT, Kyoto, Japan: Energy Procedia, vol. 37, 2013; pp. 3113–3122. doi:10.1016/j.egypro.2013.06.197.

[21] Mazzoldi A, Hill T, Colls JJ. Assessing the risk for CO_2 transportation within CCS projects, CFD modelling. *Int J Greenh Gas Con* 2011; 5(4):816–825. doi:10.1016/j.ijggc.2011.01.001.

[22] Witlox HWM, Harper M, Oke A, Stene J. Validation of discharge and atmospheric dispersion for unpressurised and pressurised carbon dioxide releases. *Process Saf Environ* 2014; 92(1):3–16. doi:10.1016/j.psep.2013.08.002.

[23] Woolley RM, Fairweather M, Wareing CJ, Proust C, Hebrard J, Jamois D, Narasimhamurthy VD, Storvik IE, Skjold T, Falle SAEG, Brown S, Mahgerefteh H, Martynov S, Gant SE, Tsangaris DM, Economou IG, Boulougouris GC, Diamantonis NI. An integrated, multi-scale modelling approach for the simulation of multiphase dispersion from accidental CO_2 pipeline releases in realistic terrain. *Int J Greenh Gas Con* 2014; 27:221–238. doi:10.1016/j.ijggc.2014.06.001.

[24] Jamois D, Proust C, Hebrard J. Hardware and instrumentation to investigate massive releases of dense phase CO_2. *Can J Chem Eng* 2015; 93(2):234–240. doi:10.1002/cjce.22120.

[25] Koornneef J, Spruijt M, Molag M, Ramírez A, Turkenburg W, Faaij A. Quantitative risk assessment of CO_2 transport by pipelines – A review of uncertainties and their impacts. *J Hazard Mater* 2010; 177(1-3):12–27. doi:10.1016/j.jhazmat.2009.11.068.

[26] Duncan IJ, Wang H. Estimating the likelihood of pipeline failure in CO_2 transmission pipelines: New insights on risks of carbon capture and storage. *Int J Greenh Gas Con* 2014; 21:49–60. doi:10.1016/j.ijggc.2013.11.005.

[27] Gernert J, Span R. EOS-CG: A Helmholtz energy mixture model for humid gases and CCS mixtures. *J Chem Thermodyn* 2016; 93:274–293. doi:10.1016/j.jct.2015.05.015.

[28] Clausen S, Munkejord ST. Depressurization of CO_2 – a numerical benchmark study. In: Røkke NA, Hägg MB, Mazzetti MJ, editors, *6th Trondheim Conference on CO_2 Capture, Transport and Storage (TCCS-6)*. BIGCCS / SINTEF / NTNU, Trondheim, Norway: Energy Procedia vol. 23, 2012; pp. 266–273. doi:10.1016/j.egypro.2012.06.021.

[29] Morin A, Aursand PK, Flåtten T, Munkejord ST. Numerical resolution of CO_2 transport dynamics. In: *SIAM Conference on Mathematics for Industry: Challenges and Frontiers (MI09)*. San Francisco, CA, USA, 2009; .

[30] Ackiewicz M, *et al*. Technical barriers and R&D opportunities for offshore, sub-seabed geologic storage of carbon dioxide. Tech. rep., Carbon Sequestration Leadership Forum (CLSF), 2015. Offshore Storage Technologies Task Force. URL `http://www.cslforum.org/documents/OffshoreStorageTaskForce_FinalCombinedReport.pdf`

[31] Tan Y, Nookuea W, Li H, Thorin E, Zhao L, Yan J. Property impacts on performance of CO_2 pipeline transport. In: Yan J, Shamim T, Chou SK, Li H, editors, *The 7th International Conference on Applied Energy (ICAE2015)*. Mälardalen University / Masdar Institute, Abu Dhabi, United Arab Emirates: Energy Procedia vol. 75, 2015; pp. 2261–2267. doi:10.1016/j.egypro.2015.07.411.

[32] Spycher N, Pruess K, Ennis-King J. CO_2-H_2O mixtures in the geological sequestration of CO_2. I. Assessment and calculation of mutual solubilities from 12 to 100°C and up to 600 bar. *Geochim Cosmochim Ac* 2003; 67(16):3015–3031. doi:10.1016/S0016-7037(03)00273-4.

[33] Austegard A, Solbraa E, De Koeijer G, Mølnvik MJ. Thermodynamic models for calculating mutual solubilities in H_2O-CO_2-CH_4 mixtures. *Chem Eng Res Des* 2006; 84(A9):781–794. doi:10.1205/cherd05023.

[34] Ahmad M, Gersen S. Water solubility in CO_2 mixtures: Experimental and modelling investigation. In: Dixon T, Herzog H, Twinning S, editors, *GHGT-12 – 12th International Conference on Greenhouse Gas Control Technologies*. University of Texas at Austin / IEAGHGT, Austin, Texas, USA: Energy Procedia, vol. 63, 2014; pp. 2402–2411. doi:10.1016/j.egypro.2014.11.263.

[35] Xiang Y, Wang Z, Yang X, Li Z, Ni W. The upper limit of moisture content for supercritical CO_2 pipeline transport. *J Supercrit Fluid* 2012; 67:14–21. doi:10.1016/j.supflu.2012.03.006.

[36] Halseid M, Dugstad A, Morland B. Corrosion and bulk phase reactions in CO_2 transport pipelines with impurities: Review of recent published studies. In: Dixon T, Herzog H, Twinning S, editors, *GHGT-12 – 12th International Conference on Greenhouse Gas Control Technologies*. University of Texas at Austin / IEAGHGT, Austin, Texas, USA: Energy Procedia, vol. 63, 2014; pp. 2557–2569. doi:10.1016/j.egypro.2014.11.278.

[37] de Koeijer G, Borch JH, Drescher M, Li H, Wilhelmsen Ø, Jakobsen J. CO_2 transport – depressurization, heat transfer and impurities. In: Gale J, Hendriks C, Turkenberg W, editors, *GHGT-10 – 10th International Conference on Greenhouse Gas Control Technologies*. IEAGHGT, Amsterdam, The Netherlands: Energy Procedia vol. 4, 2011; pp. 3008–3015. doi:10.1016/j.egypro.2011.02.211.

[38] Song KY, Kobayashi R. The water content in a CO_2-rich gas mixture containing 5.31 mol % methane along the three-phase and supercritical conditions. *J Chem Eng Data* 1990; 35(3):320–322. doi:10.1021/je00061a026.

[39] Munkejord ST, Hammer M. Depressurization of CO_2-rich mixtures in pipes: Two-phase flow modelling and comparison with experiments. *Int J Greenh Gas Con* 2015; 37:398–411. doi:10.1016/j.ijggc.2015.03.029.

[40] Løvseth SW, Skaugen G, Stang HGJ, Jakobsen JP, Wilhelmsen Ø, Span R, Wegge R. CO_2mix project: Experimental determination of thermo physical properties of CO_2-rich mixtures. In: Dixon T, Yamaji K, editors, *GHGT-11 – 11th International Conference on Greenhouse Gas Control Technologies*. RITE / IEAGHGT, Kyoto, Japan: Energy Procedia vol. 37, 2013; pp. 2888–2896. doi:10.1016/j.egypro.2013.06.174.

[41] Noothout P, Wiersma F, Hurtado O, Roelofsen P, Macdonald D. CO_2 pipeline infrastructure. Report, Global CCS Institute, IEA Greenhouse Gas R&D Programme (IEAGHG), 2014. Online pipeline database: http://www.ieaghg.org/ccs-resources/co2-pipelines.

[42] Hansen H, Eiken O, Aasum TO. The path of a carbon dioxide molecule from a gas-condensate reservoir, through the amine plant and back down

into the subsurface for storage. case study: The Sleipner area, South Viking Graben, Norwegian North Sea. In: *Offshore Europe*. SPE-96742-MS, Society of Petroleum Engineers. ISBN 978-1-55563-993-8, 2005; doi:10.2118/96742-MS.

[43] Buit L, Ahmad M, Mallon W, Hage F, Zhang X, Koenen M. Standards for CO_2. Report, Towards a transport infrastructure for large-scale CCS in Europe (CO2Europipe), 2011. URL `http://www.co2europipe.eu/`.

[44] Matuszewski M, Woods M. CO_2 impurity design parameters. Report, National Energy Technology Laboratory (NETL), 2012. URL `http://www.netl.doe.gov//research/energy-analysis/publications/`.

[45] Neades S, Davis L, Singh P, Kemper J, Basava-Reddi L, Haines M. UK feed studies 2011 - a summary. Tech. Rep. 2013/12, IEA Greenhouse Gas R&D Programme (IEAGHG), Stoke Orchard, Cheltenham, United Kingdom, 2013.

[46] Høydalsvik H. Gassnova CO_2 capture, transport and storage - Mongstad CO_2 product specification. Report, Gassnova, 2013.

[47] Hiza MJ, Kidnay AJ, Miller RC. A bibliography of important equilibria properties for fluid mixtures of cryogenic interest. Tech. rep., National Bureau of Standards, 1974.

[48] McGlashan ML, Hicks CP. *A bibliography of thermodynamic quantities for binary fluid mixtures*, *Chemical Thermodynamics*, vol. 2, pp. 275–538. Royal Society of Chemistry, 1978; doi:10.1039/9781847555830-00275.

[49] Fornari RE, Alessi P, Kikic I. High-pressure fluid phase-equilibria - experimental methods and systems investigated (1978-1987). *Fluid Phase Equilib* 1990; 57(1-2):1–33. doi:10.1016/0378-3812(90)80010-9.

[50] Dohrn R, Brunner G. High-pressure fluid-phase equilibria - experimental methods and systems investigated (1988-1993). *Fluid Phase Equilib* 1995; 106(1-2):213–282. doi:10.1016/0378-3812(95)02703-h.

[51] Christov M, Dohrn R. High-pressure fluid phase equilibria - experimental methods and systems investigated (1994-1999). *Fluid Phase Equilib* 2002; 202(1):153–218. doi:10.1016/s0378-3812(02)00096-1.

[52] Dohrn R, Peper S, Fonseca JMS. High-pressure fluid-phase equilibria: Experimental methods and systems investigated (2000-2004). *Fluid Phase Equilib* 2010; 288(1-2):1–54. doi:10.1016/j.fluid.2009.08.008.

[53] Fonseca JMS, Dohrn R, Peper S. High-pressure fluid-phase equilibria: Experimental methods and systems investigated (2005-2008). *Fluid Phase Equilib* 2011; 300(1-2):1–69. doi:10.1016/j.fluid.2010.09.017.

[54] Kroenlein K, Diky V, Muzny CD, Chirico RD, Magee JW, Frenkel M. ThermoLit - NIST literature report builder for thermophysical and thermochemical property measurements. Accessed 2015. URL `http://trc.nist.gov/thermolit/`.

[55] Kazakov A, Muzny C, Kroenlein K, Diky V, Chirico R, Magee J, Abdulagatov I, Frenkel M. NIST/TRC source data archival system: The next-generation data model for storage of thermophysical properties. *Int J Thermophys* 2012; 33(1):22–33. doi:10.1007/s10765-011-1107-7.

[56] Battino R. Sulfur dioxide - water. In: Young CL, editor, *Sulfur Dioxide, Chlorine, Fluorine and Chlorine Oxides*, *Solubility Data Series*, vol. 12, chap. 1, pp. 3–33. International Union of Pure And Applied Chemistry (IUPAC) / Pergamon Press, 1983; URL `http://srdata.nist.gov/solubility/IUPAC/SDS-12/SDS-12.pdf`.

[57] Trengove RD, Wakeham WA. The viscosity of carbon dioxide, methane, and sulfur hexafluoride in the limit of zero density. *J Phys Chem Ref Data* 1987; 16(2):175–187. doi:10.1063/1.555777.

[58] Fogg PGT. Hydrogen sulfide in aqueous solvents - water. In: Fogg PGT, Young CL, editors, *Hydrogen Sulfide, Deuterium Sulfide and Hydrogen Selenide*, *Solubility Data Series*, vol. 32, chap. 1, pp. 1–19. International Union of Pure And Applied Chemistry (IUPAC), 1988; URL `http://srdata.nist.gov/solubility/IUPAC/SDS-32/SDS-32.aspx`.

[59] Vesovic V, Wakeham W, Olchowy G, Sengers J, Watson J, Millat J. The transport properties of carbon dioxide. *J Phys Chem Ref Data* 1990; 19:763–808. doi:10.1063/1.555875.

[60] Fenghour A, Wakeman W. The viscosity of carbon dioxide. *J Phys Chem Ref Data* 1998; 27(1):31–44. doi:10.1063/1.556013.

[61] Hu J, Duan Z, Zhu C, Chou IM. PVTx properties of the CO_2–H_2O and CO_2–H_2O–NaCl systems below 647 K: Assessment of experimental data and thermodynamic models. *Chem Geol* 2007; 238(3–4):249–267. doi:10.1016/j.chemgeo.2006.11.011.

[62] Hou SX, Maitland GC, Trusler JPM. Phase equilibria of (CO_2 + H_2O + NaCl) and (CO_2 + H_2O + KCl): measurements and modeling. *J Supercrit Fluid* 2013; 78:78–88. doi:10.1016/j.supflu.2013.03.022.

[63] Al-Siyabi I. *Effect of impurities on CO_2 stream properties*. Ph.D. thesis, Heriot-Watt University, Edinburgh, Scotland, UK, 2013. URL `http://hdl.handle.net/10399/2643`. Speed of sound data plotted in I. Alsiyabi, A. Chapoy, B. Tohidi, 'Effects of impurities on speed of sound and isothermal compressibility of CO_2-rich systems', in 3rd International Forum on the Transportation of CO_2 by Pipeline, 2012.

[64] Kaminishi GI, Toriumi T. Gas-liquid equilibrium under high pressures: VI. vapor-liquid equilibrium in the carbon dioxide + hydrogen, carbon dioxide + nitrogen and carbon dioxide + oxygen systems [in japanese]. *Kogyo Kagaku Zasshi* 1966; 69:175–178.

[65] Westman SF, Stang HGJ, Løvseth SW, Austegard A, Snustad I, Størset SØ, Ertesvåg IS. Vapor-liquid equilibrium data for the carbon dioxide and nitrogen (CO_2+N_2) system at the temperatures 223, 270, 298 and 303 K and pressures up to 18 MPa. *Fluid Phase Equilib* 2016; 409:207–241. doi:10.1016/j.fluid.2015.09.034.

[66] Krichevskii IR, Khazanova NE, Lesnevskaya LS, Scandalova LU. Liquid-gas equilibria in nitrogen-carbon dioxide at high pressures [in Russian]. *Khim Promst* 1962; 3:169–171.

[67] Yorizane M, Yoshimura S, Masuoka H, Miyano Y, Kakimoto Y. New procedure for vapor-liquid equilibria. Nitrogen + carbon dioxide, methane + freon 22, and methane + freon 12. *J Chem Eng Data* 1985; 30(2):174–176. doi:10.1021/je00040a012.

[68] Kunz O, Wagner W. The GERG-2008 wide-range equation of state for natural gases and other mixtures: An expansion of GERG-2004. *J Chem Eng Data* 2012; 57(11):3032–3091. doi:10.1021/je300655b.

[69] Tsang CY, Street WB. Phase equilibria in the h2/co2 system at temperatures from 220 to 290 k and pressures to 172 mpa. *Chem Eng Sci* 1981; 36(6):993 – 1000. doi:10.1016/0009-2509(81)80085-1.

[70] Spano JO, Heck CK, Barrick PL. Liquid-vapor equilibria of the hydrogen-carbon dioxide system. *J Chem Eng Data* 1968; 13(2):168–171. doi:10.1021/je60037a007.

[71] Bezanehtak K, Combes GB, Dehghani F, Foster NR, Tomasko DL. Vapor–liquid equilibrium for binary systems of carbon dioxide + methanol, hydrogen + methanol, and hydrogen + carbon dioxide at high pressures. *J Chem Eng Data* 2001; 47(2):161–168. doi:10.1021/je010122m.

[72] Wilson GM, Cunningham JR, Nielsen PF. Enthalpy and phase boundary measurements on mixtures of nitrogen with methane, carbon dioxide and hydrogen sulfide. GPA Research Report RR-24, Gas Processing Association, Tulsa, OK, USA, 1977.

[73] Zeck S. *Beitrag zur experimentellen Untersuchung und Berechnung von Gas-Flüssigkeits-Phasengleichgewichten*. Ph.D. thesis, Technische Universität Berlin, 1985.

[74] Shi M, Wei M, Zhang J, Wang L. Simple and speedy measurement of bubble point and dew point for VLE binary system under pressure. *Chemical Engineering (China)* 1984; 6:51–54.

[75] Bailey DM, Esper GJ, Holste JC, Hall KR, Eubank PT, Marsh KN, Rogers WJ. Properties of CO_2 mixtures with N_2 and with CH_4. GPA Research Report RR-122, Gas Processing Association, Tulsa, OK, USA, 1989.

[76] Bian B. *Measurement of Phase Equilibria in the Critical Region and Study of Equation of State*. Ph.D. thesis, University of Nanjin, 1992.

[77] Duarte-Garza H, Brugge HB, Hwang CA, Eubank PT, Holste JC, Hall KR. Thermodynamic properties of CO_2+N_2 mixtures. GPA Research Report RR-140, Gas Processing Association, Tulsa, OK, USA, 1995.

[78] Westman SF, Stang HGJ, Størset SØ, Rekstad H, Austegard A, Løvseth SW. Accurate phase equilibrium measurements of CO_2 mixtures. In: Røkke N, Svendsen H, editors, *7th Trondheim Conference on CO_2 Capture, Transport and Storage (TCCS-7)*. BIGCCS / SINTEF / NTNU, Trondheim, Norway: Energy Procedia vol. 51, 2013; pp. 392–401. doi:10.1016/j.egypro.2014.07.046.

[79] Fandiño O, Trusler JPM, Vega-Maza D. Phase behavior of (CO_2 + H_2) and (CO_2 + N_2) at temperatures between (218.15 and 303.15) K at pressures up to 15 MPa. *Int J Greenh Gas Con* 2015; 36:78–92. doi:10.1016/j.ijggc.2015.02.018.

[80] Tenorio MJ, Parrott AJ, Calladine JA, Sanchez-Vicente Y, Cresswell AJ, Graham RS, Drage TC, Poliakoff M, Ke J, George MW. Measurement of the vapour-liquid equilibrium of binary and ternary mixtures of CO_2, N_2 and H_2, systems which are of relevance to CCS technology. *Int J Greenh Gas Con* 2015; 41:68–81. doi:10.1016/j.ijggc.2015.06.009.

[81] Engberg R, Köpke D, Eggers R. Die Grenzflächenspannungen von CO_2-O_2- und Rauchgas-Mischungen. *Chem Ing Tech* 2009; 81(9):1439–1443. doi:10.1002/cite.200900052.

[82] Westman SF, Stang HGJ, Løvseth SW, Austegard A, Snustad I, Ertesvåg

IS. Vapor-liquid equilibrium data for the carbon dioxide and oxygen (CO_2+O_2) system at the temperatures 218, 233, 253, 288 and 298 K and pressures up to 14 MPa. *Submitted to Fluid Phase Equilib* 2016; .

[83] Köpke D. *Verfahrenstechnik der CO_2-Abscheidung aus CO_2-reichen Oxyfuel-Rauchgasen*. Ph.D. thesis, Technische Universität Hamburg-Harburg, 2010.

[84] Caubet F. *Liquéfaction des mélanges gazeux*. Ph.D. thesis, Université de Bordeaux, France, 1901.

[85] Caubet F. *Z Phys Chem* 1902; 40:254.

[86] Bierlein JA, Kay WB. Phase-equilibrium properties of system carbon dioxide-hydrogen sulfide. *Ind Eng Chem* 1953; 45(3):618–624. doi:10.1021/ie50519a043.

[87] Robinson DB, Bailey JA. The carbon dioxide-hydrogen sulfide-methane system. part I. phase behavior at 100°F. *Can J Chem Eng* 1957; 35:151–158.

[88] Robinson DB, Lorenzo AP, Macrygeorgos CA. The carbon dioxide-hydrogen sulfide-methane system. Part II. Phase behavior at 40°F and 160°F. *Can J Chem Eng* 1959; 37:212–217. doi:10.1002/cjce.5450370603.

[89] Morris JS, Byers CH. Near-critical-region equilibria of the CH_4-CO_2-H_2S system. *Fluid Phase Equilib* 1991; 66(3):291–308. doi:10.1016/0378-3812(91)85062-Y.

[90] Kellerman SJ, Stouffer CE, Eubank PT, Holste JC, Hall KR, Gammon BE, Marsh KN. Thermodynamic properties of CO_2 + H_2S mixtures. GPA Research Report RR-141, Gas Processing Association, Tulsa, OK, USA, 1995.

[91] Chapoy A, Coquelet C, Liu H, Valtz A, Tohidi B. Vapour–liquid equilibrium data for the hydrogen sulphide (H_2S) + carbon dioxide (CO_2) system at temperatures from 258 to 313 K. *Fluid Phase Equilib* 2013; 356:223–228. doi:10.1016/j.fluid.2013.07.050.

[92] Camy S, Letourneau JJ, Condoret JS. Experimental study of high pressure phase equilibrium of (CO_2 + NO_2/N_2O_4) mixtures. *J Chem Thermodyn* 2011; 43(12):1954–1960. doi:10.1016/j.jct.2011.07.007.

[93] Blanco ST, Rivas C, Bravo R, Fernández J, Artal M, Velasco I. Discussion of the influence of CO and CH_4 in CO_2 transport, injection, and storage for CCS technology. *Envir Sci Tech* 2014; 48(18):10984–10992. doi:10.1021/es502306k.

[94] Tsiklis DS. Heterogeneous equilibria in binary systems. *Phys Chem (USSR)* 1946; 20:181–188.

[95] Yorizane M, Yoshimura S, Masuoka H. Vapor liquid equilibrium at high pressure (N_2-CO_2, H_2-CO_2 system). *Chemical Engineering (Japan)* 1970; 34(9):953–957,a1. doi:10.1252/kakoronbunshu1953.34.953.

[96] Arai Y, Kaminishi GI, Saito S. The experimental determination of the P–V–T–x relations for the carbon dioxide-nitrogen and the carbon dioxide-methane systems. *J Chem Eng Jpn* 1971; 4(2):113–122. doi:10.1252/jcej.4.113.

[97] Hwang SC, Lin HM, Chappelear PS, Kobayashi R. Dew point study in the vapor-liquid region of the methane-carbon dioxide system. *J Chem Eng Data* 1976; 21(4):493–497. doi:10.1021/je60071a019.

[98] Devlikamov VV, Semenova LV, Repin NN. Solubility of methane in liquid carbon dioxide [in Russian]. *Izv Vyssh Uchebn Zaved, Neft Gaz* 1982; (8):42–44.

[99] Vetere A. Vapor-liquid equilibria calculations by means of an equation of state. *Chem Eng Sci* 1983; 38(8):1281–1291. doi:10.1016/0009-2509(83)80048-7.

[100] Esper GJ, Bailey DM, Holste JC, Hall KR. Volumetric behavior of near-equimolar mixtures for CO_2+CH_4 and CO_2+N_2. *Fluid Phase Equilib* 1989; 49:35–47. doi:10.1016/0378-3812(89)80004-4.

[101] Bian B, Wang Y, Shi J, Zhao E, Lu BCY. Simultaneous determination of vapor-liquid equilibrium and molar volumes for coexisting phases up to the critical temperature with a static method. *Fluid Phase Equilib* 1993; 90(1):177–187. doi:10.1016/0378-3812(93)85012-B.

[102] Wei MSW, Brown TS, Kidnay AJ, Sloan ED. Vapor + liquid equilibria for the ternary system methane + ethane + carbon dioxide at 230 K and its constituent binaries at temperatures from 207 to 270 K. *J Chem Eng Data* 1995; 40(4):726–731. doi:10.1021/je00020a002.

[103] Webster LA, , Kidnay AJ. Vapor–liquid equilibria for the methane–propane–carbon dioxide systems at 230 K and 270 K. *J Chem Eng Data* 2001; 46(3):759–764. doi:10.1021/je000307d.

[104] Sidorov IP, Kazarnovskii YS, Goldman AM. Solubility of water in compressed gases. *Tr Gosudarst Nauch Issled I Proekt Inst Azot Prom (Trudy GIAP)* 1952; (1):48–67.

[105] Rettich TR, Battino R, Wilhelm E. Solubility of gases in liquids. XVI. Henry's law coefficients for nitrogen in water at 5 to 50°C. *J Solution Chem* 1984; 13(5):335–348. doi:10.1007/BF00645706.

[106] Baranenko VI, Ostretsov IN, Kirov VS, Falkovskii LN, Piontkovskii AI. Air solubility in water. *Zh Fiz Khim* 1990; 64:3256–3261.

[107] Luker J, Gniewek T, Johnson C. Saturation composition of a steam-oxygen liquid water system and P-V-T data for a superheated steam-oxygen mixture. *Ind Eng Chem Chem Eng Data Series* 1958; 3(1):8–10. doi:10.1021/i460003a002.

[108] Taylor CD. The effect of pressure upon the solubility of oxygen in water: Implications of the deviation from the ideal gas law upon measurements of fluorescence quenching. *Arch Biochem Biophys* 1978; 191(1):375–384. doi:10.1016/0003-9861(78)90101-7.

[109] Benson BB, Krause D Jr, Peterson MA. The solubility and isotopic fractionation of gases in dilute aqueous solution. I. oxygen. *J Solution Chem* 1979; 8(9):655–690. doi:10.1007/BF01033696.

[110] Rettich TR, Battino R, Wilhelm E. Solubility of gases in liquids. 22. High-precision determination of Henry's law constants of oxygen in liquid water from T = 274 K to T = 328 K. *J Chem Thermodyn* 2000; 32(9):1145–1156. doi:10.1006/jcht.1999.0581.

[111] Prorokov VN, Dolotov VV, Krestov GA. Solubility and thermodynamic characteristics of the dissolution of argon, krypton, and xenon in water and monohydric alcohols. *Zhur Fiz Khim* 1984; 58:1888–1890.

[112] Wu G, Heilig M, Lentz H, Franck EU. High pressure phase equilibria of the water-argon system. *Ber Bunsenges Phys Chem* 1990; 94(1):24–27. doi:10.1002/bbpc.19900940106.

[113] Rettich TR, Battino R, Wilhelm E. Solubility of gases in liquids. 18. high-precision determination of Henry fugacities for argon in liquid water at 2 to 40°C. *J Solution Chem* 1992; 21(9):987–1004. doi:10.1007/BF00650874.

[114] Bichowsky FR. Equilibrium in the reaction between sulfur dioxide and water. *J Am Chem Soc* 1922; 44(1):116–132. doi:10.1021/ja01422a014.

[115] Hales JM, Sutter SL. Solubiliity of sulfur dioxide in water at low concentrations. *Atmospheric Environment* 1973; 7:997–1001.

[116] Van Berkum JG, Diepen GAM. Phase equilibria in SO_2 + H_2O: the sulfur dioxide gas hydrate, two liquid phases, and the gas phase in the temperature range 273 to 400 K and at pressures up to 400 MPa. *J Chem Thermodyn* 1979; 11(4):317–334. doi:10.1016/0021-9614(79)90053-3.

[117] Rumpf B, Maurer G. Solubilities of hydrogen cyanide and sulfur dioxide in water at temperatures from 293.15 to 413.15 K and pressures up to 2.5 MPa. *Fluid Phase Equilib* 1992; 81:241–260. doi:10.1016/0378-3812(92)85155-2.

[118] Siddiqi MA, Krissmann J, Peters-Gerth P, Luckas M, Lucas K. Spectrophotometric measurement of the vapour-liquid equilibria of (sulphur dioxide + water). *J Chem Thermodyn* 1996; 28(7):685–700. doi:10.1006/jcht.1996.0064.

[119] Mondal MK. Experimental determination of dissociation constant, Henry's constant, heat of reactions, SO_2 absorbed and gas bubble-liquid interfacial area for dilute sulphur dioxide absorption into water. *Fluid Phase Equilib* 2007; 253(2):98–107. doi:10.1016/j.fluid.2007.01.015.

[120] Shaw AC, Romero MA, Elder RH, Ewan BCR, Allen RWK. Measurements of the solubility of sulphur dioxide in water for the sulphur family of thermochemical cycles. *Int J Hydrogen Energ* 2011; 36(8):4749–4756. doi:10.1016/j.ijhydene.2011.01.105.

[121] Mannheimer M. Mutual solubility of liquefied gases and water at room temperature. *The Chemist-Analyst* 1956; 45.

[122] Gillespie PC, Wilson GM. Vapor-liquid equilibrium data on water-substitute gas components: N_2-H_2O, H_2-H_2O, CO-H_2O, H_2-CO-H_2O, and H_2S-H_2O. GPA Research Report RR-41, Gas Processing Association, Tulsa, OK, USA, 1980.

[123] Yu Q, Liu D, Liu R, Zhou H, Chen M, Chen G, Chen Y, Hu Y, Xu X, Shen L, Han SJ. VLE of H_2S-H_2O system. *Chemical Engineering (China)* 1980; 4.

[124] Gillespie PC, Wilson GM. Vapour-liquid and liquid-liquid equilibria: Water-methane, water-carbon dioxide, water-hydrogen sulphide, water-n pentane, water-methane-n-pentane. GPA Research Report RR-48, Gas Processing Association, Tulsa, OK, USA, 1982.

[125] King AD Jr, Coan CR. Solubility of water in compressed carbon dioxide, nitrous oxide, and ethane. evidence for hydration of carbon dioxide and nitrous oxide in the gas phase. *J Am Chem Soc* 1971; 93(8):1857–1862.

doi:10.1021/ja00737a004.

[126] Jaffer S, Carroll JJ, Mather AE. Vapor-liquid-liquid locus of the system nitrous oxide + water. *J Chem Eng Data* 1993; 38(2):324–325. doi:10.1021/je00010a035.

[127] Fonseca IMA, Almeida JPB, Fachada HC. Automated apparatus for gas solubility measurements. *J Chem Thermodyn* 2007; 39(10):1407–1411. doi:10.1016/j.jct.2007.05.013.

[128] Zhang G, Wu Y, Ma P, Wu G, Dinghuo L. Measurement and correlation of solubility of carbon monoxide and other gases solubility in phenol. *CIESC Journal* 2005; 56(11):2039–2045. URL `http://www.hgxb.com.cn/EN/abstract/article_4641.shtml`.

[129] Pray HA, Schweickert CE, Minnich BH. Solubility of hydrogen, oxygen, nitrogen, and helium in water at elevated temperatures. *Ind Eng Chem* 1952; 44(5):1146–1151. doi:10.1021/ie50509a058.

[130] Maslennikova VY, Goryunova NP, Subbotina LA, Tsiklis DS. The solubility of water in compressed hydrogen. *Zh Fiz Khim* 1976; 50:411–414.

[131] DeVaney W, Berryman JM, Kao PL, Eakin B. High temperature V-L-E measurements for substitute gas components. GPA Research Report RR-30, Gas Processing Association, Tulsa, OK, USA, 1978.

[132] Seward TM, Franck EU. The system hydrogen - water up to 440° and 2500 bar pressure. *Ber Bunsenges Phys Chem* 1981; 85:2–7. doi:10.1002/bbpc.19810850103.

[133] Kling G, Maurer G. The solubility of hydrogen in water and in 2-aminoethanol at temperatures between 323 K and 423 K and pressures up to 16 MPa. *J Chem Thermodyn* 1991; 23(6):531–541. doi:10.1016/S0021-9614(05)80095-3.

[134] Góral M, Shaw DG, Mączyński A, Wiśniewska-Gocłowska B, Oracz P. IUPAC-NIST solubility data series. 96. amines with water part 1. C4-C6 aliphatic amines. *J Phys Chem Ref Data* 2012; 41(4):043106. doi:10.1063/1.4755288.

[135] Dhima A, de Hemptinne JC, Jose J. Solubility of hydrocarbons and CO_2 mixtures in water under high pressure. *Ind Eng Chem Res* 1999; 38(8):3144–3161. doi:10.1021/ie980768g.

[136] Jarne C, Blanco ST, Gallardo MA, Rauzy E, Otín S, Velasco I. Dew points of ternary methane (or ethane) + carbon dioxide + water mixtures: Measurement and correlation. *Energ Fuel* 2004; 18(2):396–404. doi:10.1021/ef030146u.

[137] Qin J, Rosenbauer RJ, Duan Z. Experimental measurements of vapor-liquid equilibria of the H_2O + CO_2 + CH_4 ternary system. *J Chem Eng Data* 2008; 53(6):1246–1249. doi:10.1021/je700473e.

[138] Al Ghafri SZS, Forte E, Maitland GC, Rodriguez-Henríquez JJ, Trusler JPM. Experimental and modeling study of the phase behavior of (methane + CO_2 + water) mixtures. *J Phys Chem B* 2014; 118(49):14461–14478. doi:10.1021/jp509678g.

[139] Yasunishi A, Yoshida F. Solubility of carbon dioxide in aqueous electrolyte solutions. *J Chem Eng Data* 1979; 24(1):11–14. doi:10.1021/je60080a007.

[140] Wang LS, Lang ZX, Guo TM. Measurement and correlation of the diffusion coefficients of carbon dioxide in liquid hydrocarbons under elevated pressures. *Fluid Phase Equilib* 1996; 117(1-2):364–372. doi:10.1016/0378-3812(95)02973-7. Proceedings of the Seventh International Conference on Fluid Properties and Phase Equilibria for Chemical Process Design.

[141] Zheng DQ, Guo TM, Knapp H. Experimental and modeling studies on the solubility of CO_2, $CHC1F_2$, CHF_3, $C_2H_2F_4$ and $C_2H_4F_2$ in water and aqueous nacl solutions under low pressures. *Fluid Phase Equilib* 1997; 129(1-2):197–209. doi:10.1016/S0378-3812(96)03177-9.

[142] Gu F. Solubility of carbon dioxide in aqueous sodium chloride solution under high pressure. *Gaoxiao Huaxue Gongcheng Xuebao* 1998; 12(2):118–123.

[143] Yan W, Huang S, Stenby EH. Measurement and modeling of CO_2 solubility in NaCl brine and CO_2-saturated NaCl brine density. *Int J Greenh Gas Con* 2011; 5(6):1460–1477. doi:10.1016/j.ijggc.2011.08.004.

[144] Chapoy A, Nazeri M, Kapateh M, Burgass R, Coquelet C, Tohidi B. Effect of impurities on thermophysical properties and phase behaviour of a CO_2-rich system in ccs. *Int J Greenh Gas Con* 2013; 19:92–100. doi:10.1016/j.ijggc.2013.08.019.

[145] Coquelet C, Valtz A, Dieu F, Richon D, Arpentinier P, Lockwood F. Isothermal p, x, y data for the argon + carbon dioxide system at six temperatures from 233.32 to 299.21 K and pressures up to 14 MPa. *Fluid Phase Equilib* 2008; 273(1-2):38–43. doi:10.1016/j.fluid.2008.08.010.

[146] Khodeeva SM, Korbutova IA, Sokolova ES. Solubility H_2O and D_2O and their mixture in CO_2 and N_2O near the solubility critical point. *Zh Fiz Khim* 1985; 59(6):1565–1567.

[147] Fedorova MF. *Zh Fiz Khim* 1940; 14:422–426.

[148] Sonntag RE, Van Wylen GJ. The solid-vapor equilibrium of carbon dioxide-nitrogen. In: Timmerhaus KD, editor, *Advances in Cryogenic Engineering*, vol. 7, pp. 99–105. Springer US. ISBN 978-1-4757-0533-1, 1962; doi:10.1007/978-1-4757-0531-7_12.

[149] Smith GE, Sonntag RE, Van Wylen GJ. Solid-vapor equilibrium of the carbon dioxide-nitrogen system at pressures to 200 atmospheres. In: Timmerhaus KD, editor, *Advances in Cryogenic Engineering*, vol. 9, pp. 197–206. Springer US. ISBN 978-1-4757-0527-0, 1964; doi:10.1007/978-1-4757-0525-6_24.

[150] Yakimenko NP, Glukh GM, Iomotev, B M, Abramova RI. *Zh Fiz Khim* 1975; 49:116–117.

[151] De Stefani V, Baba-Ahmed A, Valtz A, Meneses D, Richon D. Solubility measurements for carbon dioxide and nitrous oxide in liquid oxygen at temperatures down to 90 K. *Fluid Phase Equilib* 2002; 200(1):19–30. doi:10.1016/S0378-3812(01)00821-4.

[152] Thiele A, Schulte E. Binary equilibrium systems with solid carbon dioxide. *Z Phys Chem, Stoechiom Verwandschaftsl* 1920; 96:312–342.

[153] Donnelly HG, Katz DL. Phase equilibria in the carbon dioxide-methane system. *Ind Eng Chem* 1954; 46(3):511–517. doi:10.1021/ie50531a036.

[154] Pikaar MJ. *A Study of Phase Equilibria in Hydrocarbon-CO_2 Systems*. Ph.D. thesis, University of London, London, UK, 1959.

[155] Sterner CJ. Phase equilibria in the CO_2-methane systems. In: Timmerhaus KD, editor, *Advances in Cryogenic Engineering*, vol. 6, pp. 467–474. Springer US. ISBN 978-1-4757-0536-2, 1961; doi:10.1007/978-1-4757-0534-8_49.

[156] Davis JA, Rodewald N, Kurata F. Solid-liquid-vapor phase behavior of the methane-carbon dioxide system. *AIChE Journal* 1962; 8(4):537–539. doi:10.1002/aic.690080423.

[157] Agrawal GM, Laverman RJ. Phase behavior of the methane-carbon dioxide system in the solid-vapor region. In: Timmerhaus KD, editor, *Advances in Cryogenic Engineering*, vol. 19, pp. 327–338. Springer US. ISBN 978-1-4613-9849-3, 1995; doi:10.1007/978-1-4613-9847-9_40.

[158] Le TT, Trebble MA. Measurement of carbon dioxide freezing in mixtures of methane, ethane, and nitrogen in the solid-vapor equilibrium region. *J Chem Eng Data* 2007; 52(3):683–686. doi:10.1021/je060194j.

[159] Zhang L, Burgass R, Chapoy A, Tohidi B, Solbraa E. Measurement and modeling of CO_2 frost points in the CO_2-methane systems. *J Chem Eng Data* 2011; 56(6):2971–2975. doi:10.1021/je200261a.

[160] Jäger A, Vinš V, Gernert J, Span R, Hrubý J. Phase equilibria with hydrate formation in H_2O+CO_2 mixtures modeled with reference equations of state. *Fluid Phase Equilib* 2013; 338:100–113. doi:10.1016/j.fluid.2012.10.017.

[161] Burgass R, Chapoy A, Duchet-Suchaux P, Tohidi B. Experimental water content measurements of carbon dioxide in equilibrium with hydrates at (223.15 to 263.15) K and (1.0 to 10.0) MPa. *J Chem Thermodyn* 2014; 69:1–5. doi:10.1016/j.jct.2013.09.033.

[162] Nagashima HD, Fukushima N, Ohmura R. Phase equilibrium condition measurements in carbon dioxide clathrate hydrate forming system from 199.1 K to 247.1 K. *Fluid Phase Equilib* 2015; doi:10.1016/j.fluid.2015.09.020. In press.

[163] Dholabhai PD, Kalogerakis N, Bishnoi PR. Equilibrium conditions for carbon dioxide hydrate formation in aqueous electrolyte solutions. *J Chem Eng Data* 1993; 38(4):650–654. doi:10.1021/je00012a045.

[164] Englezos P, Hall S. Phase equilibrium data on carbon dioxide hydrate in the presence of electrolytes, water soluble polymers and montmorillonite. *Can J Chem Eng* 1994; 72(5):887–893. doi:10.1002/cjce.5450720516.

[165] Kyung D, Lee K, Kim H, Lee W. Effect of marine environmental factors on the phase equilibrium of CO_2 hydrate. *Int J Greenh Gas Con* 2014; 20:285–292. doi:10.1016/j.ijggc.2013.11.013.

[166] Sun Q, Tian H, Li Z, Guo X, Liu A, Yang L. Solubility of CO_2 in water and nacl solution in equilibrium with hydrate. part i: Experimental measurement. *Fluid Phase Equilib* 2016; 409:131–135. doi:10.1016/j.fluid.2015.09.033.

[167] Beeskow-Strauch B, Schicks JM, Spangenberg E, Erzinger J. The influence of SO_2 and NO_2 impurities on CO_2 gas hydrate formation and stability. *Chem – Eur J* 2011; 17(16):4376–4384. doi:10.1002/chem.201003262.

[168] Daraboina N, Ripmeester J, Englezos P. The impact of SO_2 on post combustion carbon dioxide capture in bed of silica sand through hydrate formation. *Int J Greenh Gas Con* 2013; 15:97–103. doi:10.1016/j.ijggc.2013.02.008.

[169] Trusler JPM. Equation of state for solid phase I of carbon dioxide valid for temperatures up to 800 K and pressures up to 12 GPa. *J Phys Chem Ref Data* 2011; 40(4). doi:10.1063/1.3664915. Article 043105.

[170] Jäger A, Span R. Equation of state for solid carbon dioxide based on the Gibbs free energy. *J Chem Eng Data* 2012; 57(2):590–597. doi:10.1021/je2011677.

[171] Edwards AE, Roseveare WE. The second virial coefficients of gaseous mixtures. *J Am Chem Soc* 1942; 64(12):2816–2819. doi:10.1021/ja01264a028.

[172] Gunn RD. *The volumetric properties of nonpolar gaseous mixtures*. Master's thesis, Univ. of California, Berkeley, CA, USA, 1958.

[173] Muirbrook NK. *Experimental and thermodynamic study of the high-pressure vapour-liquid equilibria for the nitrogen-oxygen-carbon dioxide system*. Ph.D. thesis, University of California, 1964.

[174] Brewer J. Tech. Rep. AFOSR-TR 67-2795, Air Force Off. Sci. Res., 1967.

[175] Lopatinskii ES, Rozhnov MS, Zhdanov VI, Parnovskii SL, Kudrya YN. Second virial coefficients of gas mixtures of hydrocarbons, carbon dioxide, and hydrogen with nitrogen and argon. *Zh Fiz Khim* 1991; 61:2060–2065.

[176] Yang X, Richter M, Wang Z, Li Z. Density measurements on binary mixtures (nitrogen+ carbon dioxide and argon+ carbon dioxide) at temperatures from (298.15 to 423.15) K with pressures from (11 to 31) MPa using a single-sinker densimeter. *J Chem Thermodyn* 2015; 91:17–29. doi:10.1016/j.jct.2015.07.014.

[177] Lichtenthaler RN, Schaefer K. Intermolecular forces of spherical and nonspherical molecules determined from second virial coefficients. *Ber Bunsenges Phys Chem* 1969; 73(1):42–48.

[178] Schmiedel H, Gehrmann R, Schramm B. Die zweiten Virialkoeffizienten verschiedener Gasmischungen im Temperaturbereich von 213 bis 475 K. *Ber Bunsenges Phys Chem* 1980; 84(8):721–724. doi:10.1002/bbpc.19800840806.

[179] Schramm B, Müller W. Messungen des zweiten Virialkoeffizienten von Gasen und Gasmischungen bei Zimmertemperatur mit einer Expansionsapparatur. *Ber Bunsenges Phys Chem* 1982; 86(2):110–112. doi:10.1002/bbpc.19820860204.

[180] Bell TN, Bignell CM, Dunlop PJ. Second virial coefficients for some polyatomic gases and their binary mixtures with noble gases. *Physica A* 1992; 181(1):221–231. doi:10.1016/0378-4371(92)90203-3.

[181] Wang J, Wang Z, Ryan D, Lan C. A study of the effect of impurities on CO_2 storage capacity in geological formations. *Int J Greenh Gas Con* 2015; 42:132–137. doi:10.1016/j.ijggc.2015.08.002.

[182] Robinson RL Jr, Jacoby RH. Better compressibility factors. *Hydrocarb Process* 1965; 44(4):141–145.

[183] Liu CH. *Experimental Densities, Entropies and Energies for Pure H_2S and Equimolar Mixtures of H_2S/CH_4 and H_2S/CO_2 Between 300 and 500 K*. Ph.D. thesis, Texas A & M University, 1985.

[184] Bailey DM, Liu CH, Holste JC, Hall KR, Eubank PT, Mars KM. Thermodynamic properties of pure hydrogen sulfide and mixtures containing hydrogen sulfide with methane, carbon dioxide, methyl-cyclohexane and toluene. GPA Research Report RR-107, Gas Processing Association, Tulsa, OK, USA, 1987.

[185] Bailey DM, Liu CH, Holste JC, Eubank PT, Hall KR. Energy functions for hydrogen sulfide. Part 3. Near-equimolar mixture with carbon dioxide. *Hydrocarb Process* 1987; 66(1):73–74.

[186] Stouffer CE, Kellerman SJ, Hall KR, Holste JC, Gammon BE, Marsh KN. Densities of carbon dioxide + hydrogen sulfide mixtures from 220 K to 450 K at pressures up to 25 MPa. *J Chem Eng Data* 2001; 46(5):1309–1318. doi:10.1021/je000182c.

[187] Nicola GD, Giuliani G, Polonara F, Stryjek R. Isochoric PVTx measurements for the CO_2 + N_2O system. *J Chem Eng Data* 2005; 50(2):656–660. doi:10.1021/je049633+.

[188] McElroy PJ, Moser J. Excess and unlike-interaction second virial coefficients and excess molar enthalpy of (0.500CO + 0.500CO_2). *J Chem Thermodyn* 1995; 27(3):267–271. doi:10.1006/jcht.1995.0025.

[189] Rivas C, Blanco ST, Fernández J, Artal M, Velasco I. Influence of methane and carbon monoxide in the volumetric behaviour of the anthropogenic CO_2: Experimental data and modelling in the critical region. *Int J Greenh Gas Con* 2013; 18:264–276. doi:10.1016/j.ijggc.2013.07.019.

[190] Cottrell TL, Hamilton RA, Taubinger RP. The second virial coefficients of gases and mixtures. Part 2.–mixtures of carbon dioxide with nitrogen, oxygen, carbon monoxide, argon and hydrogen. *Trans Faraday Soc* 1956; 52:1310–1312. doi:10.1039/TF9565201310.

[191] Jaeschke M, Humphreys AE. *The GERG Databank of High Accuracy Compressibility Factor Measurements*, *GERG Technical Monograph*, vol. 4. Groupe Européen de Recherches Gazières (GERG), 1990.

[192] Vilcu R, Gainar I, Anitescu G. The second interaction virial coefficient of gas mixtures. III. Carbon dioxide + hydrogen mixture. *Rev Roum Chim* 1990; 35:951–959.

[193] Abadio BD, McElroy PJ. (pressure, amount-of-substance density, temperature) of (1-x)CO_2 +xH_2 using a direct method. *J Chem Thermodyn* 1993; 25(12):1495–1501. doi:10.1006/jcht.1993.1149.

[194] Magee JW, Howley JA, Ely JFA. Predictive model for the thermophysical properties of carbon dioxide rich mixtures gas processors association a predictive model for the thermophysical properties of carbon dioxide rich mixtures. GPA Research Report RR-136, Gas Processing Association, Tulsa, OK, USA, 1994.

[195] Sanchez-Vicente Y, Drage TC, Poliakoff M, Ke J, George MW. Densities of the carbon dioxide + hydrogen, a system of relevance to carbon capture and storage. *Int J Greenh Gas Con* 2013; 13:78–86. doi:10.1016/j.ijggc.2012.12.002.

[196] Cipollina A, Anselmo R, Scialdone O, Filardo G, Galia A. Experimental P-T-ρ measurements of supercritical mixtures of carbon dioxide, carbon monoxide, and hydrogen and semiquantitative estimation of their solvent power using the solubility parameter concept. *J Chem Eng Data* 2007; 52(6):2291–2297. doi:10.1021/je700307r.

[197] Simon R, Fesmire CJ, Dicharry RM, Vorhis FH. Compressibility factors for CO_2-methane mixtures. *J Petrol Technol* 1977; 29(1):81–85. doi:10.2118/5052-PA.

[198] Katayama T, Ohgaki K, Ohmori H. Measurement of interaction second virial coefficients with high accuracy. *J Chem Eng Jpn* 1980; 13(4):257–262. doi:10.1252/jcej.13.257.

[199] Martin ML, Trengove RD, Harris KR, Dunlop PJ. Excess second virial coefficients for some dilute binary gas mixtures. *Aust J Chem* 1982; 35(8):1525–1529. doi:10.1071/CH9821525.

[200] Ohgaki K, Nakamura Y, Ariyasu H, Katayama T. Interaction second virial coefficients for six binary systems containing carbon dioxide, methane, ethylene and propylene at 125°C. *J Chem Eng Jpn* 1982; 15(2):85–90. doi:10.1252/jcej.15.85.

[201] Yupin TJL. The experimental study and correlation of PVT relation of binary gas mixture of carbon dioxide-methane. *J Eng Thermophys* 1984; 5(2):119–124. URL `http://en.cnki.com.cn/Article_en/CJFDTotal-GCRB198402001.htm`.

[202] Lemming W. *Experimentelle Bestimmung akustischer und thermischer Virialkoeffizienten von Arbeitsstoffen der Energietechnik*. Fortschritt-Berichte VDI / 19: Wärmetechnik, Kältetechnik, VDI-Verlag, 1989. ISBN 9783181432198. URL `https://books.google.no/books?id=KSTTtgAACAAJ`.

[203] McElroy PJ, Kee LL, Renner CA. Excess second virial coefficients for binary mixtures of carbon dioxide with methane, ethane, and propane. *J Chem Eng Data* 1990; 35(3):314–317. doi:10.1021/je00061a024.

[204] Seitz JC, Blencoe JG, Bodnar RJ. Volumetric properties for $(1-x)CO_2 + xCH_4$, $(1-x)CO_2 + xN_2$, and $(1-x)CH_4 + xN_2$ at the pressures (9.94, 19.94, 29.94, 39.94, 59.93, 79.93, and 99.93) MPa and temperatures (323.15, 373.15, 473.15, and 573.15) K. *J Chem Thermodyn* 1996; 28(5):521–538. doi:10.1006/jcht.1996.0049.

[205] Hwang CA, Iglesias-Silva GA, Holste JC, , Hall KR, Gammon BE, Marsh KN. Densities of carbon dioxide + methane mixtures from 225 K to 350 K at pressures up to 35 MPa. *J Chem Eng Data* 1997; 42(5):897–899. doi:10.1021/je970042b.

[206] May TO. *Fluid Properties and Adsorption Measurements*. Master's thesis, Washington State University, 2003.

[207] Pollitzer F, Strebel E. Über den Einfluß indifferenter Gase auf die Sättigungs-Dampfkonzentration von Füssigkeiten. *Z Phys Chem* 1924; 110:768–785.

[208] Skripka VG. Volume behavior of nonpolar component-water gaseous mixtures at high temperatures. *Zh Fiz Khim* 1979; 53:1407–1409.

[209] Moore JC, Battino R, Rettich TR, Handa YP, Wilhelm E. Partial molar

volumbes of gases at infinite dilution in water at 298.15 K. *J Chem Eng Data* 1982; 27(1):22–24. doi:10.1021/je00027a005.
[210] McBride-Wright M, Maitland GC, Trusler JPM. Viscosity and density of aqueous solutions of carbon dioxide at temperatures from (274 to 449) K and at pressures up to 100 MPa. *J Chem Eng Data* 2014; 60(1):171–180. doi:10.1021/je5009125.
[211] Novikov II, Trelin YS. A new method of calculation of the thermodynamic diagram of working fluids. *Teploenergetika* 1962; 9:79–85.
[212] Rank DH, Wiggins TA, Wick RV, Eastman DP, Guenther AH. Stimulated brillouin effect in high-pressure gases. *J Opt Soc Am* 1966; 56(2):174–175. doi:10.1364/JOSA.56.000174.
[213] Sharif MAR, Groves TK. Apparatus for the measurement of decompression wave front velocity based sound speeds and of associated densities and isothermal compressibility coefficients in moderately dense gases. *Chem Eng Commun* 1989; 86(1):199–223. doi:10.1080/00986448908940372.
[214] Estrada-Alexanders AF, Trusler JPM. Speed of sound in carbon dioxide at temperatures between (220 and 450) K and pressures up to 14 MPa. *J Chem Thermodyn* 1998; 30(12):1589–1601. doi:10.1006/jcht.1998.0428.
[215] Estrada-Alexanders AF, Hurly JJ. Kinematic viscosity and speed of sound in gaseous CO, CO_2, SiF_4, SF_6, C_4F_8, and NH_3 from 220 K to 375 K and pressures up to 3.4 MPa. *J Chem Thermodyn* 2008; 40(2):193–202. doi:10.1016/j.jct.2007.07.002.
[216] Herget CM. Ultrasonic velocity in carbon dioxide and ethylene in the critical region. *J Chem Phys* 1940; 8(7):537–542. doi:10.1063/1.1750708.
[217] Pitaevskaya LL, Bilevich AV. The velocity of ultrasound in carbon dioxide at pressures up to 4.5 kbar. *Russ J Phys Chem* 1973; 47:126–127.
[218] Pecceu W, Van Dael W. Ultrasonic velocity in liquid carbon dioxide. *Physica* 1973; 63(1):154–162. doi:10.1016/0031-8914(73)90184-5.
[219] Lin CW, Trusler JPM. Speed of sound in (carbon dioxide+ propane) and derived sound speed of pure carbon dioxide at temperatures between (248 and 373) k and at pressures up to 200 mpa. *J Chem Eng Data* 2014; 59(12):4099–4109. doi:10.1021/je5007407.
[220] Kachanov Y, Kanishchev B, Pitaevskaya L. Velocity of sound in argon and in helium-argon and nitrogen-carbon dioxide gas mixtures at high pressures. *Inz Fiz Zh* 1983; 44:8–14.
[221] Wegge R, McLinden MO, Perkins RA, Richter M, Maurer A, Span R. Speed of sound measurements on (argon + carbon dioxide) in the temperature range from (275 to 500) K at pressures up to 8 MPa. Presented at the 19th Symposium on Thermophysical Properties, Boulder, CO, USA, 2015.
[222] Radovskii IS, Trelin YS, Zaitsev VN. Experimental study of the speed of sound dispercy in wet carbon dioxide. *Inz Fiz Zh* 1980; 39(6):1077–1083.
[223] Qin J, Li M, Li J, Chen R, Duan Z, Zhou Q, Li F, Cui Q. High temperatures and high pressures Brillouin scattering studies of liquid H_2O+CO_2 mixtures. *J Chem Phys* 2010; 133(15):154513. doi:10.1063/1.3495972.
[224] Borisov SF, Kalinin BA, Porodnov BT, Suetin PE. Measurements of the viscosity coefficients of gases by the method of non steady-state flow. *Inzh-Fiz Zh* 1973; 24(1).
[225] Timrot DL, Traktueva SA. Temperature dependence of carbon dioxide and sulfur hexafluoride viscosities at medium densities. *Teploenergetika* 1975; (9):81–83.
[226] Lyusternik VE, Kuzovkina VI. Measurements of the viscosity of CO_2 up to 1870 K at 1 atm. *Teplofiz Vys Temp* 1986; 24(1):169–170. URL `http://mi.mathnet.ru/eng/tvt4893`.
[227] Abramson EH. Viscosity of carbon dioxide measured to a pressure of 8 GPa and temperature of 673 K. *Phys Rev E* 2009; 80:021201. doi:10.1103/PhysRevE.80.021201.
[228] Berg RF, Moldover MR. Critical exponent for the viscosity of carbon dioxide and xenon. *J Chem Phys* 1990; 93(3):1926–1938. doi:10.1063/1.459679.
[229] Davani E, Falcone G, Teodoriu C, McCain WD Jr. Rolling ball viscometer calibration with gas over whole interest range of pressure and temperature improves accuracy of gas viscosity measurement. *Ind Eng Chem Res* 2012; 51(46):15276–15281. doi:10.1021/ie301751y.
[230] Schäfer M, Richter M, Span R. Measurements of the viscosity of carbon dioxide at temperatures from (253.15 to 473.15) K with pressures up to 1.2 MPa. *J Chem Thermodyn* 2015; 89:7–15. doi:10.1016/j.jct.2015.04.015.
[231] Hunter IN, Marsh G, Matthews GP, Smith EB. Argon+carbon dioxide gaseous mixture viscosities and anisotropic pair potential energy functions. *Int J Thermophys* 1993; 14(4):819–833. doi:10.1007/BF00502110.
[232] Trautz M, Kurz F. Die Reibung, Wärmeleitung und Diffusion in Gasmischungen XV. Die Reibung von H_2, N_2O, CO_2 und C_3H_8 und ihren binären Gemischen. *Ann Phys* 1931; 401(8):981–1003. doi:10.1002/andp.19314010808.
[233] Davani E, Falcone G, Teodoriu C, McCain WD Jr. HPHT viscosities measurements of mixtures of methane/nitrogen and methane/carbon dioxide. *J Nat Gas Sci Eng* 2013; 12:43–55. doi:10.1016/j.jngse.2013.01.005.
[234] Uchida T, Ohmura R, Nagao J, Takeya S, Ebinuma T, Narita H. Viscosity of aqueous CO_2 solutions measured by dynamic light scattering. *J Chem Eng Data* 2003; 48(5):1225–1229. doi:10.1021/je034041x.
[235] Harvey AH, Huber ML, Laesecke AR, Muzny CD, Perkins RA. Progress toward new reference correlations for the transport properties of carbon dioxide. In: *The 4th International Symposium on Supercritical CO_2 Power Cycles*. Pittsburgh, PA, USA, 2014; pp. 1–14. URL `http://www.nist.gov/customcf/get_pdf.cfm?pub_id=916275`.
[236] Vogel E, Barkow L. Precision measurements of the viscosity coefficient of carbon dioxide between room temperature and 650 K. *Z phys Chem (Leipzig)* 1986; 267.
[237] Hendl S, Neumann AK, Vogel E. The viscosity of carbon dioxide and its initial density dependence. *High Temp High Press* 1993; 25:503–511.
[238] Chaikin AM, Markevich AM. *Zh Fiz Khim* 1958; 32:116–120.
[239] Cheung H, Bromley LA, Wilke CR. Thermal conductivity of gas mixtures. *AIChE Journal* 1962; 8(2):221–228. doi:10.1002/aic.690080219.
[240] Pátek, J, Klomfar J, Čapla L, Buryan P. Thermal conductivity of carbon dioxide-methane mixtures at temperatures between 300 and 425 K and at pressures up to 12 MPa. *Int J Thermophys* 2005; 26(3):577–592. doi:10.1007/s10765-005-5566-6.
[241] Zheng XY, Yamamoto S, Yoshida H, Masuoka H, Yorizane M. Measurement and correlation of the thermal conductivities for several dense fluids and mixtures. *J Chem Eng Jpn* 1984; 17(3):237–245. doi:10.1252/jcej.17.237.
[242] Dohrn R, Treckmann R, Heinemann T. Vapor-phase thermal conductivity of 1,1,1,2,2-pentafluoropropane, 1,1,1,3,3-pentafluoropropane, 1,1,2,2,3-pentafluoropropane and carbon dioxide. *Fluid Phase Equilib* 1999; 158-160:1021–1028. doi:10.1016/S0378-3812(99)00126-0.
[243] Span R, Wagner W. A new equation of state for carbon dioxide covering the fluid region from the triple-point temperature to 1100 K at pressures up to 800 MPa. *J Phys Chem Ref Data* 1996; 25(6):1509–1596. doi:10.1063/1.555991.
[244] Hammer M, Ervik Å, Munkejord ST. Method using a density-energy state function with a reference equation of state for fluid-dynamics simulation of vapor-liquid-solid carbon dioxide. *Ind Eng Chem Res* 2013; 52(29):9965–9978. doi:10.1021/ie303516m.
[245] Peng DY, Robinson DB. A new two-constant equation of state. *Ind Eng Chem Fund* 1976; 15(1):59–64. doi:10.1021/i160057a011.
[246] Demetriades TA, Drage TC, Graham RS. Developing a new equation of state for carbon capture and storage pipeline transport. *P I Mech Eng E-J Pro* 2013; 227(2):117–124. doi:10.1177/0954408913481552.
[247] Jacobsen RT, Stewart RB. Thermodynamic properties of nitrogen including liquid and vapor phases from 63K to 2000K with pressures to 10,000 bar. *J Phys Chem Ref Data* 1973; 2(4):757–922. doi:10.1063/1.3253132.
[248] Kunz O, Klimeck R, Wagner W, Jaeschke M. *The GERG-2004 wide-range equation of state for natural gases and other mixtures. GERG TM15 2007.* Düsseldorf: VDI Verlag GmbH., 2007. ISBN 978-3-18-355706-6. `http://www.gerg.info/publications`.
[249] Demetriades TA, Graham RS. A new equation of state for CCS pipeline transport: Calibration of mixing rules for binary mixtures of CO_2 with N_2, O_2 and H_2. *J Chem Thermodyn* 2015; doi:10.1016/j.jct.2015.07.045.
[250] Gernert J, Span R. EOS-CG: An accurate property model for application in CCS processes. In: *Proc. Asian Thermophys. Prop. Conf.* Beijing, 2010; .
[251] Span R, Eckermann T, Herrig S, Hielscher S, Jäger A, Thol M. TREND. Thermodynamic reference and engineering data 2.0. 2015. Lehrstuhl für Thermodynamik, Ruhr-Universitaet Bochum.
[252] Tillner-Roth R. *Die thermodynamischen Eigenschaften von R152a, R134a und ihren Gemischen: Messungen und Fundamentalgleichungen*. Forschungsberichte des Deutschen Kälte- und Klimatechnischen Vereins, Nr. 41, 1993. ISBN 3-922-42942-4.
[253] Lemmon EW. *A generalized model for the prediction of the thermodynamic properties of mixtures including vapor-liquid equilibrium*. PhD

dissertation, University of Idaho, Moscow, Idaho, USA, 1996.

[254] Lemmon EW, Jacobsen RT. A generalized model for the thermodynamic properties of mixtures. *Int J Thermophys* 1999; 20:825–835.

[255] Lemmon EW, Tillner-Roth R. A Helmholtz energy equation of state for calculating the thermodynamic properties of fluid mixtures. *Fluid Phase Equilib* 1999; 165:1–21.

[256] Wilhelmsen Ø, Skaugen G, Jørstad O, Li H. Evaluation of SPUNG and other equations of state for use in carbon capture and storage modelling. In: Røkke NA, Hägg MB, Mazzetti MJ, editors, *6th Trondheim Conference on CO_2 Capture, Transport and Storage (TCCS-6)*. BIGCCS / SINTEF / NTNU, Trondheim, Norway: Energy Procedia vol. 23, 2012; pp. 236–245. doi:10.1016/j.egypro.2012.06.024.

[257] Soave G. Equilibrium constants from a modified Redlich-Kwong equation of state. *Chem Eng Sci* 1972; 27(6):1197–1203. doi:10.1016/0009-2509(72)80096-4.

[258] Péneloux A, Rauzy E, Fréze R. A consistent correction for Redlich-Kwong-Soave volumes. *Fluid Phase Equilib* 1982; 8(1):7–23. doi:10.1016/0378-3812(82)80002-2.

[259] Lee BI, Kesler MG. A generalized thermodynamic correlation based on three-parameter corresponding states. *AIChE J* 1975; 21(3):510–527.

[260] Jørstad O. *Equations of State for Hydrocarbon Mixtures*. Dissertation, Norwegian Institute of Technology (NTH), 1993.

[261] Younglove BA, Ely JF. Thermophysical properties of fluids. II. Methane, ethane, propane, isobutane, and normal butane. *J Phys Chem Ref Data* 1987; 16(4):577–798. doi:10.1063/1.555785.

[262] Chapman W, Gubbins K, Jackson G, Radosz M. SAFT: Equation-of-state solution model for associating fluids. *Fluid Phase Equilib* 1989; 52:31 – 38. doi:10.1016/0378-3812(89)80308-5.

[263] Huang SH, Radosz M. Equation of state for small, large, polydisperse, and associating molecules. *Ind Eng Chem Res* 1990; 29(11):2284–2294. doi:10.1021/ie00107a014.

[264] Diamantonis NI, Boulougouris GC, Mansoor E, Tsangaris DM, Economou IG. Evaluation of cubic, SAFT, and PC-SAFT equations of state for the vapor-liquid equilibrium modeling of CO_2 mixtures with other gases. *Ind Eng Chem Res* 2013; 52(10):3933–3942. doi:10.1021/ie303248q.

[265] Gross J, Sadowski G. Perturbed-chain SAFT: An equation of state based on a perturbation theory for chain molecules. *Ind Eng Chem Res* 2001; 40(4):1244–1260. doi:10.1021/ie0003887.

[266] Redlich O, Kwong JNS. On the thermodynamics of solutions. V. An equation of state. Fugacities of gaseous solutions. *Chem Rev* 1949; 44(1):233–244. doi:10.1021/cr60137a013.

[267] Avendaño C, Lafitte T, Galindo A, Adjiman CS, Jackson G, Müller EA. SAFT-γ force field for the simulation of molecular fluids. 1. A single-site coarse grained model of carbon dioxide. *J Phys Chem B* 2011; 115(38):11154–11169. doi:10.1021/jp204908d.

[268] Lymperiadis A, Adjiman CS, Galindo A, Jackson G. A group contribution method for associating chain molecules based on the statistical associating fluid theory (SAFT-γ). *J Chem Phys* 2007; 127(23). doi:10.1063/1.2813894.

[269] Lobanova O, Mejía A, Jackson G, Müller EA. SAFT-γ force field for the simulation of molecular fluids 6: Binary and ternary mixtures comprising water, carbon dioxide, and n-alkanes. *J Chem Thermodyn* 2016; 93:320–336. doi:10.1016/j.jct.2015.10.011.

[270] Herdes C, Totton TS, Müller EA. Coarse grained force field for the molecular simulation of natural gases and condensates. *Fluid Phase Equilib* 2015; 406:91–100. doi:10.1016/j.fluid.2015.07.014.

[271] Li H, Yan J. Evaluating cubic equations of state for calculation of vapor liquid equilibrium of CO_2 and CO_2-mixtures for CO_2 capture and storage processes. *Appl Energ* 2009; 86(6):826–836. doi:10.1016/j.apenergy.2008.05.018.

[272] Li H, Yan J. Impacts of equations of state (EOS) and impurities on the volume calculation of CO_2 mixtures in the applications of CO_2 capture and storage (CCS) processes. *Appl Energ* 2009; 86(12):2760–2770. doi:10.1016/j.apenergy.2009.04.013.

[273] Chapoy A, Burgass R, Tohidi B, Austell JM, Eickhoff C. Effect of common impurities on the phase behavior of carbon-dioxide-rich systems: Minimizing the risk of hydrate formation and two-phase flow. *SPE J* 2011; 16(4):921–930. doi:10.2118/123778-PA.

[274] Chapoy A, Burgass R, Tohidi B, Alsiyabi I. Hydrate and phase behavior modeling in CO_2-rich pipelines. *J Chem Eng Data* 2015; 60(2):447–453. doi:10.1021/je500834t.

[275] Kontogeorgis GM, Voutsas EC, Yakoumis IV, Tassios DP. An equation of state for associating fluids. *Ind Eng Chem Res* 1996; 35(11):4310–4318. doi:10.1021/ie9600203.

[276] Sloan ED, Koh CA. *Clathrate Hydrates of Natural Gases*. CRC Press, 2008.

[277] Duan Z, Sun R. A model to predict phase equilibrium of CH_4 and CO_2 clathrate hydrate in aqueous electrolyte solutions. *Am Mineral* 2006; 91(8–9):1346–1354. doi:10.2138/am.2006.2017.

[278] Ely JF, Hanley HJM. Prediction of transport properties. 1. Viscosity of fluids and mixtures. *Ind Eng Chem Fund* 1981; 20(4):323–332. doi:10.1021/i100004a004.

[279] Ely JF, Hanley HJM. Prediction of transport properties. 2. Thermal conductivity of pure fluids and mixtures. *Ind Eng Chem Fund* 1983; 22(1):90–97. doi:10.1021/i100009a016.

[280] Quiñones-Cisneros SE, Zéberg-Mikkelsen CK, Stenby EH. The friction theory (f-theory) for viscosity modeling. *Fluid Phase Equilib* 2000; 169(2):249–276. doi:10.1016/S0378-3812(00)00310-1.

[281] Giljarhus KET, Munkejord ST, Skaugen G. Solution of the Span-Wagner equation of state using a density-energy state function for fluid-dynamic simulation of carbon dioxide. *Ind Eng Chem Res* 2012; 51(2):1006–1014. doi:10.1021/ie201748a.

[282] Hammer M, Morin A. A method for simulating two-phase pipe flow with real equations of state. *Comput Fluids* 2014; 100:45–58. doi:10.1016/j.compfluid.2014.04.030.

[283] Brown S, Martynov S, Mahgerefteh H, Chen S, Zhang Y. Modelling the non-equilibrium two-phase flow during depressurisation of CO_2 pipelines. *Int J Greenh Gas Con* 2014; 30:9–18. doi:10.1016/j.ijggc.2014.08.013.

[284] Aursand E, Dørum C, Hammer M, Morin A, Munkejord ST, Nordhagen HO. CO_2 pipeline integrity: Comparison of a coupled fluid-structure model and uncoupled two-curve methods. In: Røkke N, Svendsen H, editors, *7th Trondheim Conference on CO_2 Capture, Transport and Storage (TCCS-7)*. BIGCCS / SINTEF / NTNU, Trondheim, Norway: Energy Procedia, vol. 51, 2014; pp. 382–391. doi:10.1016/j.egypro.2014.07.045.

[285] Michelsen ML. State function based flash specifications. *Fluid Phase Equilib* 1999; 158-160:617–626. doi:10.1016/S0378-3812(99)00092-8.

[286] Elshahomi A, Lu C, Michal G, Liu X, Godbole A, Venton P. Decompression wave speed in CO_2 mixtures: CFD modelling with the GERG-2008 equation of state. *Appl Energ* 2015; 140:20–32. doi:10.1016/j.apenergy.2014.11.054.

[287] Henderson LF. General laws for propagation of shock waves through matter. In: Ben-Dor G, Igra O, Elperin T, editors, *Handbook of Shock Waves*, vol. 1, chap. 2, pp. 144–183. San Diego, CA, USA: Academic Press, 2000; .

[288] Martynov S, Brown S, Mahgerefteh H, Sundara V. Modelling choked flow for CO_2 from the dense phase to below the triple point. *Int J Greenh Gas Con* 2013; 19:552–558. doi:10.1016/j.ijggc.2013.10.005.

[289] Martynov S, Brown S, Mahgerefteh H, Sundara V, Chen S, Zhang Y. Modelling three-phase releases of carbon dioxide from high-pressure pipelines. *Process Saf Environ* 2014; 92(1):36–46. doi:10.1016/j.psep.2013.10.004.

[290] Martynov S, Brown S, Mahgerefteh H. An extended peng-robinson equation of state for carbon dioxide solid-vapor equilibrium. *Greenh Gas Sci Tech* 2013; 3(2):136–147. doi:10.1002/ghg.1322.

[291] Trusler JPM. Erratum: Equation of state for solid phase I of carbon dioxide valid for temperatures up to 800 K and pressures up to 12 GPa [J. Phys. Chem. Ref. Data 40, 043105 (2011)]. *J Phys Chem Ref Data* 2012; 41(3). doi:10.1063/1.4745598. Article 039901.

[292] Hammer M, Wahl PE, Anantharaman R, Berstad DO, Lervåg KY. CO_2 capture from off-shore turbines using supersonic gas separation. In: Dixon T, Herzog H, Twinning S, editors, *GHGT-12 – 12th International Conference on Greenhouse Gas Control Technologies*. University of Texas at Austin / IEAGHGT, Austin, Texas, USA: Energy Procedia, vol. 63, 2014; pp. 243–252. doi:10.1016/j.egypro.2014.11.026.

[293] Dugstad A, Halseid M, Morland B. Effect of SO_2 and N_2 on corrosion and solid formation in dense phase CO_2 pipelines. In: Dixon T, Yamaji K, editors, *GHGT-11 – 11th International Conference on Greenhouse Gas Control Technologies*. RITE / IEAGHGT, Kyoto, Japan: Energy Procedia, vol. 37, 2013; pp. 2877–2887. doi:0.1016/j.egypro.2013.06.173.

[294] Brown S, Beck J, Mahgerefteh H, Fraga ES. Global sensitivity analysis of the impact of impurities on CO_2 pipeline failure. *Reliab Eng Syst Safe* 2013; 115:43–54. doi:10.1016/j.ress.2013.02.006.

[295] Armstrong K, Allason D. 2" NB shocktube releases of dense phase CO_2. Tech. rep., GL Noble Denton, Gilsland Cumbria, UK, 2014. URL `https://www.dnvgl.com/oilgas/innovation-development/joint-industry-projects/co2pipetrans.html`.

[296] Botros KK, Hippert E Jr, Craidy P. Measuring decompression wave speed in CO_2 mixtures by a shock tube. *Pipelines International* 2013; 16:22–28.

[297] Brown S, Martynov S, Mahgerefteh H, Proust C. A homogeneous relaxation flow model for the full bore rupture of dense phase CO_2 pipelines. *Int J Greenh Gas Con* 2013; 17:349–356. doi:10.1016/j.ijggc.2013.05.020.

[298] Clausen S, Oosterkamp A, Strøm KL. Depressurization of a 50 km long 24 inches CO_2 pipeline. In: Røkke NA, Hägg MB, Mazzetti MJ, editors, *6th Trondheim Conference on CO_2 Capture, Transport and Storage (TCCS-6)*. BIGCCS / SINTEF / NTNU, Trondheim, Norway: Energy Procedia vol. 23, 2012; pp. 256–265. doi:10.1016/j.egypro.2012.06.044.

[299] Cosham A, Jones DG, Armstrong K, Allason D, Barnett J. The decompression behaviour of carbon dioxide in the dense phase. In: *9th International Pipeline Conference, IPC2012*, vol. 3. Calgary, Canada: ASME, IPTI, 2012; pp. 447–464. doi:10.1115/IPC2012-90461.

[300] Drescher M, Varholm K, Munkejord ST, Hammer M, Held R, de Koeijer G. Experiments and modelling of two-phase transient flow during pipeline depressurization of CO_2 with various N_2 compositions. In: Dixon T, Herzog H, Twinning S, editors, *GHGT-12 – 12th International Conference on Greenhouse Gas Control Technologies*. University of Texas at Austin / IEAGHGT, Austin, Texas, USA: Energy Procedia, vol. 63, 2014; pp. 2448–2457. doi:10.1016/j.egypro.2014.11.267.

[301] Jie HE, Xu BP, Wen JX, Cooper R, Barnett J. Predicting the decompression characteristics of carbon dioxide using computational fluid dynamics. In: *9th International Pipeline Conference IPC2012*. Calgary, Canada: ASME, IPTI, 2012; pp. 585–595. doi:10.1115/IPC2012-90649.

[302] Bendiksen KH, Malnes D, Moe R, Nuland S. The dynamic two-fluid model OLGA: Theory and application. *SPE Production Engineering* 1991; 6(2):171–180. doi:10.2118/19451-PA.

[303] Håvelsrud M. Improved and verified models for flow of CO_2 in pipelines. In: *The Third International Forum on the Transportation of CO_2 by Pipeline*. Gateshead, UK: Clarion Technical Conferences, 2012; .

[304] Huh C, Cho MI, Hong S, Kang SG. Effect of impurities on depressurization of CO_2 pipeline transport. In: Dixon T, Herzog H, Twinning S, editors, *GHGT-12 – 12th International Conference on Greenhouse Gas Control Technologies*. University of Texas at Austin / IEAGHGT, Austin, Texas, USA: Energy Procedia, vol. 63, 2014; pp. 2583–2588. doi:10.1016/j.egypro.2014.11.280.

[305] Cho MI, Huh C, Kang SG, Baek JH. Evaluation of the two phase pressure drop during the CO_2-N_2 mixture pipeline transport. In: Dixon T, Herzog H, Twinning S, editors, *GHGT-12 – 12th International Conference on Greenhouse Gas Control Technologies*. University of Texas at Austin / IEAGHGT, Austin, Texas, USA: Energy Procedia, vol. 63, 2014; pp. 2710–2714. doi:10.1016/j.egypro.2014.11.293.

[306] Tu R, Xie Q, Yi J, Li K, Zhou X, Jiang X. An experimental study on the leakage process of high pressure CO_2 from a pipeline transport system. *Greenh Gas Sci Tech* 2014; 4(6):777–784. doi:10.1002/ghg.1423.

[307] Botros KK. Measurements of speed of sound in lean and rich natural gas mixtures at pressures up to 37 MPa using a specialized rupture tube. *Int J Thermophys* 2010; 31(11–12):2086–2102. doi:10.1007/s10765-010-0888-4.

[308] Mahgerefteh H, Brown S, Martynov S. A study of the effects of friction, heat transfer, and stream impurities on the decompression behavior in CO_2 pipelines. *Greenh Gas Sci Tech* 2012; 2(5):369–379. doi:10.1002/ghg.1302.

[309] Xu BP, Jie HE, Wen JX. A pipeline depressurization model for fast decompression and slow blowdown. *Int J Pres Ves Pip* 2014; 123–124:60–69. doi:10.1016/j.ijpvp.2014.07.003.

[310] Stryjek R, Vera JH. PRSV: An improved Peng–Robinson equation of state for pure compounds and mixtures. *Can J Chem Eng* 1986; 64(2):323–333. doi:10.1002/cjce.5450640224.

[311] Friedel L. Improved friction pressure drop correlations for horizontal and vertical two phase pipe flow. In: *Proceedings, European Two Phase Flow Group Meeting*. Ispra, Italy, 1979; Paper E2.

[312] Spedding PL, Hand NP. Prediction in stratified gas-liquid co-current flow in horizontal pipelines. *Int J Heat Mass Tran* 1997; 40(8):1923–1935. doi:10.1016/S0017-9310(96)00252-9.

[313] Gungor KE, Winterton RHS. Simplified general correlation for saturated flow boiling and comparisons of correlations with data. *Chem Eng Res Des* 1987; 65(2):148–156.

[314] Bejan A. *Heat Transfer*. New York: John Wiley & Sons, Inc., 1993. ISBN 0-471-50290-1.

[315] Maxey WA. Long shear fractures in CO_2 lines controlled by regulating saturation, arrest pressures. *Oil Gas J* 1986; 84(31):44–46.

[316] Aihara S, Misawa K. Numerical simulation of unstable crack propagation and arrest in CO_2 pipelines. In: *The First International Forum on the Transportation of CO_2 by Pipeline*. Gateshead, UK: Clarion Technical Conferences, 2010; .

[317] Maxey WA. Fracture initiation, propagation and arrest. In: *Fifth Symposium on Line Pipe Research*. Houston, Texas, USA: American Gas Association, 1974; pp. J1–J31.

[318] Jones DG, Cosham A, Armstrong K, Barnett J, Cooper R. Fracture-propagation control in dense-phase CO_2 pipelines. In: *6th International Pipeline Technology Conference*. Ostend, Belgium: Lab. Soete and Tiratsoo Technical, 2013; Paper no. S06-02.

[319] Mahgerefteh H, Atti O. Modeling low-temperature–induced failure of pressurized pipelines. *AIChE J* 2006; 52(3):1248–1256. doi:10.1002/aic.10719.

[320] Nordhagen HO, Kragset S, Berstad T, Morin A, Dørum C, Munkejord ST. A new coupled fluid-structure modelling methodology for running ductile fracture. *Comput Struct* 2012; 94–95:13–21. doi:10.1016/j.compstruc.2012.01.004.

[321] O'Donoghue PE, Green ST, Kanninen MF, Bowles PK. The development of a fluid/structure interaction model for flawed fluid containment boundaries with applications to gas transmission and distribution piping. *Comput Struct* 1991; 38(5–6):501–513. doi:10.1016/0045-7949(91)90002-4.

[322] O'Donoghue PE, Kanninen MF, Leung CP, Demofonti G, Venzi S. The development and validation of a dynamic fracture propagation model for gas transmission pipelines. *Int J Pres Ves Pip* 1997; 70(1):11–25. doi:10.1016/S0308-0161(96)00012-9.

[323] You XC, Zhuang Z, Huo CY, Zhuang CJ, Feng YR. Crack arrest in rupturing steel gas pipelines. *Int J Fracture* 2003; 123(1–2):1–14. doi:10.1023/B:FRAC.0000005791.79914.82.

[324] Greenshields CJ, Venizelos GP, Ivankovic A. A fluid-structure model for fast brittle fracture in plastic pipes. *J Fluid Struct* 2000; 14(2):221–34. doi:10.1006/jfls.1999.0258.

[325] Makino H, Takeuchi I, Tsukamoto M, Kawaguchi Y. Study on the propagating shear fracture in high strength line pipes by partial-gas burst test. *ISIJ Int* 2001; 41(7):788–794. doi:10.2355/isijinternational.41.788.

[326] Berstad T, Dørum C, Jakobsen JP, Kragset S, Li H, Lund H, Morin A, Munkejord ST, Mølnvik MJ, Nordhagen HO, Østby E. CO_2 pipeline integrity: A new evaluation methodology. In: Gale J, Hendriks C, Turkenberg W, editors, *GHGT-10 – 10th International Conference on Greenhouse Gas Control Technologies*. IEAGHGT, Amsterdam, The Netherlands: Energy Procedia vol. 4, 2011; pp. 3000–3007. doi:10.1016/j.egypro.2011.02.210.

[327] Aihara S, Østby E, Lange HI, Misawa K, Imai Y, Thaulow C. Burst tests for high-pressure hydrogen gas line pipes. In: *Proceedings of IPC2008, 7th International Pipeline Conference*. Calgary, Alberta, Canada: ASME, 2008; .

[328] Aursand E, Dumoulin S, Hammer M, Lange HI, Morin A, Munkejord ST, Nordhagen HO. Fracture propagation contol in CO_2 pipelines: Validation of a coupled fluid-structure model. *Submitted* 2015; .

[329] Morin A, Kragset S, Munkejord ST. Pipeline flow modelling with source terms due to leakage: The straw method. In: Røkke NA, Hägg MB, Mazzetti MJ, editors, *6th Trondheim Conference on CO_2 Capture, Transport and Storage (TCCS-6)*. BIGCCS / SINTEF / NTNU, Trondheim, Norway: Energy Procedia vol. 23, 2012; pp. 226–235. doi:10.1016/j.egypro.2012.06.023.

[330] Cosham A, Jones DG, Armstrong K, Allason D, Barnett J. Analysis of two dense phase carbon dioxide full-scale fracture propagation tests. In: *10th International Pipeline Conference, IPC2014*, vol. 3. Calgary, Canada, 2014; doi:10.1115/IPC2014-33080.

[331] Cosham A, Jones DG, Armstrong K, Allason D, Barnett J. Ruptures in gas pipelines, liquid pipelines and dense phase carbon dioxide pipelines. In: *9th International Pipeline Conference, IPC2012*, vol. 3. Calgary, Canada: ASME, IPTI, 2012; pp. 465–482. doi:10.1115/IPC2012-90463.

[332] Meleddu A, Bertoli M, Di Biagio M, Demofonti G. CO_2 decompression

modeling for ductile fracture propagation control in deepwater pipelines. In: *Twenty-fourth International Offshore and Polar Engineering Conference*. Busan, South Korea: ISOPE, 2014; pp. 198–204.

[333] Munkejord ST. Comparison of Roe-type methods for solving the two-fluid model with and without pressure relaxation. *Comput Fluids* 2007; 36(6):1061–1080. doi:10.1016/j.compfluid.2007.01.001.

[334] Munkejord ST. A numerical study of two-fluid models with pressure and velocity relaxation. *Adv Appl Math Mech* 2010; 2(2):131–159.

[335] Flåtten T, Morin A, Munkejord ST. Wave propagation in multicomponent flow models. *SIAM J Appl Math* 2010; 70(8):2861–2882. doi:10.1137/090777700.

[336] Martínez Ferrer PJ, Flåtten T, Munkejord ST. On the effect of temperature and velocity relaxation in two-phase flow models. *ESAIM – Math Model Num* 2012; 46(2):411–442. doi:10.1051/m2an/2011039.

[337] Flåtten T, Lund H. Relaxation two-phase flow models and the subcharacteristic condition. *Math Mod Meth Appl S* 2011; 21(12):2379–2407. doi:10.1142/S0218202511005775.

[338] Lund H. A hierarchy of relaxation models for two-phase flow. *SIAM J Appl Math* 2012; 72(6):1713–1741. doi:10.1137/12086368X.

[339] Linga G. A hierarchy of non-equilibrium two-phase flow models. *Submitted* 2015; .

[340] Saurel R, Petitpas F, Abgrall R. Modelling phase transition in metastable liquids: application to cavitating and flashing flows. *J Fluid Mech* 2008; 607:313–350. doi:10.1017/S0022112008002061.

[341] Zein A, Hantke M, Warnecke G. Modeling phase transition for compressible two-phase flows applied to metastable liquids. *J Comput Phys* 2010; 229(8):2964–2998. doi:10.1016/j.jcp.2009.12.026.

[342] Rodio MG, Abgrall R. An innovative phase transition modeling for reproducing cavitation through a five-equation model and theoretical generalization to six and seven-equation modelsl *Int J Heat Mass Tran* 2015; 89:1386–1401. doi:10.1016/j.ijheatmasstransfer.2015.05.008.

[343] Menikoff R, Plohr BJ. The Riemann problem for fluid flow of real materials. *Rev Mod Phys* 1989; 61(1):75–130. doi:10.1103/RevModPhys.61.75.

[344] Menikoff R. Empirical equations of state for solids. In: Horie Y, editor, *Shock Wave Science and Technology Reference Library*, vol. 2, pp. 143–188. Berlin: Springer, 2007; doi:10.1007/978-3-540-68408-4_4.

[345] Lund H, Flåtten T, Munkejord ST. Depressurization of carbon dioxide in pipelines – models and methods. In: Gale J, Hendriks C, Turkenberg W, editors, *GHGT-10 – 10th International Conference on Greenhouse Gas Control Technologies*. IEAGHGT, Amsterdam, The Netherlands: Energy Procedia vol. 4, 2011; pp. 2984–2991. doi:10.1016/j.egypro.2011.02.208.

[346] Lund H, Aursand P. Two-phase flow of CO_2 with phase transfer. In: Røkke NA, Hägg MB, Mazzetti MJ, editors, *6th Trondheim Conference on CO_2 Capture, Transport and Storage (TCCS-6)*. BIGCCS / SINTEF / NTNU, Trondheim, Norway: Energy Procedia vol. 23, 2012; pp. 246–255. doi:10.1016/j.egypro.2012.06.034.

[347] Benintendi R. Non-equilibrium phenomena in carbon dioxide expansion. *Process Saf Environ* 2014; 92(1):47–59. doi:10.1016/j.psep.2013.11.001.

[348] Tian H, Ma Y, Li M, Zhang M. Theoretical analysis on expansion mechanism in carbon dioxide expander. *Science China Technological Sciences* 2011; 54(6):1469–1474. doi:10.1007/s11431-011-4328-x.

[349] Heermann DW, Wang T, Lee WD. Nucleation and metastability in the CO_2 system. *Int J Mod Phys C* 2003; 14(1):81–94. doi:10.1142/S0129183103004231.

[350] Bredesen A, Hafner A, Pettersen J, Nekså P, Aflekt K. Heat transfer and pressure drop for in-tube evaporation of CO_2. In: *Proceedings of the International Conference on Heat Transfer Issues in Natural Refrigerants*. University of Maryland, USA: IIF-IIR, 1997; pp. 1–15.

[351] Pettersen J. Flow vaporization of CO_2 in microchannel tubes. In: *4th International Conference on Compact Heat Exchangers and Enhancement Technology for the Process Industries*. Grenoble, France, 2002; pp. 111–121. doi:10.1016/S0894-1777(03)00029-3. Exp. Therm. Fluid Sci. 28 (2–3), 2004.

[352] Yun R, Kim Y. Two-phase pressure drop of CO_2 in mini tubes and microchannels. In: *1st International Conference on Microchannels and Minichannels*. Rochester, NY, USA: ASME, 2003; pp. 259–270. doi:10.1080/10893950490477554. Microscale Therm. Eng. 8 (3), 2004.

[353] Cheng L, Ribatski G, Quibén JM, Thome JR. New prediction methods for CO_2 evaporation inside tubes: Part I – A two-phase flow pattern map and a flow pattern based phenomenological model for two-phase flow frictional pressure drops. *Int J Heat Mass Tran* 2008; 51(1–2):111–124. doi:10.1016/j.ijheatmasstransfer.2007.04.002.

[354] Aakenes F, Munkejord ST, Drescher M. Frictional pressure drop for two-phase flow of carbon dioxide in a tube: Comparison between models and experimental data. In: Røkke N, Svendsen H, editors, *7th Trondheim Conference on CO_2 Capture, Transport and Storage (TCCS-7)*. BIGCCS / SINTEF / NTNU, Trondheim, Norway: Energy Procedia vol. 51, 2013; pp. 373–381. doi:10.1016/j.egypro.2014.07.044.

[355] Mitsubishi. Carbon dioxide handling involves using liquefied petroleum gas ship for conveying carbon dioxide. Patent JP2004125039-A, Mitsubishi Jukogyo KK, 2002.

[356] Kaarstad O, Hustad CW. Delivering CO_2 to Gullfaks and the Tampen Area. Cens project report, Elsam, Kinder Morgan, Statoil, 2003.

[357] Aspelund A, Mølnvik MJ, de Koeijer G. Ship transport of CO_2: Technical solutions and analysis of costs, energy utilization, exergy efficiency and CO_2 emissions. *Chem Eng Res Des* 2006; 84(9):847–855. doi:10.1205/cherd.5147.

[358] Vermeulen TN. Knowledge sharing report - CO_2 liquid logistics shipping concept (LLSC): Overall supply chain optimization. Tech. rep., Global CCS Institute, Anthony Veder, Vopak, 2011.

[359] Roussanaly S, Bureau-Cauchois G, Husebye J. Costs benchmark of CO_2 transport technologies for a group of various size industries. *Int J Greenh Gas Con* 2013; 12:341–350. doi:10.1016/j.ijggc.2012.05.008.

[360] Skagestad R, Eldrup N, Hansen HR, Belfroid S, Mathisen A, Lach A, Haugen HA. Ship transport of CO_2- status and technology gaps. Tech. Rep. 2214090, Tel-Tek, 2014.

[361] Nam H, Lee T, Lee J, Lee J, Chung H. Design of carrier-based offshore CCS system: Plant location and fleet assignment. *Int J Greenh Gas Con* 2013; 12:220–230. doi:10.1016/j.ijggc.2012.05.008.

[362] Omata A. Preliminary feasibility study on CO_2 carrier for ship-based CCS. Tech. Rep. CCSC-RPT-10-002, Chiyoda cooperation for GCCSI, 2011.

[363] Brownsort P. Ship transport of CO_2 for enhanced oil recovery - literature survey. Tech. rep., Scottish Carbon Capture & Storage, Edinburgh, Scotland, 2015.

[364] Eggers R, Green V. Pressure discharge from a pressure vessel filled with CO_2. *J Loss Prevent Proc* 1990; 3(1):59–63. doi:10.1016/0950-4230(90)85025-5.

[365] Gebbeken B, Eggers R. Blowdown of carbon dioxide from initially supercritical conditions. *J Loss Prevent Proc* 1996; 9(4):285–293. doi:10.1016/0950-4230(96)00021-6.

[366] Fredenhagen A, Eggers R. High pressure release of binary mixtures of CO_2 and N_2. Experimental investigation and simulation. *Chem Eng Sci* 2001; 56(16):4879–4885. doi:10.1016/S0009-2509(01)00129-4.

[367] Zhang J, Zhu D, Tian W, Qiu S, Su G, Zhang D. Depressurization study of supercritical fluid blowdown from simple vessel. *Ann Nucl Energy* 2014; 66:94–103. doi:10.1016/j.anucene.2013.11.004.

[368] Han SH, Chang D, Kim J, Chang W. Experimental investigation of the flow characteristics of jettisoning in a CO_2 carrier. *Process Saf Environ* 2014; 92(1):60–69. doi:10.1016/j.psep.2013.10.003.

[369] Vree B, Ahmad M, Buit L, Florisson O. Rapid depressurization of a CO_2 pipeline – experimental study. *Int J Greenh Gas Con* 2015; 41:41–49. doi:10.1016/j.ijggc.2015.06.011.

[370] Clayton WE, Griffin ML. Catastrophic failure of a liquid carbon dioxide storage vessel. *Process Saf Prog* 1994; 13(4):202–209. doi:10.1002/prs.680130405.

[371] Abbasi T, Abbasi SA. The boiling liquid expanding vapour explosion (BLEVE): Mechanism, consequence assessment, management. *J Hazard Mater* 2007; 141(3):489–519. doi:10.1016/j.jhazmat.2006.09.056.

[372] Bjerketvedt D, Egeberg K, Ke W, Gaathaug A, Vaagsaether K, Nilsen SH. Boiling liquid expanding vapour explosion in CO_2 small scale experiments. In: Gale J, Hendriks C, Turkenberg W, editors, *GHGT-10 – 10th International Conference on Greenhouse Gas Control Technologies*. IEAGHGT, Amsterdam, The Netherlands: Energy Procedia vol. 4, 2011; pp. 2285–2292. doi:10.1016/j.egypro.2011.02.118.

[373] Tosse S, Vaagsaether K, Bjerketvedt D. An experimental investigation of rapid boiling of CO_2. *Shock Waves* 2015; 25(3):277–282. doi:10.1007/s00193-014-0523-6.

[374] van der Voort MM, van den Berg AC, Roekaerts DJEM, Xie M, de Bruijn PCJ. Blast from explosive evaporation of carbon dioxide: experiment, modeling and physics. *Shock Waves* 2012; 22(2):129–140. doi:10.1007/s00193-012-0356-0.

[375] van der Voort MM, van Wees RMM, Ham JM, Spruijt MPN, van den Berg AC, de Bruijn PCJ, van Ierschot PGA. An experimental study on the temperature dependence of CO_2 evaporation. *J Loss Prevent Proc* 2013; 26(4):830–838. doi:10.1016/j.jlp.2013.02.016.

[376] Paterson L, Lu M, Connell L, Ennis-King JP. Numerical modeling of pressure and temperature profiles including phase transitions in carbon dioxide wells. In: *SPE Annual Technical Conference and Exhibition*. Denver, Colorado, USA: Society of Petroleum Engineers, 2008; doi:10.2118/115946-MS. Paper SPE-115946-MS.

[377] Lu M, Connell LD. Non-isothermal flow of carbon dioxide in injection wells during geological storage. *Int J Multiphase Flow* 2008; 2(2):248–258. doi:10.1016/S1750-5836(07)00114-4.

[378] Lindeberg E. Modelling pressure and temperature profile in a CO_2 injection well. In: Gale J, Hendriks C, Turkenberg W, editors, *GHGT-10 – 10th International Conference on Greenhouse Gas Control Technologies*. IEAGHGT, Amsterdam, The Netherlands: Energy Procedia vol. 4, 2011; pp. 3935–3941. doi:10.1016/j.egypro.2011.02.332.

[379] Cronshaw MB, Bolling JD. A numerical model of the non-isothermal flow of carbon dioxide in wellbores. In: *SPE California Regional Meeting*. San Francisco, California, USA: Society of Petroleum Engineers, 1982; doi:10.2118/10735-MS. Paper SPE-10735-MS.

[380] Pan L, Oldenburg CM, Wu YS, Pruess K. Wellbore flow model for carbon dioxide and brine. In: Gale J, Herzog H, Braitsch J, editors, *GHGT-9 – 9th International Conference on Greenhouse Gas Control Technologies*. MIT / IEA GHG, Washington DC, USA: Energy Procedia vol. 1, 2009; pp. 71–78. doi:10.1016/j.egypro.2009.01.012.

[381] Lu M, Connell LD. Transient, thermal wellbore flow of multispecies carbon dioxide mixtures with phase transition during geological storage. *Int J Multiphase Flow* 2014; 63:82–92. doi:10.1016/j.ijmultiphaseflow.2014.04.002.

[382] Lu M, Connell LD. The transient behaviour of CO_2 flow with phase transition in injection wells during geological storage – Application to a case study. *J Petrol Sci Eng* 2014; 124:7–18. doi:10.1016/j.petrol.2014.09.024.

[383] Ruan B, Xu R, Wei L, Ouyang X, Luo F, Jiang P. Flow and thermal modeling of CO_2 in injection well during geological sequestration. *Int J Greenh Gas Con* 2013; 19:271–280. doi:10.1016/j.ijggc.2013.09.006.

[384] Musivand Arzanfudi M, Al-Khoury R. A compressible two-fluid multiphase model for CO_2 leakage through a wellbore. *Int J Numer Meth Fl* 2015; 77(8):477–507. doi:10.1002/fld.3990.

[385] de Koeijer G, Hammer M, Drescher M, Held R. Need for experiments on shut-ins and depressurizations in CO_2 injection wells. In: Dixon T, Herzog H, Twinning S, editors, *GHGT-12 – 12th International Conference on Greenhouse Gas Control Technologies*. University of Texas at Austin / IEAGHGT, Austin, Texas, USA: Energy Procedia, vol. 63, 2014; pp. 3022–3029. doi:10.1016/j.egypro.2014.11.325.

[386] Lund H, Torsæter M, Munkejord ST. Study of thermal variations in wells during CO_2 injection. In: *SPE Bergen One Day Seminar*. Bergen, Norway: Society of Petroleum Engineers, 2015; doi:10.2118/173864-MS. Paper SPE-173864-MS.